U.PORTO

DOUTORAMENTO

Biologia Básica e Aplicada

Aiptasia sp. larva as a model to study the cellular mechanisms of coral-algae symbiosis

Iliona Wolfowicz

D

2017

Iliona Wolfowicz. *Aiptasia* sp. larva as a model to study the cellular mechanisms of coral-algae symbiosis

Aiptasia sp. larva as a model to study the cellular mechanisms of coral-algae symbiosis

Iliona Pereira Dias Wolfowicz

D.ICBAS **2017**

SEDE ADMINISTRATIVA

INSTITUTO DE CIÊNCIAS BIOMÉDICAS ABEL SALAZAR
FACULDADE DE CIÊNCIAS
FACULDADE DE MEDICINA

Iliona Pereira Dias Wolfowicz

Aiptasia sp. larva as a model to study the cellular mechanisms of coral-algae symbiosis

Tese de Candidatura ao grau de Doutor em Biologia Básica e Aplicada submetida ao Instituto de Ciências Biomédicas Abel Salazar da Universidade do Porto.

Orientador – Dr. Annika Guse

Categoria – Independent Group Leader

Afiliação – Heidelberg University, Centre for Organismal Studies

Coorientador – Dr. Ana Xavier Carvalho

Categoria – Group Leader

Afiliação – Instituto de Investigação e Inovação em Saúde, Instituto de Biologia Molecular e Celular

Abstract

Symbiosis between animals and microorganisms is widespread throughout the tree of life, often providing ecological advantages to the partners. One striking example is the endosymbiosis between corals and photosynthetic dinoflagellate algae (genus *Symbiodinium*), which provide essential nutrients to their coral host. This nutrient transfer is key for the productivity and biodiversity of coral reef ecosystems. Most corals establish symbiosis anew each generation during larval stages and take up algae through phagocytosis into the endodermal cells. However, corals are unsuitable as model system and sexually reproduce only once a year severely limiting access to larvae for dissecting the molecular mechanisms underlying symbiosis establishment. During my thesis, I established critical resources for *Aiptasia*, a small tropical marine sea anemone as a model system for coral symbiosis. First, I contributed to developing a robust spawning induction protocol for *Aiptasia* that allows unlimited access to larvae for experimentation. I then compared symbiosis specificity between *Aiptasia* larvae and two coral species using several defined symbiont types. I found that specificity patterns during symbiosis establishment are similar suggesting that the underlying mechanisms are conserved between *Aiptasia* and corals further strengthening *Aiptasia* as a model system. I refined an assay to quantitatively assess symbiosis establishment efficiency in *Aiptasia* during development and, importantly, established confocal microcopy as a powerful means to visualize the intracellular localization of symbionts in the larvae's endodermal cells. Building up on these tools and techniques, I asked how symbionts escape digestion by the host. I used various lysosomal markers to test if symbionts reside in lysosomal-like organelles. I found evidence that symbionts co-localize with multiple lysosomal markers indicating that symbionts withstand acidic and proteolytic environments as a prerequisite to avoid lysosomal digestion by the host. Together, my work was fundamental to further develop *Aiptasia* as a powerful platform for analyzing the cellular mechanisms of coral symbiosis, a phenomenon of immense importance for coral reef ecosystems worldwide.

Resumo

A simbiose entre animais e microrganismos está vastamente representado na árvore da vida, e muitas vezes para conferir vantagens aos organismos envolvidos nesta interação. Um exemplo flagrante é o da endossimbiose entre corais e dinoflagelados, algas fotossintéticas do género *Symbiodinium*, que fornecem nutrientes essenciais ao coral hospedeiro. Esta transferência de nutrientes é essencial para a produtividade e biodiversidade dos ecossistemas em recifes de corais. A maioria dos corais re-estabelece simbiose a cada geração durante os estadios larvares, incorporando algas por fagocitose nas células da endoderme. No entanto, os corais são inadequados como sistemas modelo pois reproduzem-se sexualmente apenas uma vez por ano o que limita drasticamente o acesso a larvas para dissecar os mecanismos moleculares subjacentes ao processo de simbiose. Durante o desenvolvimento desta tese, estabeleci recursos fundamentais de um modelo animal para o estudo da simbiose de corais, a anémona tropical e marinha *Aiptasia*. Primeiro contribuí para o desenvolvimento de um protocolo robusto para indução da desova em *Aiptasia*, permitindo o acesso ilimitado a larvas para experimentação. De seguida, comparei a especificidade da simbiose em larvas de *Aiptasia* e duas espécies de coral com diferentes tipos definidos de simbiontes. Verifiquei que os padrões de especificidade do processo de simbiose são semelhantes, o que sugere que os mecanismos adjacentes são conservados entre *Aiptasia* e corais, evidenciando assim o potencial da *Aiptasia* como sistema modelo. Optimizei o procedimento de quantificação da eficiência do processo de simbiose durante o desenvolvimento larvar do modelo *Aiptasia* e, além disso, estabeleci microscopia confocal como método ideal para visualizar a localização intracelular de simbiontes nas células da endoderme da larva. Com as técnicas desenvolvidas e a descrição fundamental do processo de simbiose neste organismo, avancei no sentido de perceber como os simbiontes evitam a digestão pela célula do hospedeiro. Usei marcadores do lisossoma para testar se os simbiontes residem num organelo com características lisossomais. Observei que os simbiontes co-localizam com marcadores do lisossoma, o que indica que estes resistem a condições acídicas e proteolíticas - pré-requisito para evitar a digestão pelos lisossomas do hospedeiro. Em suma, o meu trabalho foi fundamental para o desenvolvimento do modelo

Aiptasia como uma plataforma apropriada para a análise dos mecanismos celulares da simbiose de corais – fenómeno de extrema importância nos ecossistemas de recifes de coral no mundo.

Publication list

Grawunder, D., Hambleton, E. A., Bucher, M., **Wolfowicz, I.**, Bechtoldt, N., Guse, A. (2015). Induction of gametogenesis in the cnidarian endosymbiosis model *Aiptasia* sp. *Sci. Rep.*, **5**: 15677.

Bucher, M., **Wolfowicz, I.**, Voss, P. A., Hambleton, E. A., Guse, A. (2016). Development and symbiosis establishment in the cnidarian endosymbiosis model *Aiptasia* sp. *Sci. Rep.*, **6**: 19867.

Wolfowicz, I., Baumgarten, S., Voss, P.A., Hambleton, E.A, Hatta, M., Voolstra, C., Guse, A. (2016). *Aiptasia* sp. larvae as a model to reveal mechanisms of symbiont selection in cnidarians. *Sci. Rep*. **6**: 32366.

Acknowledgements

I am deeply grateful to my supervisor Dr. Annika Guse for support and guidance throughout my PhD and for the exceptional opportunities of travelling and doing fieldwork. I am very grateful to my co-supervisor Dr. Ana Xavier Carvalho in Porto for her support and for being always available when needed. To Prof. Masayuki Hatta at Ochanomizu University in Tokyo, for his dedicated guidance in my first experiments with coral larvae, I am profoundly thankful. I would like to show my gratitude to Prof. Dr. Thomas Holstein and Dr. Suat Özbek for advices and for sharing laboratory space and equipment. I was very fortunate to integrate the Centre for Organismal Studies (COS) at Heidelberg University, such dedicated, dynamic and multidisciplinary community of researchers and educators. I am thankful to Dr. Nico Dross, Dr. Christian Ackermann and Dr. Ulrike Engel at the Nikon Imaging Center for their technical help and advices with confocal microscopy. I would like to show all my thanks to the Guse Lab, a wonderful group of people – their team spirit was key for the development of my PhD. My thanks go especially to Natascha Bechtoldt, Désirée Grawunder, Madeline Bucher, Philipp Voss, Sebastian Baumgarten and Liz Hambleton for collaborative work, support and fruitful discussions. Thank you to the Guse team, Holstein team and Grossmann team for fun moments outside of the lab. I am so thankful to the GABBA program for this incredible opportunity, for the inspiration, for the chance of making part of the GABBA community. Thank you to my family and friends for giving me so much love, support and encouragement.

Table of contents

Abbreviations

ASW	Artificial sea water
ATP	Adenosine triphosphate
BCA	Bicinchoninic acid
BSA	Bovine serum albumin
Cas9	CRISPR associated protein 9
CRISR	Clustered regularly interspaced short palindromic repeats
DABO	1,4-Diazabicyclo [2.2.2] octan
DAPI	4',6-diamidino-2-phenylindole
DMSO	Dimethyl sulfoxide
DNA	Deoxyribonucleic acid
ECL	Enhanced chemiluminescence
FITC	Fluorescein isothiocyanate
GTP	Guanosine-5'-triphosphate
GTPae	Guanosine-5'-triphosphate hydrolase
kDa	Kilodalton
mRNA	Messenger RNA
NA	Numerical aperture
PAR	Photosynthetically active radiation
PBS	Phosphate buffered saline
rDNA	Ribosomal DNA
RNA	Ribonucleic acid
RNA-Seq	RNA-sequencing
SDS	Sodium dodecyl sulfate
SEM	Standard error of the mean
Tris	Tris(hydroxymethyl)aminomethane
TRITC	Tetramethylrhodamine
vATPase	Vacuolar-type H^+-ATP enzyme

Chapter 1- Introduction

1. Coral reefs, ecological and economical important ecosystems

Coral reefs are prominent ecosystems, which possess immense ecological and economic importance. Particularly, coral reef's three-dimensional structures are home of more than 25% of all marine species, while covering only 0.1-0.5% of the total ocean area (Spalding et al. 2001, Morberg and Falke 1999). Thus, coral reefs are biodiversity "hot spots". Moreover, coral reefs have the important capability of sequestration of carbon from the atmosphere. The global estimated value of coral reefs is around 30 billion US dollars (Cesar et al. 2003, Conservation International 2008). By contributing to fisheries, giving shore protection and serving as tourism attraction, coral reefs are a main source of income for around 350 million people living near reef regions (Wilkinson 1996). Main reef areas include tropical and subtropical parts of the western Atlantic and the Indo-Pacific (Spalding et al. 2001, Morberg & Falke 1999).

2. Coral reefs depend on a functional symbiosis with dinoflagellate algae

The fact that corals can successfully grow in tropical, oligotrophic waters is due to the corals' capability to establish symbiotic interactions. Symbiosis is defined as the intimate association between two or more organisms of different species. Such associations are known to shape the phenotype of the hosts and to modulate their physiology. Corals are found in symbiosis with a wide variety of microorganisms such as virus, bacteria, and eukaryotes (Rosenberg et al. 2007, Bosch et al. 2014). Particularly important for the survival of corals is the endosymbiosis with dinoflagellate photosynthetic algae from the genus *Symbiodinium*. *Symbiodinium* is highly efficient in light harvesting (Brodersen et al. 2014) and, once stably integrated into the coral endodermal cells, provides photosynthetic products, such as glucose, glycerol and amino acids to the coral host (Falkowski et al. 1984, Burriesci et al. 2012). Photosynthates contribute to more than 90% of corals' energetic needs (Muscatine 1990) and thus to increase fitness and survival in nutrient-poor environments (Wernegreen et al. 2012). While

the coral host receives algae photosynthates as nutrients, it provides the algae with inorganic nutrients such as CO_2, NH_3, PO_4^{3-} and increased access to light for photosynthesis (Muscatine 1990, Yellowlees et al. 2008). This interaction with photosynthetic algae enhances corals' calcification ability through a carbon concentrating mechanism, to build the three-dimensional structures of reefs that are the habitat for a wide range of species (Birkeland 1997, Paulay 1997, McCook et al. 2010). Besides establishing symbiosis with corals, *Symbiodinium* is also found in symbiosis with marine invertebrates such as sponges, anemones, jellyfish, flatworms, mollusks and bivalves (Coffroth et al. 2006, Porto et al. 2008, Rumpho et al. 2011, Nitschke et al. 2016, Stat el al. 2006, Manning & Gates 2008).

3. Threats to coral reefs

Coral reefs are fragile and severely endangered by environmental changes and other external stressors leading to repeated coral loss (Hughes et al. 2003, Hoegh-Guldberg et al. 2007, Pandolfi et al. 2003, Sweatman et al. 2011, De'ath et al. 2012). As symbiosis is essential for increased corals' fitness, stressors that lead to the breakdown of coral-algae endosymbiosis may lead to coral death. This phenomenon is known as "coral-bleaching", because symbiont loss reveals the white color of the calcareous skeleton of corals (Hoegh-Guldberg et al. 2007). Most of these stressors to corals stem from human activity, such as water pollution, overfishing, ocean acidification by increased atmospheric CO_2 concentration and increase of seawater temperature. This can trigger the breakdown of symbiosis, ultimately leading to coral death and consequently to loss of reefs' biodiversity (Hughes et al. 2003, Hoegh-Guldberg 1999, Weis 2008, Holbrook et al. 2015). Therefore, it is urgent to understand the fundamental aspects of symbiosis in steady state, to later reveal how stress factors lead to the breakdown of symbiosis. This may help develop effective strategies to conserve one of the globally most valuable ecosystems, the coral reef.

4. Coral biology and the mode of algal symbiont acquisition

Corals are cnidarians, a diverse phylum of animals defined by the presence of two tissue layers - outer ectoderm and inner endoderm – external radial symmetry, a single anatomical opening and the presence of nematocysts, specialized stinging cells (reviewed in Technau & Steele 2011). Cnidaria comprises approximately 9000 species that are further sub-divided in five major classes: Anthozoa, Scyphozoa, Cubozoa, Hydrozoa and Staurozoa (reviewed in Technau & Steele 2011). Corals and sea anemones belong to the class of the anthozoans, characterized by the lack of a medusa stage in their life cycle (Kayal et al. 2013). Reef-building corals mostly belong to the order Scleractinia (stony corals) that encompass approximately 1300 species (Cairns 1999, Spalding et al. 2001). Typically, scleractinian corals reproduce sexually by release of sperm and eggs into the water for external fertilization – known as broadcast spawning (Baird et al. 2009). To increase the chances of fertilization, broadcasting corals synchronize the release of gametes (Babcock et al. 1986, Harrison 2011). The synchronicity of gametes release leads to massive spawning events that typically occur once per year (Babcock et al. 1986). After fertilization, the embryo develops into a free-swimming planula (Babcock et al. 1986, Hayashibara et al. 1997).

Corals use two strategies to acquire symbiotic algae: in the first strategy, known as horizontal transmission, dinoflagellate algae are acquired anew each generation by larvae from the environment (Fadlallah 1983, van Oppen et al. 2001, Baird et al. 2009, Harii et al. 2009) (Figure 1). In the second strategy, known as vertical transmission, symbionts are integrated into the germ-line by the mother; however, the latter strategy is less common (Smith & Douglas 1987, reviewed in Baird et al. 2009). Thus, the non-symbiotic planula larval stage is the most relevant developmental stage during which symbiosis is established for the first time in nature (Figure 1). Adult corals may re-establish symbiosis after bleaching events by recapturing of symbionts from the environment and/or by multiplication of remaining symbiotic algal cells in the endoderm of the coral host. However, symbiosis re-establishment in adult corals is not very efficient (Lewis & Coffroth 2004, Jones et al. 2008, Coffroth et al. 2010). Therefore, acquisition of algae

during early ontogeny in corals is likely to be key for the establishment of a stable and functional symbiosis through the whole coral life cycle.

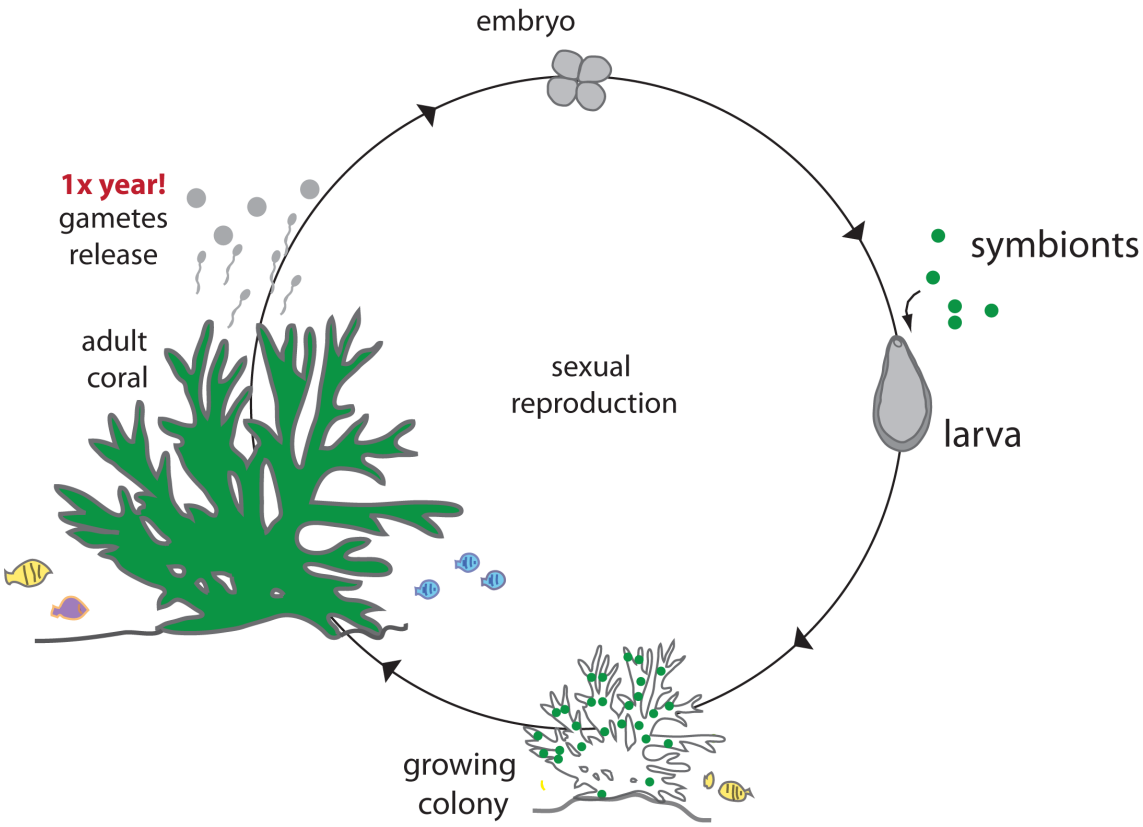

Figure 1 Coral life cycle. For most corals, sexual reproduction occurs only once a year. Corals release gametes, fertilization occurs externally in the water and the embryo develops into a larva. Larvae are naturally symbiont-free and take up symbionts from the environment. Therefore, symbiosis establishment occurs for the first time during larval stages of many corals. Larvae metamorphose into juvenile polyps that settle on substrate to grow and form an adult colony.

4.1 Coral-algae symbiosis establishment during larval development

In the larva, symbiosis establishment may be beneficial for dispersal, settlement and survival (Baird et al. 2009, Suzuki et al. 2013, Cumbo et al. 2013). Initially, larvae from certain reef-building corals were believed to establish symbiosis only after larval settlement and metamorphosis into juvenile polyps (Harrison & Wallace 1990). However, later it was shown that coral larvae from *Fungia scutaria* and *Acropora millepora* establish symbiosis during larval development, which subsequently increased settlement efficiency (Schwarz et al. 1999, vanOppen 2001). Later studies that tested the competency of larvae from

several coral species indicated that, like *Fungia*, many scleractinian coral larvae are competent to take up algae via phagocytosis into their endodermal cells at early developmental stages essentially as soon as the mouth opening and the gastric cavity (lined by the endoderm) are developed (Schwartz et al. 1999, Marlow & Martindale 2007, Harii et al. 2009). Symbiont density increases over time in coral larvae and has been shown to increase coral larvae survival (in comparison to symbiont-free larvae in non-stress conditions), possibly indicating a contribution of algae to the larva's nutrition and increasing time for dispersal (Richmond 1988, Baird et al. 2006, Suzuki et al. 2013).

5. Relevance of algal symbionts diversity and ecology in symbiosis

Free-living *Symbiodinium* can be found in the water column, the vicinity of corals, the benthic sediments and in seagrass. Particularly, benthic sediments were shown to facilitate *Symbiodinium* uptake by coral larva and juvenile polyps (Adams et al. 2009, Nitschke et al. 2016). The genus *Symbiodinium* is very diverse and many studies focus on genotyping different populations of these algae to reveal their phylogenetic relationships. The analysis of sequences from molecular markers of ribosomal origin such as the nuclear small subunit ribosomal DNA (18S-rDNA), the Domain V of chloroplast large subunit 23S ribosomal DNA (cp23S-rDNA) and the Internal Transcribed Spacer 2 (ITS2) allowed the classification of *Symbiodinium* in different clades, subclades and types (Rowan & Powers 1991, LaJeunesse 2001, Santos et al. 2002, Coffroth & Santos 2005, Pochon et al. 2006). Using such techniques, *Symbiodinium* was divided into nine clades from A to I with several types within each clade (also referred as subclades, types or strains) (Coffroth & Santos 2005, Pochon & Gates 2010) (Figure 2). To date, *Symbiodinium* types in clades A, B, C, D and F have been shown to establish symbiosis with scleractinian corals (Figure 2), others are found in symbiosis with unicellular eukaryotes such as Foraminifera or are not found in stable symbiotic interactions with other organisms, e.g. clade E (Pochon & Pawlowski 2006, Pochon & Gates 2010). A single host is not limited to a specific symbiont and scleractinian corals, but also other cnidarians, mollusk, sponges and foraminifera are found to even establish symbiosis with multiple *Symbiodinium*

populations simultaneously (Silverstein et al. 2012, Fay & Weber 2012). However, corals associate with some *Symbiodinium* types but not others, undergoing a process of symbiont selection leading to a specific host:symbiont combination often referred in the literature as “symbiosis specificity” (LaJeunesse et al. 2004, Coffroth et al. 2010). In light of changing environments, symbiosis establishment with the most suitable symbiont type possibly confers higher resilience or capability to adapt and may be key for coral survival (Jones et al. 2008, Coffroth et al. 2010).

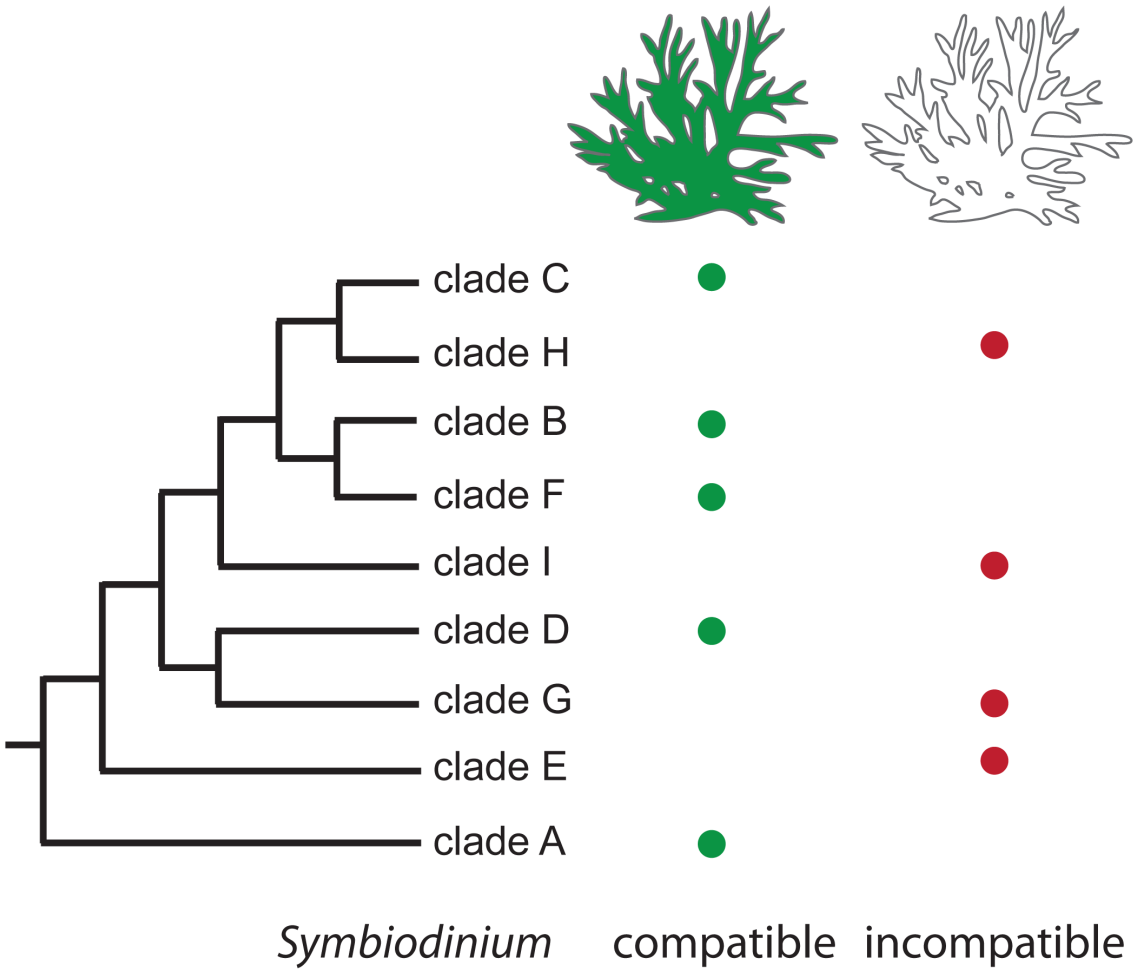

Figure 2 Phylogenetic relationship of *Symbiodinium* clades and their association with the corals. Simplified phylogenetic tree based on nuclear and chloroplast ribosomal markers showing the relationship between *Symbiodinium* clades A to I (adapted from Pochon et al. 2004). Each clade comprises many sub-types; *Symbiodinium* types within clades A, B, C, D and F have been found to establish symbiosis with scleractinian corals (compatible; green dots), whereas the others have not been detected in corals (incompatible; red dots).

6. Patterns of symbiosis establishment in the larva

Symbiont types that establish symbioses with corals are known as “compatible” and, in contrast, symbionts that are not able to do so are “incompatible”. Literature is divergent when it comes to define symbiont specificity and it is not yet clear which factors are prevailing when determining which symbiont(s) will form a stable long-lasting interaction with its host: statistical factors, host-symbiont taxa (fixed), external environmental factors (adaptable), or a combination of all of these (Weis et al. 2001, Rodriguez-Lanetty et al. 2006b, Silverstein et al. 2012, Baker 2003, Lewis & Coffroth 2004). The degree of fixed or adaptable symbiosis establishment may be a trait of the specific coral species (Putnam et al. 2012). Complexity in symbiont specificity is further increased in cases where symbiosis is established anew each generation, because horizontal symbiont transmission may lead to combinations of coral larvae and symbionts that can differ from those of the parental coral colony (Baird et al. 2009). As larvae are highly dispersive, it might be key for survival to select and maintain symbionts which best fulfill the larval needs in a particular environment. Consequently, the symbionts found in such larvae may not reflect the most abundant *Symbiodinium* type but rather the most suitable for the host in that particular niche (Yamashita et al. 2013), speaking for external factors to modulate host-symbiont association (Rodriguez-Lanetty et al. 2006b, Kamezaki et al. 2013, Wicks et al. 2010). An unclear influence of fixed or adaptable factors is also apparent when observing that larvae and juvenile polyps can harbor *Symbiodinium* types that differs from those of the adult colony but nonetheless later form a stable lasting symbiosis with homologous (i.e. from the parent colony) *Symbiodinium* types. This indicates that either symbiont availability or stringent selection mechanisms come into play (Abrego et al. 2009, Little et al. 2004). However, most of these studies were performed under less controlled conditions but rather in the natural environment. Other studies, under more controlled conditions, show that certain coral larvae prefer homologous over heterologous symbionts (i.e. isolated from neighbor coral species) arguing in the line of stringent selection (Weis et al. 2001, Rodriguez-Lanetty et al. 2006b).

Taken together, although different studies aim to specify whether symbiont selection is strict or flexible, no conclusion has been reached yet. Controlled

experiments under laboratory conditions are needed to systematically dissect the mechanisms underlying the selection and maintenance of certain types of symbionts.

7. Cellular mechanisms underlying the establishment of a stable host-symbiont symbiosis

The selection of specific symbionts by a host is defined by a set of events that lead to a stable symbiotic interaction, known to follow a “winnowing” process (Nyholm & McFall-Ngai 2004). The cellular mechanisms involved in symbiosis establishment can be divided into the following steps: (1) host-symbiont initial contact; (2) symbiont phagocytosis by endodermal cells; (3) intracellular symbiont maintenance; (4) symbiont proliferation within the host tissue and exchange of nutrients (Figure 3). Each step, individually or in combination with others, influences symbiosis establishment and the overall stability of the host-symbiont interaction (Davy et al. 2012).

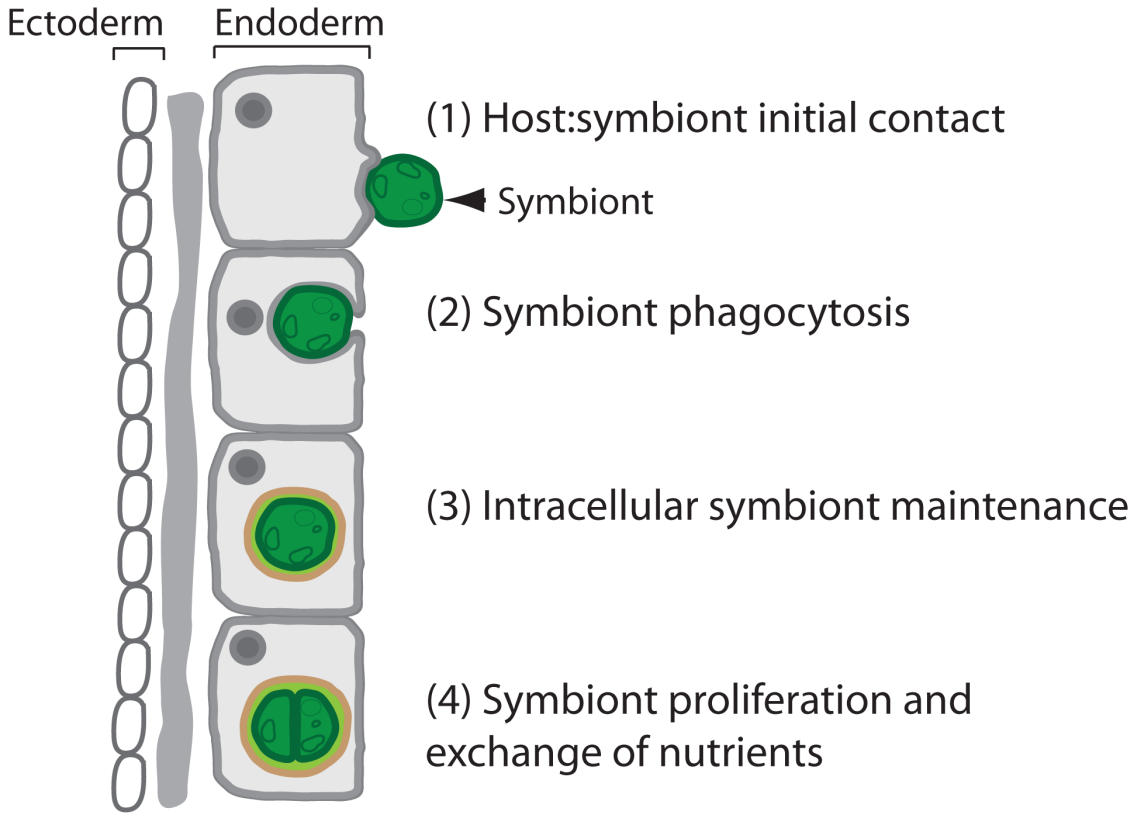

Figure 3 Phases of symbiosis establishment in cnidarian-algal symbiosis. (1) Initial host and symbiont contact; (2) symbiont engulfment/phagocytosis by host endodermal cell; (3) intracellular symbiont sorting/maintenance and formation of the symbiont-containing vacuole with an outer

membrane of host origin and inner membranes of symbiont origin; (4) symbiont proliferation and exchange of nutrients between the symbiotic partners (adapted from Davy et al. 2012).

(1) host-symbiont initial contact: after mouth development, mucus production and/or chemical attractants may be important to facilitate initial host-symbiont contact (Schwarz et al. 1999, Harii et al. 2009, Hagedorn et al. 2015). Next, a specific recognition mechanism is believed to precede symbiont phagocytosis by the host (Pool 1979, McNeil 1981). This recognition may involve receptors such as lectins at the host cell surface that recognize carbohydrates on the *Symbiodinium* cell surface (Bay et al. 2011, Koyke et al. 2004, Kuniya et al. 2015). However, no specific molecular recognition mechanism involved in symbiont recognition has been identified to date.

(2) Symbiont phagocytosis (entry into the host cell): Phagocytosis, the uptake of particles > 0.5 µm (reviewed in Flannagan et al. 2012), is generally accepted as the mode of symbiont entry into host cells (Davy et al. 2012). Phagocytosis requires active cytoskeleton rearrangement and formation and scission of vesicles out of the host plasma membrane. Cells use phagocytosis mainly for food particle incorporation and microbial elimination (reviewed in Flannagan et al. 2012). It is unclear if phagocytosis differs in case of symbiont uptake and symbiosis establishment (Davy et al. 2012).

(3) intracellular symbiont maintenance: The membrane-bound compartment formed upon particle entry into the host cell is known as a phagosome. In case the engulfed particle is a symbiont, the phagosome is called a “symbiosome” in which the symbiont is maintained in a functional and dynamic interaction with the host (Wakefield et al. 2000). Its outer membrane is of host- and its inner layers of several membranes of symbiont origin (Kazandjian et al. 2008, Wakefield et al. 2000).

Once the symbiont is inside the cell, it can either be eliminated or maintained, leading to the formation of a stable symbiosome and suggesting the underlying selection processes after uptake exist (Dunn et al. 2009, Davy et al. 2012, Nyholm & McFall-Ngai 2004). The symbiosome allows the maintenance of a stable interaction between partners with exchange of material between them. Very little is yet known about the properties and proteins that constitute the symbiosome (Wakefield & Kempf 2001). The mechanisms that allow for a positive selection and

permit stable symbiosome formation thereby contributing to the establishment of symbiosis and maintenance are poorly understood. Section 7.1 is dedicated to discuss this topic in more detail.

(4) symbiont proliferation within host tissue and exchange of nutrients: little is known about symbiont division *in hospite*. One study in *Hydra viridissima* (another symbiotic cnidarian belonging to the Hydrozoa) indicated that the distribution of available resources between symbiont and host *in hospite* regulates the division rate of interacting partners (Douglas & Smith 1984, McAuley 1985a, McAuley 1985b). Other studies in corals, sea anemones and in *Hydra* indicated a correlation between light intensity and division rate shown by a division peak of symbionts *in hospite* at dawn (Fitt & Trench 1983a, Yacobovitch et al. 2004). However, algal symbiosis is crucial for corals' nutrition and exchange of nutrients between the two partners has to be coordinated to allow proliferation. Thus metabolic limitations may regulate/restrict symbiont growth (Cook et al. 1994, Jackson & Yellowlees 1990).

Recently, glucose has been shown to be the most abundant photosynthate transferred to the host (Burriesci et al. 2012) while the symbionts get inorganic nutrients such as carbon, nitrogen and phosphorus in return (Trench 1971a, Trench 1971b, Trench 1974). Other compounds such as glycerol, amino acids, glycoproteins, fatty acids and lipids translocate to the host (Muscatine & Hand 1958, von Holt & von Holt 1968). Particularly, photosynthetically fixed carbon is translocated to the host where it is has a fundamental role in the host metabolism such as for growth, respiration and reproduction (Muscatine 1990). Much attention has been given to the fact that the host gets glucose and other photosynthetic products from the symbiont, but little focus has been given to the identity of other compounds released by the symbiont to the host (Davy et al. 2012). To learn more about the compounds transferred between symbiotic partners a characterization of the symbiosome membrane is crucial as it can be key to identify specific transporters and the compounds that are transferred (Davy et al. 2012).

In summary, many fundamental questions about the cellular processes underpinning coral-algae symbiosis are still unanswered. A better understanding of coral-algal symbiosis at the cellular level may reveal the mechanisms of

symbiont selection as well as generally conserved mechanisms underlying symbiosis between two distinct species.

7.1. Algal symbiont maintenance mechanisms

Algae are taken up into host endodermal cells by phagocytosis, a pathway generally utilized by cells for food particle digestion and microbial elimination (Davy et al. 2012, Marlow & Martindale 2007, reviewed in Flannagan et al. 2012). After particle uptake, the particle-containing phagosome matures into the digestive phagolysosome characterized by low pH and high protease activity – lysosomal hydrolases from the family of the Cathepsins - to ultimately digest the phagocytosed particle (reviewed in Flannagan et al. 2012).

Phagosome maturation is orchestrated by Rab GTPases, which coordinate the transition from early to late phagosome and are important markers of the different stages of phagosome maturation. More specifically, Rab5 is associated with the early phagosome and is required for the transformation into the mature phagosome. In contrast, Rab7 promotes fusion with lysosomes and together with the lysosomal-associated membrane glycoproteins 1 and 2 (Lamp-1 and Lamp-2) it associates with late phagosomes, lysosomes and phagolysosomes (Fairn & Grinstein 2012).

Interestingly, some pathogens have evolved effective strategies to interfere with phagolysosomal destruction. The animal pathogens *Trypanosoma cruzi* and *Listeria monocytogenes* invade the host cell but escape the phagosome through a pore they make (Flannagan et al. 2009). But, for example, *Mycobacterium*, *Leishmania donovani*, *Salmonella* and *Legionella* pathogens interfere with the normal process of phagosome maturation, re-directing it in a way that maturation is compromised and therefore phagosome-lysosomes fusion is inhibited (reviewed in Schwarz 2008, Flannagan et al. 2009). A way to achieve this is to interfere with Rab-proteins, especially Rab5 and Rab7. This strategy is termed “arrest of phagosome maturation”. Other microbes such as *Coxiella burnetti* and *Leishmania mexicana* simply adapt to the acidic environment of the lysosome being able to

persist and multiply in the phagolysosome (Davy et al. 2012, Flannagan et al. 2009).

Previous studies in various cnidarian symbioses (e.g., *Hydra viridissima-Chlorella*, *Paramecium bursaria-Chlorella* and *Cassiopea xamachana-Symbiodinium*) suggest that symbionts may, similar to pathogens, inhibit phagosome-lysosome fusion. This is based on the fact that electron microscopy shows that phagosome-containing algae, in contrast to phagosomes with dead algae or food particles, do not co-localize with ferritin-labelled lysosomes (Karakashian & Karakashian 1973, Karakashian & Rudzinska 1981, Hohman et al. 1982, Fitt & Trench 1983b, O'Brien et al. 1982). Supporting this idea, it was shown that in symbiotic cells, the protein Rab5 is distributed around symbiotic algae whereas Rab7 is not. Instead, Rab7 is present around phagocytosed heat-killed algae and inert beads (Chen et al. 2003, Chen et al. 2004). However, more recently, Barott and colleagues measured the symbiosome luminal pH and found that it had a highly acidic lumen (pH ~ 4). Moreover they found that low pH, and therefore acidity, increased algae's photosynthetic activity *in hospite*, which is at least in part due to the presence of vATPases in the symbiosome membrane (Barott et al. 2015).

Thus, to date it is still unclear how phagocytosed symbionts avoid digestion by the host cell. It is unclear whether symbionts are capable to withstand the acidic and proteolytic conditions in the phagolysosome or whether symbionts actively manipulate phagolysosome maturation to escape proteolysis. Revealing the molecular composition of the symbiosome may help to test whether it resembles an arrested or a mature phagolysosome and thus to distinguish between the two possibilities.

8. The sea anemone *Aiptasia* - a model system approach to dissect coral-algae symbiosis at the molecular level

Many questions related to the cellular and molecular mechanisms underlying coral-algae symbiosis including symbiont selection and maintenance remain unexplored mostly because corals are not suitable as laboratory model

organisms. Corals have a calcareous skeleton that complicates the use of modern cellular and molecular biology techniques such as microscopy or biochemical extraction. Corals are protected, grow slowly and are difficult to maintain under laboratory conditions. Moreover, corals reproduce sexually only once a year severely limiting access to coral larvae for experimentation under controlled conditions.

To overcome these limitations, the small sea anemone *Aiptasia* is being developed as a tractable model system for the study of coral-algae symbiosis (Weis et al. 2008). *Aiptasia* establishes symbiosis with the same types of *Symbiodinium* as corals, with the advantage of being possible to maintain in symbiont-free (aposymbiotic) state if provided with food to allow survival (Kinzie & Chee 1979, Hambleton et al. 2014, Weis et al. 2008, Matthews et al. 2016).

Aiptasia has been used since decades for the study of symbiosis (Kinzie & Chee 1979), but only recently resources and techniques for molecular analysis are becoming available. Defined clonal lines of *Aiptasia* are available as well as clonal and axenic cultures of major *Symbiodinium* clades to allow controlled experiments (Sunagawa et al. 2009, Xiang et al. 2013, Thornhill et al. 2013). The *Aiptasia* genome sequence was published during the course of this thesis (Baumgarten et al. 2015) and the genome of the coral *Acropora digitifera* (Shinzato et al. 2011) is available for comparative studies. Other important resources including *Aiptasia* transcriptomes comparing symbiotic and non-symbiotic anemones as well as a first proteomic analysis became available (Lehnert et al. 2012, Lehnert et al. 2014, Oakley et al. 2016). Likewise, genomic and transcriptomic resources for *Symbiodinium* were reported, which paved the way for studying coral-algae symbiosis at the cellular and molecular level (Shoguchi et al. 2013, Lin et al. 2015, Bayer et al. 2012, Xiang et al. 2015). Like corals, *Aiptasia* produces natural symbiont-free larvae and establishes symbiosis anew each generation (Hambleton et al. 2014) (Figure 4). Moreover, *Aiptasia* larvae distinguish between compatible and incompatible symbionts and specificity is maintained in adult anemones indicating conserved molecular mechanisms (Hambleton et al. 2014). Importantly, *Aiptasia* produces larvae under laboratory conditions allowing regular access to larvae for experimentation and repetition/optimization of experiments (Hambleton

et al. 2014). Together, this makes *Aiptasia* larvae ideally suited to analyze fundamental aspects of symbiosis establishment such as symbiont selection and symbiosome formation.

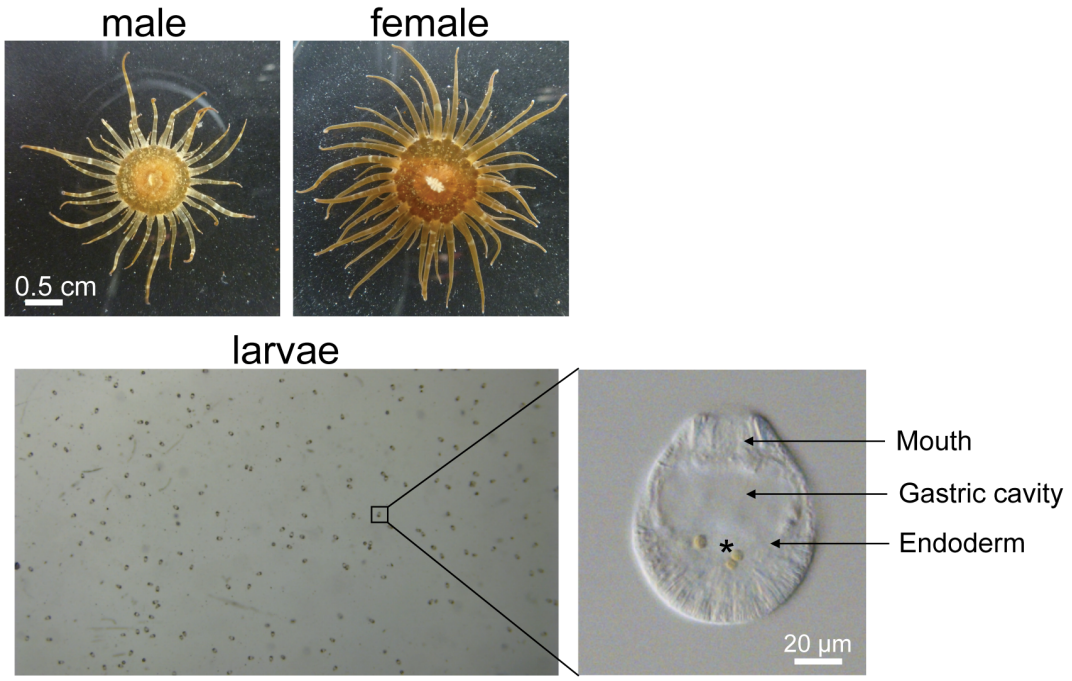

Figure 4 The sea anemone *Aiptasia* and its larva. Male and female anemone lines are grown and maintained under laboratory conditions for larvae production. *Aiptasia* larvae, like corals, are naturally symbiont-free and take up *Symbiodinium* from the environment during larval development through the mouth into the gastric cavity for subsequent incorporation into endodermal cells. Asterisk (*) indicates symbionts.

Chapter 2 - Aims

Many fundamental questions about the mechanisms underlying intracellular coral-algae symbiosis are still unanswered. Important questions include how symbiont selection and thus symbiosis specificity is achieved. It is also unclear how symbionts survive in the "symbiosome", a phagolysosomal-like organelle, inside the host cells without being digested. The aim of this thesis is to develop and use *Aiptasia* larva as a model for symbiosis establishment in order to start dissecting symbiosis specificity and symbiosome formation at the molecular level.

In this cumulative thesis, I contributed to three peer-reviewed publications that are foundational to develop the model system. In the first publication, the aim was to develop a robust *Aiptasia* spawning induction protocol under controlled laboratory conditions to generate larvae for experimentation. In the second manuscript, the aim was to provide a detailed overview of *Aiptasia* embryonic and larval development, and to develop a quantitative symbiosis establishment assay including microscopic tools to analyze symbiosis at the cellular level. In the third publication, the aim was to generate a comparative dataset for selection of distinct symbiont types between *Aiptasia* and two reef-building coral species, *Acropora digitifera* and *Acropora tenuis*, to further validate *Aiptasia* as a model for corals as well as to use RNA-Seq to identify a first set of candidate genes involved in symbiosis establishment.

Finally, I aimed to build up on the achievements in developing *Aiptasia* as a model system for cell biological approaches and establish a platform for characterization of the lysosomal distribution of *Aiptasia* larva and the symbiosome of the endodermal cells. This is a first step to better understand the properties of the symbiosome as a phagolysosomal-like organelle, and thereafter understand how symbionts avoid destruction to stably integrate into host cells.

My specific contributions to each publication precede each individual result section in chapter 3.

Chapter 3 - Results

Preface

Chapter 3 consists of three peer-reviewed publications followed by a section of unpublished data. Preceding each publication is a brief description of my contributions and main highlights.

Publication 1: “Induction of gametogenesis in the cnidarian endosymbiosis model *Aiptasia* sp.”

Highlights

In this publication, we reveal a robust protocol for induction of sexual reproduction in *Aiptasia*, with frequent collection of larvae in a predictable and reliable way. In short, the highlights are:

- Mimicking the lunar cycle artificially with blue-light is a necessary cue to promote gamete production and synchronous gamete release;
- Increased efficiency of larvae production is achieved when animals are fed with *Artemia nauplii* shrimp 5 days a week for more than 2 months and, during artificial lunar cycle, the temperature shifted from 27°C to 29°C;
- Peak larvae production is between day 13 and day 17 of the artificial lunar cycle;
- *Aiptasia* female clonal line F003 has higher rates of sexual reproduction when compared to the female clonal line H2, which shows preference for asexual reproduction instead.

Author contribution

I contributed to this manuscript by performing *Symbiodinium* typing experiments from the *Aiptasia* line F003 (Figure 2b), and by collecting partial of the spawning data presented in Supplementary Table S1.

This is an “Open access” publication.

SCIENTIFIC REPORTS

OPEN

Induction of Gametogenesis in the Cnidarian Endosymbiosis Model *Aiptasia* sp.

Received: 30 June 2015
Accepted: 01 October 2015
Published: 26 October 2015

Désirée Grawunder[1,*], Elizabeth A. Hambleton[1,*], Madeline Bucher[1], Iliona Wolfowicz[1,2], Natascha Bechtoldt[1] & Annika Guse[1]

Endosymbiosis is widespread among cnidarians and is of high ecological relevance. The tropical sea anemone *Aiptasia* sp. is a laboratory model system for endosymbiosis between reef-building corals and photosynthetic dinoflagellate algae of the genus *Symbiodinium*. Here we identify the key environmental cues to induce reproducible spawning in *Aiptasia* under controlled laboratory conditions. We find that simulating a lunar cycle with blue-wavelength light is necessary to promote abundant gamete production and synchronous release in well-fed animals. Sexual reproduction rates are genetically determined and differ among clonal lines under similar conditions. We also find the inverse difference in rates of asexual reproduction. This study provides the requisite basis for further development of the *Aiptasia* model system, allowing analysis of basic cellular and molecular mechanisms in the laboratory as well as investigations of broad questions of ecological and evolutionary relevance.

Cnidarians exhibit enormous plasticity in their morphologies and life cycles, and have emerged as key models in a broad range of research fields from evolution to ecology. As the sister group to the Bilateria (Fig. 1a), cnidarians are important model systems for studying development[1,2], pattern formation[3], regeneration[4] and stem cell biology[5,6] (Fig. 1a). The cnidarians' evolutionary success over 500 million years has been proposed to be due in part to their ability to form symbioses with prokaryotic and/or eukaryotic microorganisms[7]. Major symbiotic partners include complex communities of viruses, archaea, bacteria (including cyanobacteria), and eukaryotic algae[8,9]. More broadly, such symbioses with photosynthetic microbes are also found in mollusks, sponges, acoel flatworms, and vertebrates (salamander) and in all, the translocation of photosynthetically fixed carbon from the symbiont to the host represents a significant energy source[10,11].

The most common eukaryotic endosymbiont among the cnidarians is the dinoflagellate *Symbiodinium* spp.; associations with *Symbiodinium* are found in many species including the majority of hexacorallia (e.g. reef-building corals, sea anemones), octocorallia (e.g. gorgonians, soft corals, sea pens), hydrozoa (e.g. fire corals) and scyphozoa (e.g. jellyfish)[12] (Fig. 1a). Genus *Symbiodinium* is diverse, containing hundreds of strains worldwide that have been categorized into clades based on ribosomal DNA markers[13]; species assignments and functional characterizations of strains are an active area of research[14]. The unicellular *Symbiodinium* reside intracellularly in cnidarian endodermal tissues and transfer photosynthates to the host. Thus, this widespread phenomenon is likely a key factor in the extensive adaptive radiation of cnidarians in diverse aquatic niches.

The most economically and ecologically critical cnidarian-*Symbiodinium* symbiosis is that of reef-building corals, which rely so heavily on symbiont-produced nutrition that the relationship is obligatory for the hosts to persist[15,16]. As such, the breakdown of this symbiosis, termed "coral bleaching", has become a major threat to coral reefs worldwide[17]. Despite this importance, much remains unknown about the cellular and molecular basis of the coral-*Symbiodinium* symbiosis, including its establishment,

[1]Centre for Organismal Studies (COS), Heidelberg University, Heidelberg 69120, Germany. [2]University of Porto, Porto 4200-465, Portugal. *These authors contributed equally to this work. Correspondence and requests for materials should be addressed to A.G. (email: annika.guse@cos.uni-heidelberg.de)

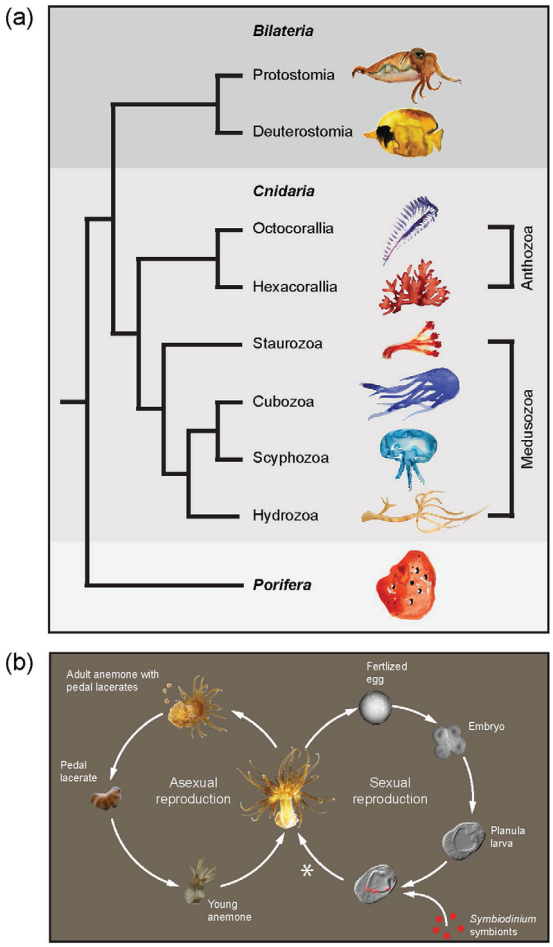

Figure 1. Symbiosis throughout the cnidarians and the anthozoan life cycle. (**a**) Phylogenetic tree of the major metazoan clades, with phyla shown in bold. Cnidarians represent a sister group to the bilaterians and are at the base of metazoan evolution. Symbiosis with dinoflagellates and green algae occur in species throughout the classes Medusozoa and Anthozoa, the latter of which contains *Aiptasia* sp. Illustrations were drawn by Stephanie Guse and are used with permission. (**b**) Overview of *Aiptasia* life cycle showing dual reproductive modes. *metamorphosis and settlement in the laboratory have not yet been reported, and as such remains an active experimental area.

maintenance, and breakdown in response to stress[18]. The majority of corals produce symbiont-free planula larvae that must take up symbionts from the environment each generation[19]. However, most reef-building corals spawn only once per year[20], greatly restricting the experimental availability of larvae and thereby severely limiting the systematic study of endosymbiosis establishment.

To address this limitation, a practicable symbiotic laboratory model has been developed with the small sea anemone *Aiptasia* sp. Although *Aiptasia* is not suited to every application relevant to coral biology (e.g. calcification), it holds many advantages including its symbiotic relationship with the same types of *Symbiodinium* strains as corals[21–23]. Most importantly, the process of endosymbiosis establishment is similar to that of many reef-building corals: *Aiptasia* planula larvae are initially non-symbiotic and establish endosymbiosis anew each generation[23] (Fig. 1b). Both reef-building corals and *Aiptasia* live primarily as a sessile polyp stage that switches between asexual reproduction and sexual production of motile planula larvae (Fig. 1b). Based on molecular analysis, *Aiptasia* sp. is regarded as a single panglobal species with two distinct genetic networks: one on the United States South Atlantic coast and the other consisting of all other *Aiptasia* sp. sampled worldwide[24]. Clonal anemone lines can be generated through asexual reproduction via pedal laceration[25] (Fig. 1b), and the majority of *Aiptasia* resources have been developed from clonal line CC7, including transcriptomes[26,27] and the genome[28]. Transcriptomic and genomic resources for many *Symbiodinium* strains are likewise available[29–31].

Despite these advantages, a critical aspect remains underdeveloped in *Aiptasia*: consistent induction of sexual reproduction in the laboratory, a prerequisite to investigations of symbiosis establishment and development of state-of-the-art functional tools such as morpholinos and transgenesis[32–34]. *Aiptasia* is demonstrably capable of year-round gametogenesis[35] and spawning in laboratory conditions[23,36], but laboratory-induced spawning has been inefficient and unpredictable and currently no publically available

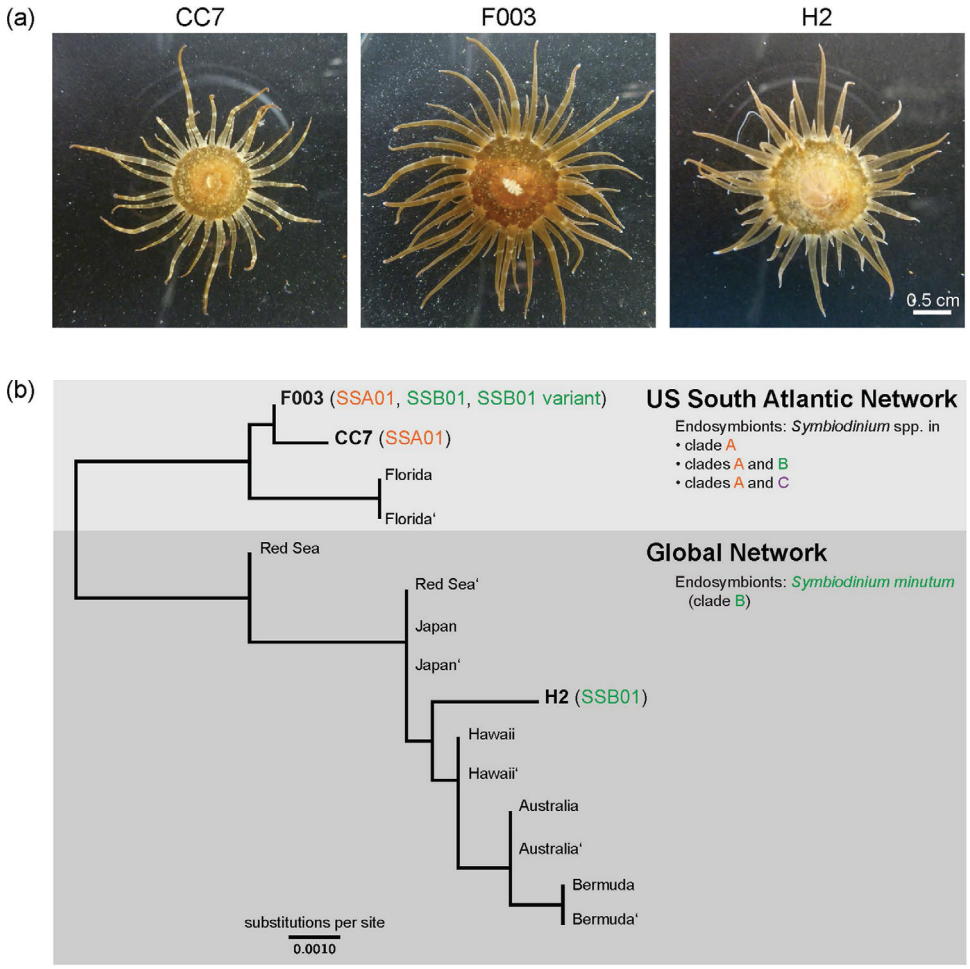

Figure 2. Characterization of *Aiptasia* clonal lines CC7 (male), F003 (female), and H2 (female). (**a**) Clonal lines appear morphologically similar, with minor variation in coloration and body size. (**b**) Maximum likelihood tree of ~2 kb concatenated *SCAR* genotyping markers[24] showing the relationship of the three clonal lines to twelve field-sampled *Aiptasia* sp. individuals[24] grouped into two genetic networks. Clonal lines are indicated by name; field-sampled individuals are named by their sampling location, with the second animal from the same location designed by'. Shown also are the endogenous *Symbiodinium* spp. (clades A-C and strain names) hosted by *Aiptasia* in the given genetic networks[24] and in the three laboratory clonal lines[22,26]; F003 symbiont characterization from this study.

protocols exist to overcome this limitation. Laboratory-induced spawning in the cnidarian *Nematostella* has been achieved through manipulation of food, temperature, and light alone or in combination[37,38]. In the wild, coral spawning is correlated with the lunar cycle and blue light appears to play a major role in synchronized spawning[39–42]. Similarly, oogenesis in *Aiptasia* is increased by feeding[43] and peaks in relation to the lunar cycle[35]. Thus, we hypothesized that ample feeding and blue-light cues simulating moonlight may efficiently stimulate laboratory spawning in *Aiptasia*.

To test this hypothesis, we used three *Aiptasia* clonal lines used in laboratories worldwide. We first further characterized these clonal lines—CC7 (male) and F003 and H2 (both female)—and used molecular phylogeny to place them into a biogeographical context. Next, we systematically tested different conditions to determine major cues for coordinated and copious gametogenesis and spawning. We found that blue-light cues (presumably mimicking a lunar cycle) together with slight temperature increases produce synchronous and efficient spawning in well-fed CC7 and F003 couples and, to a lesser extent, in CC7 and H2 couples. Quantitative differences of spawning efficiencies between female lines F003 and H2 were inversely correlated to their asexual reproduction rates.

Results

Characterization of *Aiptasia* clonal lines. The three clonal lines of *Aiptasia* CC7, F003, and H2 we routinely maintain in the laboratory (see *Aiptasia* culture conditions in Methods) appear morphologically similar (Fig. 2a). However, their genetic relationship to each other and to other *Aiptasia* populations was unclear. We therefore determined the relationship of our lines to wild *Aiptasia* populations

worldwide by sequencing the four independent "*SCAR*" ("sequence characterized amplified region") genotyping markers[24] of two individuals from each of the three clonal *Aiptasia* lines. Within each of the lines, both individuals sampled yielded identical sequences for each *SCAR* marker, demonstrating the continued clonality of the lines. Each clonal line produced a haplotype distinct from the others. In CC7 and F003, two alleles were found in the following three loci and both animals carried the alleles: *SCAR3*, *SCAR4*, and *SCAR5* (CC7 only). In those cases, the alleles were collapsed together to produce a consensus sequence containing the appropriate base ambiguity. The Maximum Likelihood tree in Fig. 2b shows the relationship of these three clonal lines to twelve globally field-sampled *Aiptasia* representing eight distinct haplotypes[24]. As expected, lines CC7 and F003 (founders collected from US South Atlantic coast) and line H2 (founder collected from Hawaii) all cluster closest with individuals collected from the same respective geographic region by Thornhill and colleagues[24] (Fig. 2b). Thus, these laboratory clonal lines represent members of both identified *Aiptasia* genetic networks found worldwide: US South Atlantic network (CC7, F003) and global network (H2).

Endogenous *Symbiodinium* hosted by *Aiptasia* clonal lines. Thornhill and colleagues[24] found that the two worldwide *Aiptasia* genetic networks differ in their symbiont composition: the global *Aiptasia* network harbors only the clade B species *Symbiodinium minutum*, while members of the US South Atlantic network harbor clade A *Symbiodinium* strains either solely or, to a lesser extent, in combination with either variants of clade B *S. minutum* or (rarely) clade C strains (Fig. 2b). Accordingly, clonal line H2 (global network) harbors only the *S. minutum* strain SSB01[22], while clonal line CC7 (US South Atlantic network) hosts a single clade A strain[26] designated SSA01 (Fig. 2b). To identify the as-yet-unknown endogenous symbiont(s) of *Aiptasia* clonal line F003 (US South Atlantic network), we sequenced the chloroplast ribosomal 23S subunit (*cp23S*) of three independent F003 animals as previously described[22]. Within each individual, we consistently found three distinct *cp23S* sequences in relatively constant proportions: ~57% of sequences were a single variant of *S. minutum* (i.e. identical to strain SSB01 [GenBank #JX221048.1] except for a SNP at SSB01 nt250 and a deletion in SSB01 nt363–nt498); ~35% were identical to SSA01 (GenBank #KT186239); ~8% were identical to *S. minutum* strain SSB01. The first two sequences are consistent with the typical patterns of the US South Atlantic *Aiptasia* network[24]. The third sequence, *S. minutum* strain SSB01, was not detected during a similar but cursory analysis >1.5 years ago; its current presence may be due to either its previously undetected natural occurrence or to an accidental introduction during extended culture in close proximity to SSB01. Taken together, F003 and CC7 are therefore each representatives of different symbiont patterns typically observed in the US South Atlantic *Aiptasia* network.

Spawning induction for *Aiptasia* clonal lines CC7, Foo3, and H2 under laboratory conditions. To test whether the simulation of a lunar cycle can trigger spawning in *Aiptasia*, we subjected spawning couples to a blue-intensive moon cue for five nights per 29-day cycle (Fig. 3a–c and Supplementary Fig. S1 online). Beforehand, animals were fed with *Artemia* nauplii five times per week for over two months. To avoid competition for food and other resources, animals were cultured in low densities and pedal lacerates were removed on a regular basis (we observed that such treatment markedly increases animal size [Supplementary Fig. S2 online]). We monitored in total 13 couples of [F003xCC7] and 37 couples of [H2xCC7] for two subsequent cycles (Fig. 3a–c). For crosses with F003, spawning was tightly clustered between Day 13 and Day 20 of the 29-day artificial lunar cycle, with peak larvae production on Days 13–17 (Fig. 3b). Spawning in crosses with H2 was likewise synchronous, with a peak of larvae production also around Day 13–18 (Fig. 3c). Overall, couples with F003 were more synchronous and spawned more often than those with H2 (Fig. 3b,c) (see below for more on observed line-specific differences). In both lines, however, the variability of larvae occurrences between couples was relatively high, which may be due to differences in culture conditions prior to spawning induction (Supplementary Fig. S1 online). We monitored couples for only two spawning cycles because spawning frequencies decreased afterwards, somewhat depending on the duration in the pre-induction high-feeding conditions (data not shown).

Because we sought to modify our spawning protocol to maximize spawning efficiency and predictability, during these experiments we intermittently tested other conditions previously known to stimulate spawning in other cnidarians. We compared spawning when animals were fed *Artemia* nauplii twice weekly versus five times per week; we observed that increased feeding improved spawning, especially for F003-containing couples (Supplementary Fig. S3 online). We tested whether a very low amount of blue light during the pre-spawning-induction period (see Methods) would enhance spawning efficiency during the lunar cycle inductions, yet saw no discernable effect of these treatments (Supplementary Fig. S1 online). Because warming water temperatures appear correlated with gametogenesis and spawning in anthozoans[36,38,39,44], we simultaneously tested the effects of temperature shifts during spawning induction. We saw no obvious trend, but interpretation was difficult because the animals in the experiments were subjected to different conditions prior to spawning induction (Supplementary Fig. S1 online). We therefore sought to parse which cues were key to promote efficient and synchronous spawning.

Blue light is the key cue to induce efficient and synchronous spawning to produce larvae. To determine the distinct effects of temperature and simulated moon cue to effectively induce spawning,

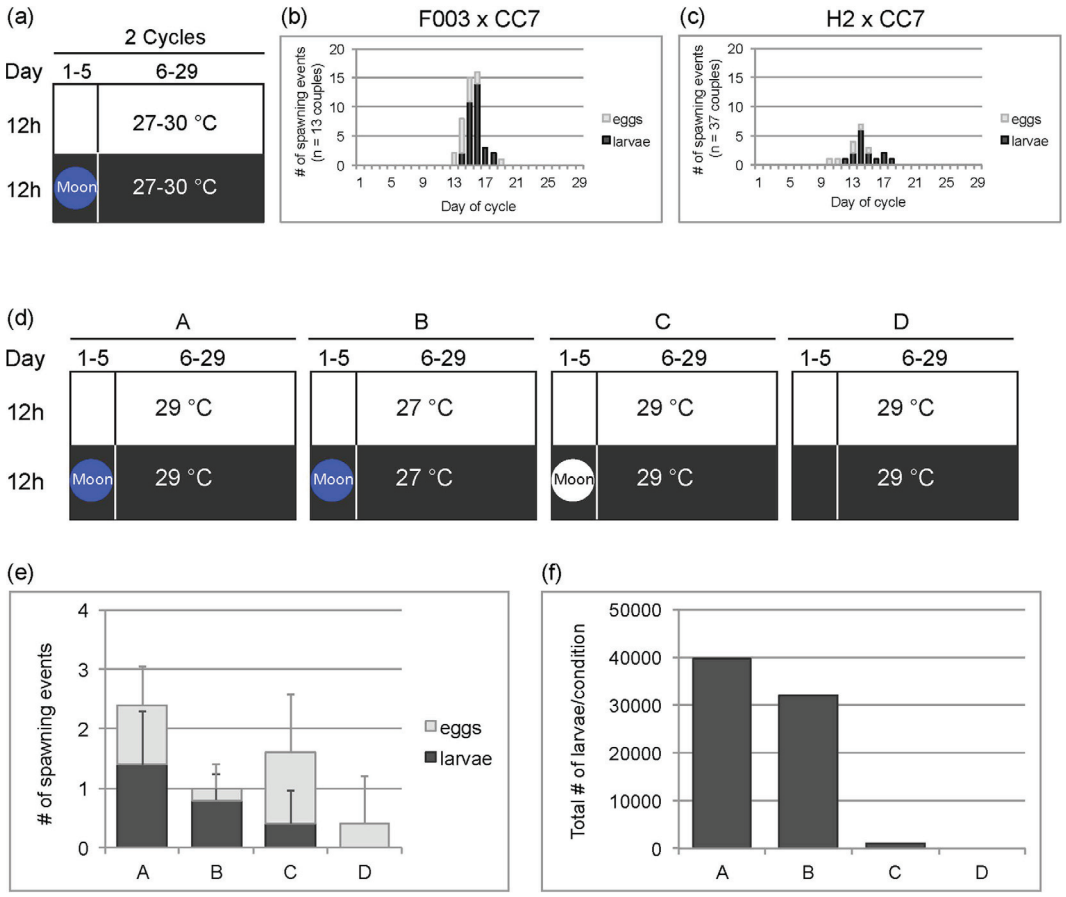

Figure 3. Induction of spawning in *Aiptasia*. (**a**) Schematic of initial spawning induction conditions during two consecutive 29-day artificial lunar cycles. Temperature and moon cue indicated; color of the circle refers to color of the simulated moon cue (see text). (**b**,**c**) Spawning synchronicity and efficiency in [F003 x CC7] couples (**b**) and [H2 x CC7] couples (**c**) under the induction conditions in (**a**).(**d**) Schematics of various spawning induction conditions A-D for a direct comparison of spawning cues in [F003xCC7] couples. (**e**) Number of spawning events by five couples in each of the four induction conditions in (**d**) over one 29-day artificial lunar cycle. Error bars are standard deviations. (**f**) Quantification of total larvae per condition produced during the larvae spawning events shown in (**e**).

we conducted a side-by-side comparison of different spawning cues using only couples of [F003xCC7] originating from identical pre-induction culture conditions. Couples were grown at 26 °C and fed well for seven months prior to exposure to the following conditions: (A) blue-light simulated moon at 29 °C; (B) blue-light simulated moon at 27 °C; (C) white-light simulated moon at 29 °C; (D) no simulated moon (Fig. 3d). Blue light appeared to be the most important cue, as these conditions (A and B) produced efficient and synchronized spawning of larvae (Fig. 3e) as well as copious production of tens of thousands of larvae (Fig. 3f). The temperature increase from growth conditions to 29 °C (Conditions A, C, and D) appeared to be beneficial to egg release (Fig. 3e), although this temperature shift alone or with a white-light cue results in inefficient larvae production, with either no or very low numbers of larvae generated (Fig. 3f). White light, which in this case is composed of ~20% blue wavelengths (see Methods), does stimulate some spawning, but mostly eggs (Condition C, Fig. 3e) and over a wider range of days in the cycle (Days 16–21, Supplementary Fig. S4 online). This poor synchronization and low output resulted in very little larvae, especially when compared to condition A in which the only difference is the blue spectrum of the light (Fig. 3f). All data for these experiments are found in Supplementary Fig. S4 online.

Quantification of line-specific differences in larvae production. To confirm and quantify the differences we observed in spawning efficiencies between females of clonal lines F003 and H2 (Fig. 3b,c), we performed additional experiments under the best spawning induction parameters from above. We chose F003, H2, and CC7 animals of similar body size and cultured them in low-density cultures that were fed five times a week for five months, after which five couples of [F003xCC7] and five couples of [H2xCC7] were subjected to the blue-light lunar cycle cue (Condition A, Fig. 3d) and larval output was quantified. Consistent with our observations in the earlier experiments (Fig. 3b,c), we again found that

(a)

Lines	Couple #	Cycle 1						Cycle 2						Spawnings/Couple/Cycle		
		Day 13	Day 14	Day 15	Day 16	Day 17	Day 18	Day 13	Day 14	Day 15	Day 16	Day 17	Day 18	Eggs	Larvae	Total
F003xCC7	1			E	480000					2800	16000					
	2		E	20000	54000				2000	22000						
	3		E	300	140000				500	35000	2800			0,4	1,8	2,2
	4			4400	26000					13000						
	5		E	8200	23000					13000						
H2xCC7	1					E			E							
	2				2000					E	E					
	3	E	E	E	E						E			1,2	0,2	1,4
	4										E					
	5	E	E				50									

(b)

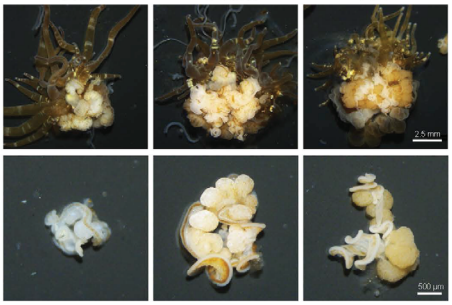

(c)

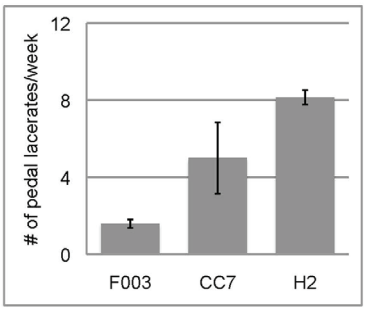

Figure 4. Line-specific differences in reproduction between *Aiptasia* female clonal lines. (**a**) Quantification of larvae and egg production by [F003 x CC7] and [H2 x CC7] couples in two cycles of spawning induction in condition A from Fig. 3d. E denotes occurrence of eggs; numbers indicate approximate quantification of larvae. (**b**) Cross-sections of longitudinally dissected anemones from the three clonal lines shows many bulbous gonads within mesentery tissues. (**c**) Weekly quantification of asexual reproduction via pedal laceration in the three clonal lines over five weeks. n = five individuals per clonal line; error bars are standard deviations.

couples with F003 spawned much more efficiently than those with H2: crosses with F003 produced larvae on average 1.8 times per couple per cycle, whereas H2 produced larvae only an average of 0.2 times per couple per cycle (Fig. 4a). Reproductive output for F003 was also far higher, typically with over 10,000 larvae per event, than for H2-containing couples that only spawned small numbers of larvae or, in most cases, eggs (Fig. 4a). Nevertheless, spawning synchrony was high in crosses with both female lines, falling between Days 13 and 18 (Fig. 4a).

Line-specific differences in gonad development. In *Aiptasia* sp. gonad development occurs within the mesentery tissue in the interior body column and is directly dependent upon food uptake[43]. We dissected well-fed CC7, F003, and H2 animals and indeed found many gonads within mesentery tissue (Fig. 4b, upper row). CC7 male gonads were typically smaller and lighter in comparison to the bigger, darker gonads from females in lines F003 and H2 (Fig. 4b, lower row). However, qualitative visual assessments consistently showed that F003 animals contained higher ratios of distinct gonads to non-gonad mesentery than H2 animals (Fig. 4b). In both F003 and H2 gonads, we observed immature oocytes with prominent germinal vesicles, in contrast to released eggs during spawning (Supplementary Fig. S5 online). Sperm isolated from CC7 gonads were morphologically similar to those naturally released during spawning (Supplementary Fig. S5 online).

Line-specific differences in asexual reproduction. A previous study of a wild clonal *Aiptasia* sp. population found no apparent tradeoff between reproductive modes, yet it was postulated that genotypes may allocate resources between reproduction modes differently, perhaps as an adaptation to the local environment[43]. To assess whether such tradeoffs or differences occur in various genotypes of *Aiptasia*, particularly in light of the observed differences in sexual reproduction (see above), we monitored the asexual reproduction rates of clonal lines CC7, F003, and H2. Asexual reproduction is achieved via pedal laceration[25], wherein symbiont-containing lacerates bud off the pedal disc and migrate away from the parental animal over the course of several days, after which they develop tentacles (Fig. 1b). We quantified the number of pedal lacerates (pl) produced per animal per week and found that under standard growth conditions, H2 produces significantly more pedal lacerates (8 pl/week) than F003 (1.7 pl/week) (Fig. 4c). Male clonal line CC7 produces on average 5 pl/week (Fig. 4c). Thus, the rates of asexual reproduction differ greatly between genotypes with no clear correlation to the sex of the clonal line; within females, H2 asexually reproduces faster than F003 in these conditions.

Discussion

Here we have developed a robust protocol to induce spawning in three clonal lines of the model symbiotic cnidarian *Aiptasia*, thereby opening new possibilities in analysis of symbiosis establishment, early

development, and other key processes. Similar to the model cnidarian *Nematostella*, we find that extensive feeding of *Aiptasia* over multiple months in low-density culture is an important prerequisite for subsequent efficient spawning, especially for females. However, in resemblance to reef-building corals rather than to *Nematostella*, we have identified the key trigger to induce the synchronous release of gametes in well-fed *Aiptasia* animals to be the simulation of full moon by blue light during five nights within an artificial lunar monthly cycle. Interestingly, the wavelength of the applied light is consequential: LEDs exclusively emitting light between 400–460 nm effectively stimulate the release of gametes, while LEDs with white light, even when enriched in the blue wavelengths (such as actinic spectra) have minimal effect. This indicates that *Aiptasia*, similar to reef-building corals, may have specific blue-light-sensing photoreceptors (e.g. cryptochromes) that are thought to mediate synchronous mass spawning events of corals worldwide[40,41]. Indeed, we identified in the *Aiptasia* genome[28] a homolog of the *Acropora millepora* blue-light cryptochrome receptor *cry2* (data not shown) that is expressed in correlation with coral spawning[41]. Many reef-building corals release gametes synchronously after the increase in water temperature (occurring during spring) in correlation to the last full moon and sunset[39]. Accordingly, we observed that a modest temperature shift (+3 °C) is not sufficient to induce efficient spawning in *Aiptasia* alone, but in combination with the simulation of full moon appears to be beneficial. However, *Aiptasia* collected in the wild has been proposed to spawn year-round in correlation with the lunar cycle[35], suggesting no strict inherent temperature limitations, although influences of seasonal changes in spawning efficiency cannot be ruled out[36]. Taken together, our data support the idea that the blue light is the key spawning cue with minor influences of water temperature.

In studies of gonad development of *Aiptasia* populations in the wild, Chen and colleagues found that *Aiptasia* eggs appeared to be released about 8–14 days after the natural full moon[35]. In the studies herein, we observe the synchronous release of gametes on Day 13–17 within a 29-day cycle; because our simulated full-moon cues occurs on Days 1–5, this spawning corresponds to 8–12 days after the moon cue (i.e. peak of moonlight followed by increasingly darkening conditions). Thus, our studies match up remarkably well, with the timing of gamete release nearly identical between natural *Aiptasia* populations and our populations kept in the laboratory for over five years and stimulated by an artificial light cue. The persistence of this innate ability to respond to the stimuli indicates that synchronized spawning is strongly genetically encoded and shared worldwide throughout *Aiptasia* sp. including across the major global genetic networks. Moreover, we observe that *Aiptasia* gametes are released a few hours after diurnal onset of darkness (data not shown), which is likewise identical to reef-building corals that spawn a few hours after sunset, varying by species[45,46]. Taken together, the monthly timing (i.e. new moon) and diurnal timing (i.e. after sunset) ensure spawning during a period of the darkest possible conditions. This is hypothesized to not only aid in predation avoidance but also to ensure embryos pass through fragile cleavage stages prior to exposure to potentially damaging UV radiation during daylight[47].

Interestingly, we find that the two female lines F003 and H2 differ in their reproductive strategies: under standard growths conditions and extensive feeding, the H2 colony expands more efficiently by asexual pedal laceration than F003, which in turn appears to invest a major part of incoming nutrients into oocyte production. The consistency of these responses indicates that they stem from genetically encoded differences[24,48]. It has been hypothesized that distinct genotypes with different allocation ratios between asexual and sexual reproduction may be favored in different habitats[49]. Consistent with the high asexual reproduction rates in H2, Thornhill and colleagues[24] propose that efficient clonal propagation and associated vertical symbiont transmission of members of the global *Aiptasia* network primarily led to its worldwide distribution and status as an invasive species in aquaria and in the wild[35,50,51], and the low-level genetic population structure of its associated endosymbiont *S. minutum*. Such extensive distribution therefore likely occurred quickly, via anthropogenic vectoring such as ballast waters, fouling of ships, aquaculture, or the aquarium trade[24]. In contrast, its lower asexual reproduction rates apparently restrict F003 to a more local distribution, yet its enhanced sexual reproduction rates would increase the genotypic diversity of its community. Indeed, this is recapitulated in the diversity of the sequenced *SCAR* markers: we found that F003 and CC7 showed greater genotypic diversity, with two alleles at several loci, whereas H2 was monoallelic at all four loci investigated. Such genotypic diversity might lead to the observed greater flexibility with associated symbionts[24], and indeed we find that F003 hosts multiple endogenous *Symbiodinium* strains from different clades.

This study opens the door to a steady supply of *Aiptasia* larvae for a number of crucial purposes, not least of which is addressing what may be considered one of the final steps in the establishment of the *Aiptasia* model system: closing the life cycle in the laboratory via metamorphosis and settlement of planula larvae. To date this has not been reported, although metamorphosis and settlement under laboratory conditions has been established for corals[52–54], providing vital guidance on how to approach this in *Aiptasia*. The protocol provided here allows sufficient *Aiptasia* larvae to systematically test and thereby identify metamorphosis and settlement cues in the laboratory. Although larvae production allows new techniques to be developed and important biological questions to be addressed in areas like development, endosymbiosis establishment and photobiology, microscopic imaging, gene knockdown, and transformation, settlement will further this by opening other paths like classical genetics and generation of transgenic lines.

These developments will bring *Aiptasia* fully into the stable of cnidarian laboratory models, which have proven to be vital in gaining basic biological insights. Yet *Aiptasia* also represents a new type of model

system because of its additional feature of an ecologically relevant endosymbiosis. That photosynthetic symbioses appear in organisms across the tree of life makes comparative analyses of these critical relationships interesting in evolutionary and ecological contexts. The symbioses inherent in nearly all higher metazoans (including humans) have been increasingly recognized in the molecular age, and particularly in the global context of accelerating environmental change, *Aiptasia* will contribute to opening new paths in emerging fields that seek to describe the ever-more-recognized complexity of organisms in a changing world.

Methods

***Aiptasia* clonal lines.** The founder animals for male line CC7[26] and female line F003 (courtesy of the John Pringle lab) were originally collected by Carolina Biological Supply Company (#162865; Burlington, USA) from an area approximately centered on Wilmington, North Carolina, USA. The founder animal for line H2 was collected off Coconut Island, Hawaii[22].

Genotypic characterization of *Aiptasia* clonal lines. To genotypically characterize the three clonal lines CC7, F003, and H2, we used the *SCAR* markers developed by Thornhill and colleagues[24]. Genomic DNA was extracted from two representative animals of each line with the DNeasy Blood and Tissue Kit (#69504; Qiagen, Venlo, Netherlands) according to the manufacturer's protocol for animal tissue. The gDNA of each animal was then amplified with each of the four *SCAR* marker primer pairs[24]: *ApSCAR3F* and *ApSCAR3R*; *ApSCAR4F* and *ApSCAR4R*; *ApSCAR5F* and *ApSCAR5R*; *ApSCAR7F* and *ApSCAR7R2*. Amplification reactions of 50 μL contained 2 U *Taq* polymerase, 0.2 μM of each primer, 200 μM dNTPs, 20 mM Tris-HCl (pH 8.8), 10 mM $(NH_4)SO_4$, 10 mM KCl, 2 mM $MgSO_4$, 0.1% Triton®X-100, and 150 ng gDNA template. Amplification conditions were as follows: initial denaturation at 95 °C for two min; 30 cycles of denaturation at 95 °C, annealing at 58 °C for 45 s, extension at 60 °C for 1.5 min; final extension at 68 °C for 5 min. Products were purified with the Wizard SV Gel and PCR Clean-Up System (#A9281; Promega, Madison, USA), cloned, and four or more positive bacterial clones were sequenced with the M13F (−21) or M13R (−26) universal primers.

Sequences were processed in Geneious version 6.1.8[55] [http://www.geneious.com] by initially aligning to the reference sequences from Thornhill *et al.* and trimming and concatenating accordingly[24]. In cases where a given marker in an anemone line produced two alleles (see Results), the alleles were collapsed to create a consensus sequence containing the appropriate base ambiguity. The three clonal line sequences and the twelve reference sequences from Thornhill *et al.*[24] were aligned with ClustalW[56] and a maximum likelihood phylogenetic tree was generated using PhyML[57] with default parameters and the general time-reversible (GTR) nucleotide substitution model. Tree topology searches chose the best topologies of both Nearest Neighbor Interchanges (NNI) and Subtree Pruning and Regrafting (SPR) topological moves. Topology, branch length, and substitution rate were optimized, and branch support was estimated by bootstrap analysis of 100 replicates.

Identification of endogenous *Symbiodinium* in F003 clonal line. To determine which symbiont strain(s) are endogenous to the *Aiptasia* F003 line, we used the *Symbiodinium Domain V chloroplast large subunit ribosomal DNA* (*cp23S*) marker for phylogenetic analysis as previously described[22,58]. Three adult individuals were each homogenized with a MICCRA D1 homogenizer (Miccra, Müllheim, Germany) and algal genomic DNA was extracted using the DNeasy Plant Mini Kit (#69104; Qiagen, Venlo, Netherlands) following the manufacturer's instructions. The *cp23S* region was amplified from each gDNA sample with the *23S4F* and *23S7R* primers[58]. Amplification reactions of 50 μl contained Phusion polymerase, 0.1 μM of each primer, 200 μM dNTPs, 1X Phusion HF buffer (#B0518S; NEB, Ipswich, USA), and ~50–100 ng gDNA. Amplification conditions were as follows: initial denaturation at 94 °C for 5 min; 35 cycles of 94 °C for 30 s, 50 °C for 1 min, 72 °C for 1.5 min; and final extension at 72 °C for 5 min. For each amplification reaction, products (~650 bp) were purified with the Wizard SV Gel and PCR Clean-Up System, cloned, and 18 or more positive bacterial clones were sequenced with the M13F (−21) universal primer. In total, 60 high quality *cp23s* sequences (18, 21, and 21 sequences per animal) were aligned in Geneious version 7.1.7[55] [http://www.geneious.com] and compared to *cp23S* sequences from SSB01[22] (GenBank Accession #JX221048.1) and the CC7 endogenous clade A strain[26] SSA01 (GenBank Accession #KT186239), which was sequenced as described above.

***Aiptasia* culture conditions.** General anemone stocks were maintained at a density of 30–40 animals (unless stated otherwise) per tank in medium-sized food-grade translucent polycarbonate tanks (GN 1/4–100 cm height, #44 CW; Cambro, Huntington Beach, USA) filled with artificial seawater (ASW) (Coral Pro Salt; Red Sea Aquatics Ltd, Houston, USA) at 31–34 ppt salinity. Stock tanks were kept in Intellus Ultra Controller Incubators (Model I-36LL4LX; Percival, Perry, USA) at 26 °C on a diurnal 12L:12D cycle (12 h light:12 h dark) under white fluorescent bulbs with an intensity of ~20–25 μmol m^{-2} s^{-1} of photosynthetically active radiation (PAR), as measured with an Apogee PAR quantum meter (MQ-200; Apogee, Logan, USA). Animals were fed two to five times per week with freshly hatched *Artemia* nauplii. Seawater in the tanks was exchanged two to three times per week and tanks were cleaned with cotton-tip swabs as required.

Spawning induction of *Aiptasia*. To induce *Aiptasia* gamete release following a simulated full moon cue, individuals with oral disk diameter ~0.7 cm or greater were combined into couples ([H2xCC7] or

[F003xCC7]), transferred to ASW in small food-grade translucent polycarbonate tanks (GN 1/9–65 cm height, #92 CW; Cambro, Huntington Beach, CA, USA) and kept in standard cell culture incubators (Heracell 150i; Thermo Scientific, Waltham, USA) at 27 °C–30 °C (see temperatures indicated in Results). Tanks were fed *Artemia* nauplii five times per week and kept on a diurnal 12L:12D cycle at intensities of 20–30 μmol m^{-2} s^{-1} provided by white LED lights, which were comprised of two types of LEDs—those with wavelengths of 425 nm–705 nm (color temperature 15,000 Kelvin) and those with wavelength 460 nm – at a ratio of 5:1 respectively (SolarStinger SunStrip "Marine"; Econlux, Cologne, Germany). A 29-day lunar cycle was simulated by subjecting the tanks to constant blue light during the 12 h "dark" period in the first five nights of the cycle (Day 1–5). Blue LED lights were comprised of LEDs with wavelengths 400 nm, 420 nm, 440 nm, and 460 nm at a ratio of 1:1:1:1 (SolarStinger SunStrip "Deep Blue"; Econlux, Cologne, Germany) and were 10–16 μmol m^{-2} s^{-1} in intensity. The presence of gametes or planula larvae was checked by examining the tanks with a Leica S8APO stereoscope.

Isolation of larvae for quantification. Larvae were isolated from the spawning tanks by stepwise filtration: tank contents were first passed through a 70 or 100 μm cell strainer to withhold coarse particles and permit larval passage, after which larvae were concentrated by passage through a 40 μm cell strainer and then rinsed into glass beakers with filter-sterilized ASW. For approximate quantification, beakers were mixed well to evenly distribute larvae and six 10 μl drops were pipetted onto a glass slide. The average number of larvae per drop was used to extrapolate the approximate total.

Dissection of gonads and gametes from *Aiptasia*. To promote gonad growth in anemones, 20–25 small anemones per clonal line (~0.5 cm height and no apparent gonads) were taken from stock tanks and combined into a medium-sized food-grade translucent polycarbonate tank, with two tanks per line. Animals were kept at 27 °C, fed five times per week with *Artemia* nauplii, and sampled after seven months. Anemones were transferred to a standard petri dish containing ASW and dissected in half longitudinally with a scalpel; mucus, acontia, and remaining food particles were removed with forceps. Animals were transferred to new petri dishes with ASW and images were captured using a Leica S8APO binocular (top illumination) equipped with a Leica MC170 HD color camera. Individual gonads were then detached from the anemones with forceps, transferred to new petri dishes, and imaged under identical parameters as above but with a higher magnification.

To isolate and image gametes, small fractions of male and female gonads in ASW were opened with scalpel and forceps. Gonads were placed by forceps (female) or pipette (male) onto glass microscope slides and covered with glass coverslip. Representative images were taken with a Nikon Eclipse 80i microscope equipped with a Nikon DS-1QM monochrome camera (sperm) or a Nikon DS-1U color camera (female gonad).

Quantification of asexual reproduction rates. To determine the rate of asexual reproduction, five animals approximately three to four months old from each clonal line were individually placed into ASW in small food-grade translucent polycarbonate tanks and fed five times per week with *Artemia* nauplii. Pedal laceration was analyzed for each individual at the end of every week for five consecutive weeks. The number of pedal lacerates were counted by eye or with a stereoscope (Leica S8APO), and after counting all pedal lacerates were removed.

References

1. Darling, J. A. *et al.* Rising starlet: the starlet sea anemone, *Nematostella vectensis*. *Bioessays* **27,** 211–221 (2005).
2. Genikhovich, G. & Technau, U. The starlet sea anemone *Nematostella vectensis*: an anthozoan model organism for studies in comparative genomics and functional evolutionary developmental biology. *Cold Spring Harb. Protoc. 2009* **9,** (2009).
3. Bode, H. R. Axial patterning in Hydra. *Cold Spring Harbor Perspect. Biol. 2009* **1,** a00463 (2009).
4. Holstein, T. W., Hobmayer, E. & Technau, U. Cnidarians: an evolutionarily conserved model system for regeneration? *Dev. Dynam.* **226,** 257–267 (2003).
5. David, C. N. & Murphy, S. Characterization of interstitial stem cells in Hydra by cloning. *Dev. Biol.* **58,** 372–383 (1977).
6. Bosch, T. C. G. Hydra and the evolution of stem cells. *Bioessays* **31,** 478–486 (2009).
7. Bosch, T. C. G. *et al.* How do environmental factors influence life cycles and development? An experimental framework for early-diverging metazoans. *Bioessays* **36,** 1185–1194 (2014).
8. Rosenberg, E., Koren, O., Reshef, L., Efrony, R. & Zilber-Rosenberg, E. The role of microorganisms in coral health, disease, and evolution. *Nat. Rev. Microbiol.* **5,** 355–362 (2007).
9. Augustin, R., Fraune, S., Franzenburg, S. & Bosch, T. C. Where simplicity meets complexity: *Hydra*, a model for host-microbe interactions. *Adv. Exp. Med. Biol.* **710,** 71–81 (2011).
10. Rumpho, M. E., Pelletreau, K. N., Moustafa, A. & Bhattacharya, D. The making of a photosynthetic animal. *J. Exp. Biol.* **214,** 303–311 (2011).
11. Graham, E. R., Fay, S. A., Davey, A. & Sanders, R. W. Intracapsular algae provide fixed carbon to developing embryos of the salamander *Ambystoma maculatum*. *J. Exp. Biol.* **216,** 452–459 (2013).
12. Rodriguez-Lanetty, M. Evolving lineages of *Symbiodinium*-like dinoflagellates based on ITS1 rDNA. *Mol. Phylogenet. Evol.* **28,** 152–168 (2003).
13. Pochon, X. & Gates, R. D. A new *Symbiodinium* clade (Dinophyceae) from soritid foraminifera in Hawai'i. *Mol. Phylogenet. Evol.* **56,** 492–497 (2010).
14. Lajeunesse, T. C., Parkinson, J. E. & Reimer, J. D. A genetics-based description of *Symbiodinium minutum* sp. nov. and *S. psygmophilum* sp. nov. (Dinophyceae), two dinoflagellates symbiotic with Cnidaria. *J. Phycol.* **48,** 1380–1391 (2012).
15. Muscatine, L. The role of symbiotic algae in carbon and energy flux in coral reefs in *Coral Reefs* (ed. Zubinsky, Z.) 75–87 (Elsevier, 1990).

16. Yellowlees, D., Rees, T. A. V. & Leggat, W. Metabolic interactions between algal symbionts and invertebrate hosts. *Plant Cell Environ.* **31,** 679–694 (2008).
17. Hoegh-Guldberg, O. *et al.* Coral reefs under rapid climate change and ocean acidification. *Science* **318,** 1737–1742 (2007).
18. Davy, S. K., Allemand, D. & Weis, V. M. Cell biology of cnidarian-dinoflagellate symbiosis. *Microbiol. Mol. Biol. Rev.* **76,** 229–261 (2012).
19. Harii, S., Yasuda, N., Rodriguez-Lanetty, M., Irie, T. & Hidaka, M. Onset of symbiosis and distribution patterns of symbiotic dinoflagellates in the larvae of scleractinian corals. *Mar. Biol.* **156,** 1203–1212 (2009).
20. Harrison, P. L. Sexual reproduction of scleractinian corals in *Coral Reefs: an Ecosystem in Transition* (eds. Zubinsky, Z. & Stambler N.) 59–85 (Springer, 2011).
21. Weis, V. M., Davy, S. K., Hoegh-Guldberg, O., Rodriguez-Lanetty, M. & Pringle, J. R. Cell biology in model systems as the key to understanding corals. *Trends Ecol. Evol.* **23,** 369–376 (2008).
22. Xiang, T., Hambleton, E. A., DeNofrio, J. C., Pringle, J. R. & Grossman, A. R. Isolation of clonal axenic strains of the symbiotic dinoflagellate *Symbiodinium* and their growth and host specificity. *J. Phycol.* **49,** 447–458 (2013).
23. Hambleton, E. A., Guse, A. & Pringle, J. R. Similar specificities of symbiont uptake by adults and larvae in an anemone model system for coral biology. *J. Exp. Biol.* **217,** 1613–1619 (2014).
24. Thornhill, D. J., Xiang, Y., Pettay, D. T., Zhong, M. & Santos, S. R. Population genetic data of a model symbiotic cnidarian system reveal remarkable symbiotic specificity and vectored introductions across ocean basins. *Mol. Ecol.* **22,** 4499–4515 (2013).
25. Clayton, W. S., Jr. Pedal laceration by the anemone *Aiptasia pallida*. *Mar. Ecol. Prog. Ser.* **21,** 75–80 (1985).
26. Sunagawa, S. *et al.* Generation and analysis of transcriptomic resources for a model system on the rise: the sea anemone *Aiptasia pallida* and its dinoflagellate endosymbiont. *BMC Genomics* **10,** 258 (2009).
27. Lehnert, E. M., Burriesci, M. S. & Pringle, J. R. Developing the anemone *Aiptasia* as a tractable model for cnidarian-dinoflagellate symbiosis: the transcriptome of aposymbiotic *A. pallida*. *BMC Genomics* **13,** 271 (2012).
28. Baumgarten, S. *et al.* The genome of *Aiptasia*, a sea anemone model for coral symbiosis. *P. Natl. Acad. Sci. USA* Advance online publication, doi: 10.1073/pnas.1513318112 (2015).
29. Shoguchi, E. *et al.* Draft assembly of the *Symbiodinium minutum* nuclear genome reveals dinoflagellate gene structure. *Curr. Biol.* **23,** 1399–1408 (2013).
30. Bayer, T. *et al.* Symbiodinium transcriptomes: genome insights into the dinoflagellate symbionts of reef-building corals. *PLoS ONE* **7,** e35269 (2012).
31. Xiang, T., Nelson, W., Rodriguez, J., Tolleter, D. & Grossman, A. R. *Symbiodinium* transcriptome and global responses of cells to immediate changes in light intensity when grown under autotrophic or mixotrophic conditions. *Plant J.* **82,** 67–80 (2015).
32. Wittlieb, J., Khalturin, K., Lohmann, J. U., Anton-Erxleben, F. & Bosch, T. C. G. Transgenic Hydra allow *in vivo* tracking of individual stem cells during morphogenesis. *P. Natl. Acad. Sci. USA* **103,** 6208–6211 (2006).
33. Momose, T. & Houliston, E. Two oppositely localised Frizzled RNAs as axis determinants in a cnidarian embryo. *PLoS Biol.* **5,** e70 (2007).
34. Ikmi, A., McKinney, S. A., Delventhal, K. M. & Gibson, M. C. TALEN and CRISPR/Cas9-mediated genome editing in the early-branching metazoan *Nematostella vectensis*. *Nat. Commun.* **5,** 5486 (2014).
35. Chen, C., Soong, K. & Chen, C. A. The smallest oocytes among broadcast-spawning actiniarians and a unique lunar reproductive cycle in a unisexual population of the sea anemone, *Aiptasia pulchella* (Anthozoa: Actiniaria). *Zool. Stud.* **47,** 37–45 (2008).
36. Schlesinger, A., Kramarsky-Winter, E., Rosenfeld, H., Armoza-Zvoloni, R., Loya, Y. & Earley, R. Sexual plasticity and self-fertilization in the sea anemone. *Aiptasia diaphana. PLoS ONE* **5,** e11874 (2010).
37. Hand, C. & Uhlinger, K. R. The culture, sexual and asexual reproduction, and growth of the sea anemone *Nematostella vectensis*. *Biol. Bull.* **182,** 169–172 (1992).
38. Fritzenwanker, J. H. & Technau, U. Induction of gametogenesis in the basal cnidarian *Nematostella vectensis* (Anthozoa). *Dev. Genes Evol.* **212,** 99–103 (2002).
39. Ryland, J. S. Reproduction in Zoanthidea (Anthozoa: Hexacorallia). *Invertebr. Reprod. Dev.* **31,** 177–188 (1997).
40. Gorbunov, M. Y. & Falkowski, P. G. Photoreceptors in the cnidarian hosts allow symbiotic corals to sense blue moonlight. *Limnol. Oceanogr.* **47,** 309–315 (2002).
41. Levy, O. *et al.* Light-responsive cryptochromes from a simple multicellular animal, the coral *Acropora millepora*. *Science* **3184,** 67–470 (2007).
42. Guest, J. R., Baird, A. H., Goh, B. P. & Chou, L. M. Seasonal reproduction in equatorial reef corals. *Invertebr. Reprod. Dev.* **48,** 207–218 (2005).
43. Chen, C., Chang, H.-Y. & Soong, K. No tradeoff between sexual and asexual investments in the sea anemone *Aiptasia pulchella* (Anthozoa: Actiniaria). *Zool. Stud.* **51,** 996–1005 (2012).
44. Siebert, A. E., Jr. A description of the embryology, larval development, and feeding of the sea anemones *Anthopleura elegantissima* and *A. xanthogrammica*. *Can. J. Zool.* **52,** 1383–1388 (1974).
45. Vize, P. D., Hilton, J. D., Brady, A. K. & Davies, S. W. Light sensing and the coordination of coral broadcast spawning behavior. *Proc. 11th Int. Coral Reef Symp.* 378–381 (2008).
46. Brady, A. K., Hilton, J. D. & Vize, P. D. Coral spawn timing is a direct response to solar light cycles and is not an entrained circadian response. *Coral Reefs* **28,** 677–680 (2009).
47. Gilbert, S. F. & Epel, D. *Ecological Developmental Biology: Integrating Epigenetics, Medicine, and Evolution*. 1–462 (Sinauer, 2008).
48. Via, S. *et al.* Adaptive phenotypic plasticity: consensus and controversy. *Trends Ecol. Evol.* **10,** 212–217 (1995).
49. Roff, D. A. *The Evolution of Life Histories: Theory and Analysis*. 1–535 (Chapman & Hall, 1992).
50. Mito, T. & Uesugi, T. Invasive alien species in Japan: the status quo and the new regulation for prevention of their adverse effects. *Global Environmental Research* **8,** 171–191 (2004).
51. Rhyne, A. L., Lin, J. & Deal, K. J. Biological control of aquarium pest anemone *Aiptasia pallida* Verrill by peppermint shrimp *Lysmata* Risso. *J. Shellfish Res.* **23,** 227–229 (2004).
52. Iwao, K., Fujisawa, T. & Hatta, M. A cnidarian neuropeptide of the GLWamide family induces metamorphosis of reef-building corals in the genus *Acropora*. *Coral Reefs* **21,** 127–129 (2002).
53. Takahashi, T. & Hatta, M. The importance of GLWamide neuropeptides in cnidarian development and physiology. *J. Amino Acids* **2011,** 1–8 (2011).
54. Tebben, J. *et al.* Chemical mediation of coral larval settlement by crustose coralline algae. *Sci. Rep.* **5,** 10803 (2015).
55. Kearse, M. *et al.* Geneious Basic: an integrated and extendable desktop software platform for the organization and analysis of sequence data. *Bioinformatics* **28,** 1647–1649 (2012).
56. Thompson, J. D., Higgins D. G. & Gibson T. J. CLUSTAL W: improving the sensitivity of progressive multiple sequence alignment through sequence weighting, position-specific gap penalties and weight matrix choice. *Nucleic Acids Res.* **22,** 4673–4680 (1994).
57. Guindon, S. *et al.* New algorithms and methods to estimate Maximum-Likelihood Phylogenies: Assessing the performance of PhyML 3.0. *Syst. Biol.* **59,** 307–321 (2010).
58. Pochon, X., Montoya-Burgos, J. I., Stadelmann, B. & Pawlowski, J. Molecular phylogeny, evolutionary rates, and divergence timing of the symbiotic dinoflagellate genus *Symbiodinium*. *Mol. Phylogenet. Evol.* **38,** 20–30 (2006).

Acknowledgements

Funding was provided to A.G. by the Emmy-Noether-Programme of the German Research Foundation (DFG) (grant no. GU 1128/3–1) and by a Marie Curie Career Integration Grant (CIG) under the FP7-PEOPLE-2013-CIG program, European Commission; and to I.W. by a PhD fellowship from the Graduate Program in Areas of Basic and Applied Biology (GABBA) of University of Porto. We thank John Pringle, Santiago Perez, and Pringle lab members for providing *Aiptasia* lines and advice; Tingting Xiang and Arthur Grossman for *Symbiodinium* strains; Dan Thornhill for *Aiptasia SCAR* sequences; Steffen Lemke, Thomas Holstein, and Suat Özbek for advice and comments.

Author Contributions

D.G., E.A.H. and A.G. designed the experiments; D.G., E.A.H., M.B., I.W. and N.B. performed the experiments. E.A.H. and A.G. wrote the manuscript. All authors reviewed the manuscript.

Additional Information

Supplementary information accompanies this paper at http://www.nature.com/srep

Competing financial interests: The authors declare no competing financial interests.

How to cite this article: Grawunder, D. *et al.* Induction of Gametogenesis in the Cnidarian Endosymbiosis Model *Aiptasia* sp. *Sci. Rep.* **5**, 15677; doi: 10.1038/srep15677 (2015).

SUPPLEMENTARY INFORMATION

INDUCTION OF GAMETOGENESIS IN THE CNIDARIAN ENDOSYMBIOSIS MODEL *AIPTASIA* SP.

Authors: D. Grawunder, E. A. Hambleton, M. Bucher, I. Wolfowicz, N. Bechtoldt, A. Guse

Lines	Couple #	# of months/condition		Tp	Cycle 1											Cycle 2										
		FOO3	CC7		Day 10	Day 11	Day 12	Day 13	Day 14	Day 15	Day 16	Day 17	Day 18	Day 19	Day 20	Day 10	Day 11	Day 12	Day 13	Day 14	Day 15	Day 16	Day 17	Day 18	Day 19	Day 20
F003 x CC7	1	4 *	3 *	27						L										E	L	L				
	2			27						E										E	E	E				
	3			30					E	L	L	L							E	L						
	4			30							L									E						
	5	3 *	3 *	29					E												L					
	6			29						L	L										L	L	L			
	7			29						E																
	8	5	3 *	29							L											L				
	9			29						L	L											L				
	10			29						L	L										L	L				
	11			29							L											L				
	12	8 *	2 *	27						E	L											L	L	L	E	
	13			29				E	L	L										E	L			L		
H2 x CC7	1	3-5 *	6 *	27					L	L										L						
	2			27					L								E									
	3			27					L																	
	4			27					L	L																
	5			27					L							E										
	6	3 *	3 *	29																						
	7			29																						
	8			29																						
	9			29																						
	10			29																						
	11			29																						
	12	4 *	4 *	29					E																	
	13			29																						
	14			29																						
	15	5 *	3 *	29																						
	16			29																						
	17			29																						
	18			29																						
	19	2 *	2 *	27						E																
	20			27																						
	21			27																						
	22			29				L																		
	23			29																						
	24			29				E																		
	25			29				L	L																	
	26			29																						
	27			29				E																		
	28	5 *	4 *	29																						
	29			29																						
	30			29																						
	31			29								L														
	32			29																						
	33			29																						
	34			29																						
	35			29							L	L														
	36			29																						
	37			29																						

Supplementary Figure S1. Data of initial spawning induction of *Aiptasia* clonal lines (Fig. 3a-c). Thirteen couples of [F003 x CC7] and thirty-seven couples of [H2 x CC7] were followed for two months under a simulated lunar cycle. E = eggs; L = larvae. Some couples were simultaneously exposed to other conditions to test whether these affected spawning success (see Results); # of months/condition is the duration in higher temperature and higher feeding conditions prior to spawning induction; Tp indicates temperature; * indicates exposure to faint blue light (~6 μmol m^{-2} s^{-1}) during night periods prior to the spawning induction.

SUPPLEMENTARY INFORMATION

INDUCTION OF GAMETOGENESIS IN THE CNIDARIAN ENDOSYMBIOSIS MODEL *AIPTASIA* SP.

Authors: D. Grawunder, E. A. Hambleton, M. Bucher, I. Wolfowicz, N. Bechtoldt, A. Guse

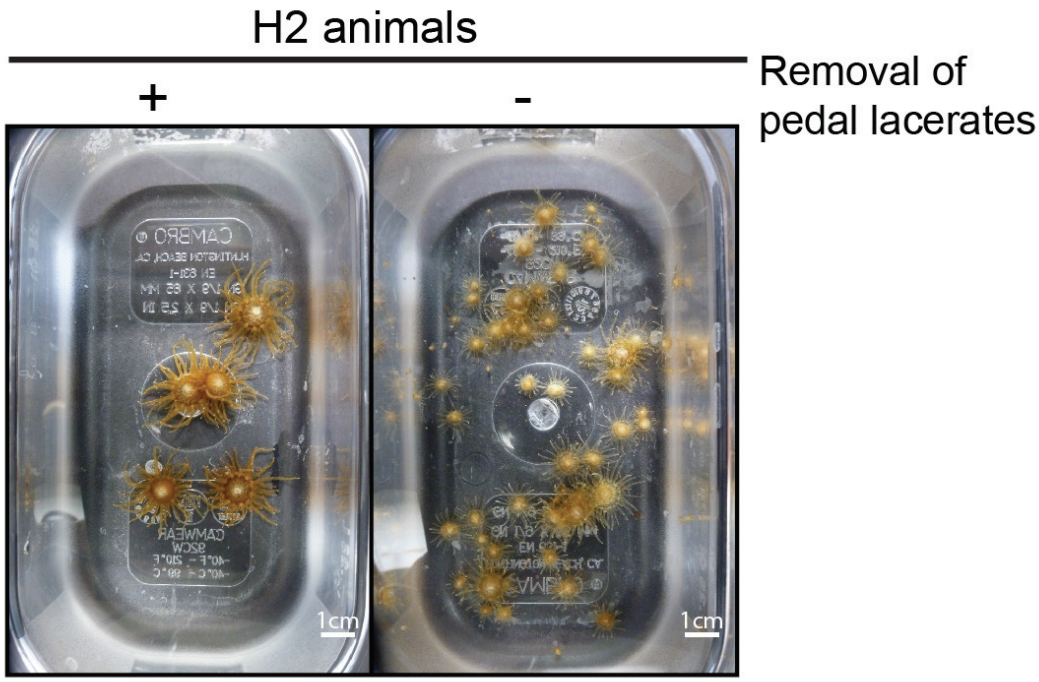

Supplementary Figure S2. Removal of pedal lacerates greatly promotes growth of individual adults. Five small adults from clonal line H2 were placed into ASW in small food-grade translucent polycarbonate tanks; two such tanks were created and kept under standard culture conditions. In the left-panel tank, all pedal lacerates were removed three times per week; in the right-panel tank, all pedal lacerates were left undisturbed. Tanks were imaged with a hand-held digital camera (Panasonic Lumix DMC-TZ18) after 7 months.

SUPPLEMENTARY INFORMATION

INDUCTION OF GAMETOGENESIS IN THE CNIDARIAN ENDOSYMBIOSIS MODEL *AIPTASIA* SP.

Authors: D. Grawunder, E. A. Hambleton, M. Bucher, I. Wolfowicz, N. Bechtoldt, A. Guse

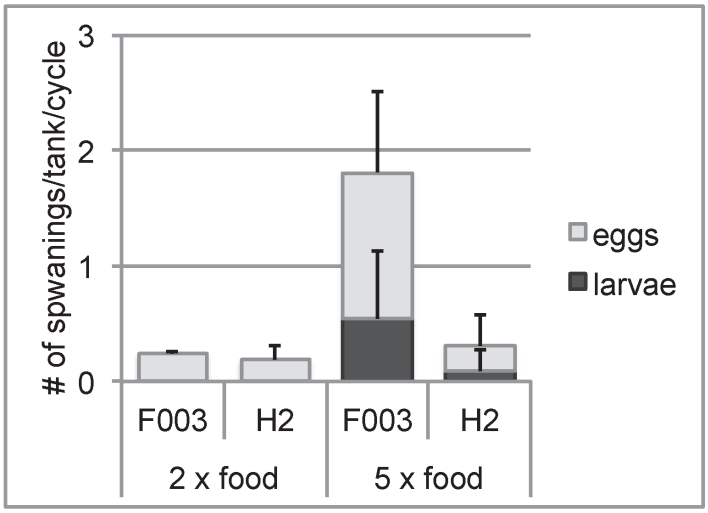

Supplementary Figure S3. Comparison of spawning efficiency before and after increased feeding shows a marked improvement in spawning, especially by [F003 x CC7] couples. Error bars are standard deviations.

SUPPLEMENTARY INFORMATION

INDUCTION OF GAMETOGENESIS IN THE CNIDARIAN ENDOSYMBIOSIS MODEL *AIPTASIA* SP.

Authors: D. Grawunder, E. A. Hambleton, M. Bucher, I. Wolfowicz, N. Bechtoldt, A. Guse

Condition	Couple #	Cycle 1									Spawnings/Couple/Cycle		
		Day 13	Day 14	Day 15	Day 16	Day 17	Day 18	Day 19	Day 20	Day 21	Eggs	Larvae	Total
A	1		L	15000							1,0	1,4	2,4
	2	E	E										
	3	E	L	5000									
	4	E (few)	L	2800									
	5		E	17000									
B	1			8000							0,2	0,8	1,0
	2			200									
	3	E		7300									
	4												
	5			16500									
C	1										1,2	0,4	1,6
	2				E (few)	50			E	E			
	3								E (few)				
	4				E (few)	1250							
	5								E (few)				
D	1										0,4	0	0,4
	2												
	3												
	4		E (few)	E (few)									
	5												

Supplementary Figure S4. Data of direct comparison of spawning induction conditions using five couples of [F003xCC7] per condition (Fig. 3d-f). Couples were followed for one 29-day artificial lunar cycle. E = eggs; L = larvae.

SUPPLEMENTARY INFORMATION

INDUCTION OF GAMETOGENESIS IN THE CNIDARIAN ENDOSYMBIOSIS MODEL *AIPTASIA* SP.

Authors: D. Grawunder, E. A. Hambleton, M. Bucher, I. Wolfowicz, N. Bechtoldt, A. Guse

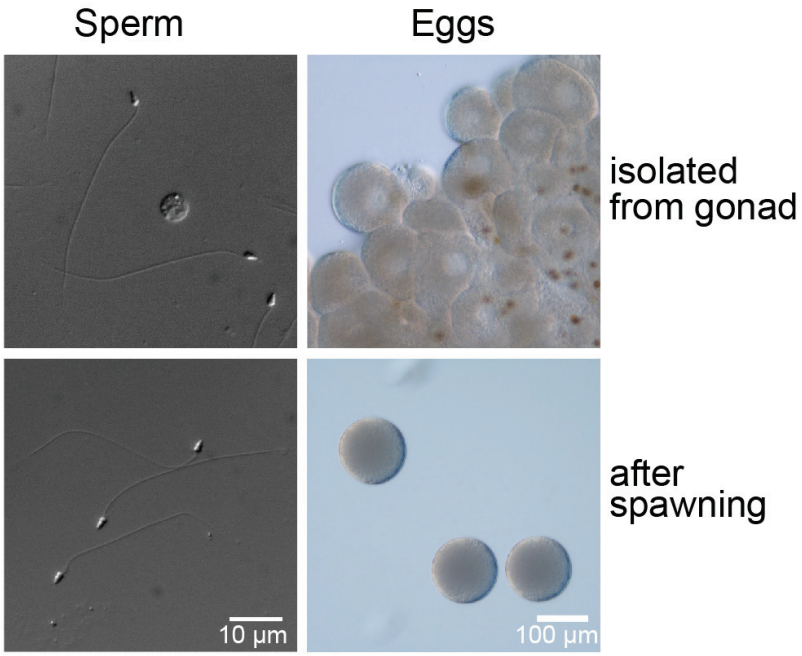

Supplementary Figure S5. Male and female gametes isolated from gonads or after spawning.

Publication 2: “Development and symbiosis establishment in the cnidarian endosymbiosis model *Aiptasia* sp.“

Highlights

In this publication, we describe how confocal scanning microscopy can be used to look at symbiosis establishment during *Aiptasia* larval development. Our major findings were:

- In *Aiptasia* larvae the gastric cavity increases accompanied by an increase of endodermal cell size, over the course of 10 days of development;
- Symbiont uptake starts as soon as the mouth is formed and continues during the first 14 days of larval development with similar efficiency;
- Algal symbionts occupy a major portion of the endodermal cell in *Aiptasia* larvae;
- The localization of symbionts in *Aiptasia* larvae varies during development, indicating developmental changes of endodermal cells.

Author contribution

For this manuscript, I developed a protocol to image symbiotic cells at the cellular level and contributed to Figure 3e. I also first noted the existence of particularly big cells within the larval endoderm (Figure 2f). I analyzed symbiosis establishment during larval development (Figure 3b), and contributed to the initial experiments describing that the preferential uptake of symbionts correlated with larval developmental (Figure 4).

This is an “Open access” publication.

SCIENTIFIC REPORTS

OPEN

Development and Symbiosis Establishment in the Cnidarian Endosymbiosis Model *Aiptasia* sp.

Received: 09 November 2015
Accepted: 16 December 2015
Published: 25 January 2016

Madeline Bucher[1], Iliona Wolfowicz[1,2], Philipp A. Voss[1], Elizabeth A. Hambleton[1] & Annika Guse[1]

Symbiosis between photosynthetic algae and heterotrophic organisms is widespread. One prominent example of high ecological relevance is the endosymbiosis between dinoflagellate algae of the genus *Symbiodinium* and reef-building corals, which typically acquire symbionts anew each generation during larval stages. The tropical sea anemone *Aiptasia* sp. is a laboratory model system for this endosymbiosis and, similar to corals, produces non-symbiotic larvae that establish symbiosis by phagocytosing *Symbiodinium* from the environment into the endoderm. Here we generate the first overview of *Aiptasia* embryogenesis and larval development and establish *in situ* hybridization to analyze expression patterns of key early developmental regulators. Next, we quantify morphological changes in developing larvae and find a substantial enlargement of the gastric cavity over time. Symbiont acquisition starts soon after mouth formation and symbionts occupy a major portion of the host cell in which they reside. During the first 14 days of development, infection efficiency remains constant while in contrast, localization of phagocytosed symbionts changes, indicating that the occurrence of functional phagocytosing cells may be developmentally regulated. Taken together, here we provide the essential framework to further develop *Aiptasia* as a model system for the analysis of symbiosis establishment in cnidarian larvae at the molecular level.

Coral reef ecosystems, of high ecological and economic relevance, strictly depend upon a functional symbiosis between corals and dinoflagellates (genus *Symbiodinium*), which reside inside host endodermal cells and provide most of the host's nutrition via transferred photosynthates, receiving inorganic nutrients and shelter in return[1]. The genus *Symbiodinium* comprises hundreds of strains[2], with reef-building coral taxa establishing relationships with some strains but not others; such symbiosis specificity produces physiological consequences, such as adaptation to certain environmental conditions[3–5]. Most scleractinian corals (>75%) transmit symbionts horizontally, thereby re-establishing symbiosis each generation and allowing symbiont-host combinations that differ from those of the parents[6,7].

In anthozoans that undergo horizontal symbiont transmission, non-symbiont-containing embryos develop into planula larvae (hereafter larvae), a ciliated postgastrula stage that, like the adult morphology, is diploblastic with defined endodermal and ectodermal tissue layers connected by the mesoglea[8–10]. Larvae of the majority of reef-building corals demonstrably have the capacity to acquire symbionts from the surrounding marine environment[11–15]. One horizontally transmitting coral species (*Fungia scutaria*) has also been shown to integrate symbionts during embryogenesis, i.e. before mouth formation[16]. However, the majority of corals appear to require an open blastopore leading into a developed gastric cavity for symbiont uptake and phagocytosis[15]. Harii and colleagues documented an increase in gastric cavity size as coral larvae age, and postulated that this enlargement may be widespread in corals and accompanied by the occurrence of well-developed, ciliated gastrodermal cells that may enhance acquisition of symbionts by late developmental stages[15].

Despite the critical importance of symbiont acquisition in coral larvae, it is not yet clear whether the larval endoderm consists of different cell types, some of which may be specialized phagocytes, and whether the occurrence of such cell types is developmentally regulated. Also unknown is whether and how symbiont phagocytosis alters the morphology and physiology of the host endoderm at the single-cell level and/or the broader tissue context. This lack of knowledge is largely because the systematic study of the detailed cellular and molecular events

[1]Centre for Organismal Studies (COS), Heidelberg University, Heidelberg 69120, Germany. [2]Graduate Program in Areas of Basic and Applied Biology (GABBA), University of Porto, Porto 4200-465, Portugal. Correspondence and requests for materials should be addressed to A.G. (email: annika.guse@cos.uni-heidelberg.de)

leading to symbiosis establishment is hindered by the once-annual spawning of most reef-building corals[7,17]. Much of our understanding of cnidarian development and larval physiology comes from well developed model systems such as *Nematostella vectensis*, *Clytia hemisphaerica*, and *Hydractinia echinata*; however, the former is non-symbiotic and the latter two are medusozoans whose larvae therefore differ considerably from corals (e.g. lack of an open blastopore and accompanying pharyngeal region lined by the endodermal epithelia)[18,19]. Thus, a tractable laboratory model of symbiont acquisition in larvae has heretofore been largely absent.

To address this limitation, a practicable symbiotic laboratory model has been developed with the sea anemone *Aiptasia* sp., an anthozoan that forms relationships with the same types of *Symbiodinium* as corals[20,21] and likewise exhibits horizontal transmission of these symbionts through production of non-symbiotic larvae[22]. Most importantly, spawning can be induced efficiently in *Aiptasia* under laboratory conditions, providing regular access to abundant larvae for experimentation[23]. Such experimentation in *Aiptasia* is particularly exploitable because of the cellular and molecular resources already generated for the system, including the *Aiptasia* genome[24] and several transcriptomes[25,26] and corresponding transcriptomic/genomic resources for several *Symbiodinium* strains[27–29].

With the *Aiptasia* model system in place, we sought to address key questions of how early development of the anthozoan larva contributes to symbiosis establishment. Here we provide for the first time an analysis of the basic features of *Aiptasia* development from embryogenesis to late larval stages, including how larval morphology changes over time. Specifically, we find that the gastric cavity enlarges over time, predominantly through remodeling of the endodermal tissue. By co-incubating larvae with a compatible *Symbiodinium* strain, we find that symbiont uptake starts after mouth formation and that uptake efficiency remains constant for two weeks. Symbionts are integrated into the host cells and appear to locally alter endodermal morphology. Interestingly, the spatial distribution of symbiont uptake within the endoderm changes as larvae age, indicating that the occurrence of symbiont-phagocytosing cells may change over time. Taken together, we provide a foundational platform for studies of the specific molecular and cellular processes of symbiont phagocytosis and other events critical to symbiosis establishment.

Results

Characterization of embryonic and larval development in *Aiptasia*. A prerequisite of symbiosis studies in larval stages is an initial characterization of *Aiptasia* embryogenesis under standard conditions, which has heretofore not been reported. To generate such an overview, we used differential interference contrast (DIC) microscopy to image development from the unfertilized egg to planula larvae 10 days post fertilization (dpf) (Fig. 1a). After fertilization of eggs (diameter 85.8 +/− 5 μm [$n = 51$]), two meridional and one equatorial cleavages produce sister cells of similar size with very stereotypic 4-cell, 8-cell and 16-cell stages (Fig. 1a, C–E). For the 16- and 32-cell stages, the formation of a small blastocoel is observed (Fig. 1a, E–F). Similar to *Nematostella*[30], we were unable to observe polar bodies, fertilization membranes, or prominent 2-cell stages (Fig. 1a, A–C). In the ciliated blastula, which begins to rotate, the nuclei are localized to the periphery (Fig. 1a, H; b, A–A"). Before gastrulation (which appears to occur predominantly via invagination), the blastula starts to elongate (Fig. 1a, I; b, B–B") and an apparent blastopore forms (Fig. 1a, J). At 24 hours post fertilization (hpf), two germ layers can be distinguished, with the endoderm filling the larval cavity; concurrently, at the aboral pole the apical ciliary tuft forms, which may be involved in settlement and metamorphosis (Fig. 1a, K)[31,32]. At 48 hpf we observed typical features of anthozoan planula larvae, including a clear oral-aboral axis with a prominent blastopore at the oral pole and a well-developed apical tuft at the aboral pole. Defined endodermal and ectodermal tissue layers form, separated by the mesoglea, and the first mature nematocytes are distinguishable within the aboral ectoderm (Fig. 1a, L). As larvae mature, the endoderm appears to get thinner and the gastric cavity more spacious (Fig. 1a, M–N). Under laboratory conditions, larvae can be maintained for approximately 30–40 days before they die; presumably, in nature larvae find a proper substrate for settlement during this time, but settlement has not been achieved in the laboratory to date (see Discussion).

To generate a molecular snapshot of early development in *Aiptasia*, we used *in situ* hybridization to determine the spatial expression of classical developmental markers involved in tissue specification and body axis formation in gastrulating embryos (Fig. 1c). Genes encoding the transcription factors *Brachyury* and *Forkhead*, as well as *β-catenin* are expressed at the blastopore (Fig. 1c, A–C), whereas *Chordin* is expressed only on one side in the anterior ectoderm (Fig. 1c, D). The *Wnt* most aborally located, *Wnt2*, forms a distinct domain in the ectoderm and *OtxA* is expectedly found throughout the endodermal tissue and around the blastopore (Fig. 1c, E–F). All six markers faithfully replicated localization patterns seen in *Nematostella* at comparable developmental stages (late gastrula to planula larva stages)[10,33–38], indicating that *Aiptasia* follows a conserved anthozoan developmental program.

Morphological changes in the symbiosis-relevant endoderm during development. We next sought to characterize changes in larval tissue morphology over the course of development, with particular attention to features that may influence the establishment of symbiosis. To do so, we examined larval tissue structure in detail by using confocal microscopy to visualize nuclei (Hoechst staining) and cell boundaries (phalloidin staining of F-actin) in larvae of different ages. Larvae 48 hpf already have clearly defined tissue layers: the endoderm and the ectoderm, which also lines the prominent pharynx connecting the mouth to the gastric cavity (Fig. 2a, A). As larvae transition to middle age (8 and 12 dpf), the pharyngeal ectoderm noticeably shrinks and the gastric cavity appears to become considerably larger (Fig. 2a, B–C).

Symbionts are taken up from the environment into the gastric cavity, where they are then phagocytosed by host endodermal cells[12,14,39]. We therefore quantified the enlargement of the gastric cavity over larval aging. By measuring the area of the gastric cavity in one medial plane as a proxy (see schematic in Fig. 2b), we find that the gastric cavity is approximately 2.5 fold larger in larvae 10 dpf (~1500 μm^2) than in larvae 48 hpf (~600 μm^2) (Fig. 2c). Quantification of larval length and width shows that neither metric differs significantly between larvae

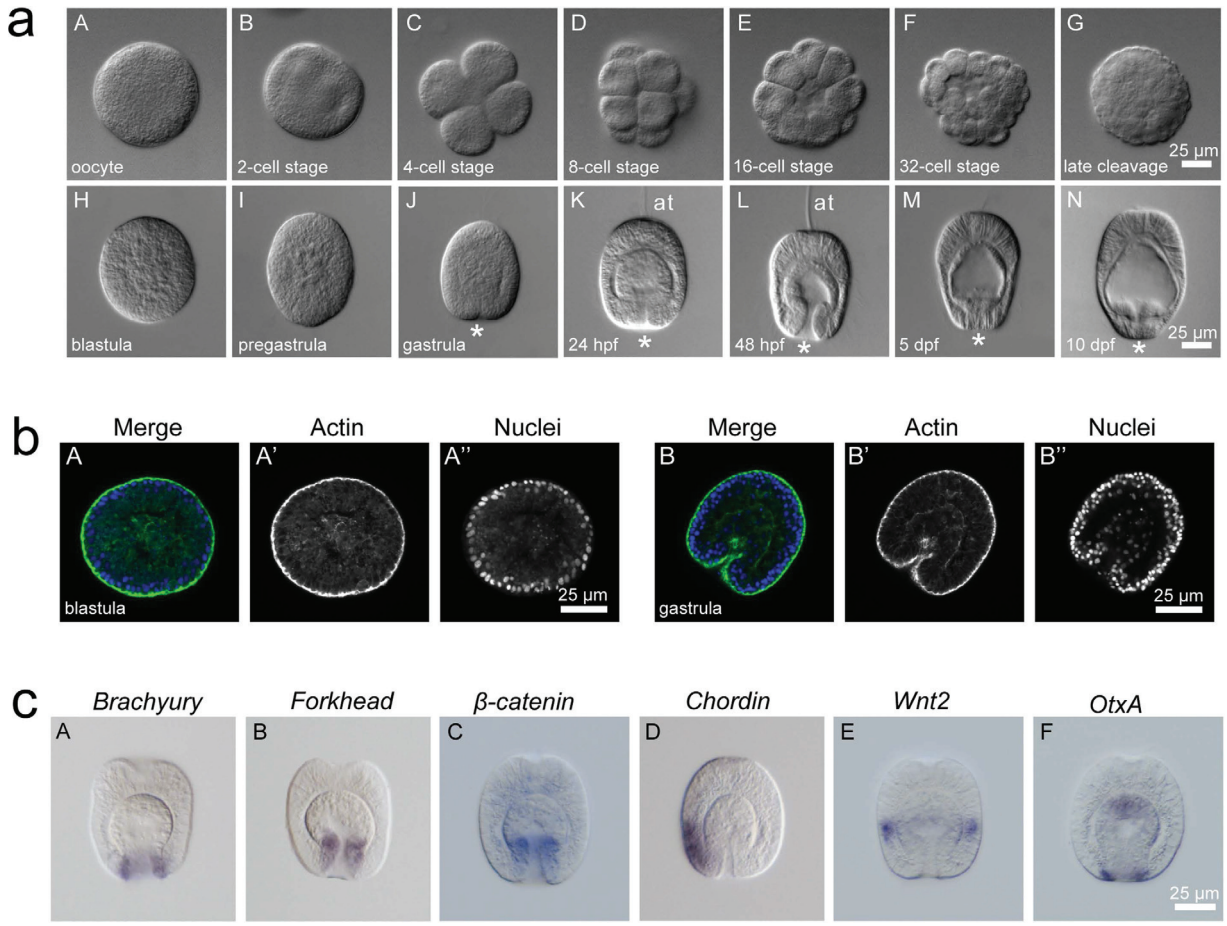

Figure 1. Development of *Aiptasia*. (**a**) Overview of *Aiptasia* embryonic and larval development using differential interference contrast (DIC) microscopy. *indicates the blastopore; hpf = hours post fertilization; dpf = days post fertilization. (**b**) Representative confocal microscopy images of *Aiptasia* blastula (A–A") and gastrula (B–B"). The left panels (A and B) show merged images of Hoechst-stained nuclei (blue) and phalloidin-stained F-actin (green), the middle panels (A' and B') only actin, and the right panels (A" and B") only nuclei. (**c**) Gene expression patterns of key classical developmental regulators in *Aiptasia* larvae ~24 hpf using *in situ* hybridization.

48 hpf and 10 dpf, demonstrating that the gastric cavity enlargement is not simply because the whole larva enlarges, as it rather remains relatively constant in size (Fig. 2b,d).

To identify the cause of the increase in gastric cavity size, we measured ecto- and endodermal thickness as well as the width of the pharynx lined by the pharyngeal ectoderm (Fig. 2b,e). The thickness of the ectoderm at the aboral region remains constant between these two larval stages. In contrast, the endodermal thickness changes substantially during this time: while the aboral endoderm is ~15 µm thick in larvae 48 hpf, it is reduced nearly 50% to ~7 µm thick in larvae 10 dpf. Likewise, the endoderm lining the sides of the gastric cavity decreases from ~9 µm to ~5 µm. Moreover, the width of the pharynx increases approximately 30%, from ~7 µm to ~10 µm (Fig. 2e). To observe these morphological changes at the cellular level, we measured the areas of the apical faces of the endodermal cells in larvae 48 hpf and 10 dpf (Fig. 2f). We find that in larvae 48 hpf, the areas of endodermal cells are substantially smaller (~17 μm^2) than those in larvae 10 dpf (~28 μm^2) (Fig. 2g). However, the cell areas in older larvae range from less than 10 μm^2 to more than 50 μm^2, whereas the cells in younger larvae are more uniform (Fig. 2f,g).

Taken together, the data above indicate that over time, the larval endodermal architecture changes from long, columnar cells with uniform cell surface areas to relatively flatter cells with more variable cell surface areas. Together with the widening of the pharynx, these morphological changes allow the gastric cavity to increase in size as the larvae age. These changes are summarized schematically in Fig. 2h.

Developmental time window of symbiosis establishment and consequent endodermal remodeling. The observed broad-scale changes in the symbiosis-relevant endoderm led us to determine the period in development in which naturally non-symbiotic *Aiptasia* larvae acquire symbionts from the environment. To test when larvae are first capable of symbiont acquisition, we added a constant environmental supply of a compatible *Symbiodinium* strain (SSB01[21]) at 10,000 algal cells/ml to developing embryos at the 4-, 8-, and 16-cell stages and fixed a subset of embryos at different time-points early in development to measure infection efficiencies

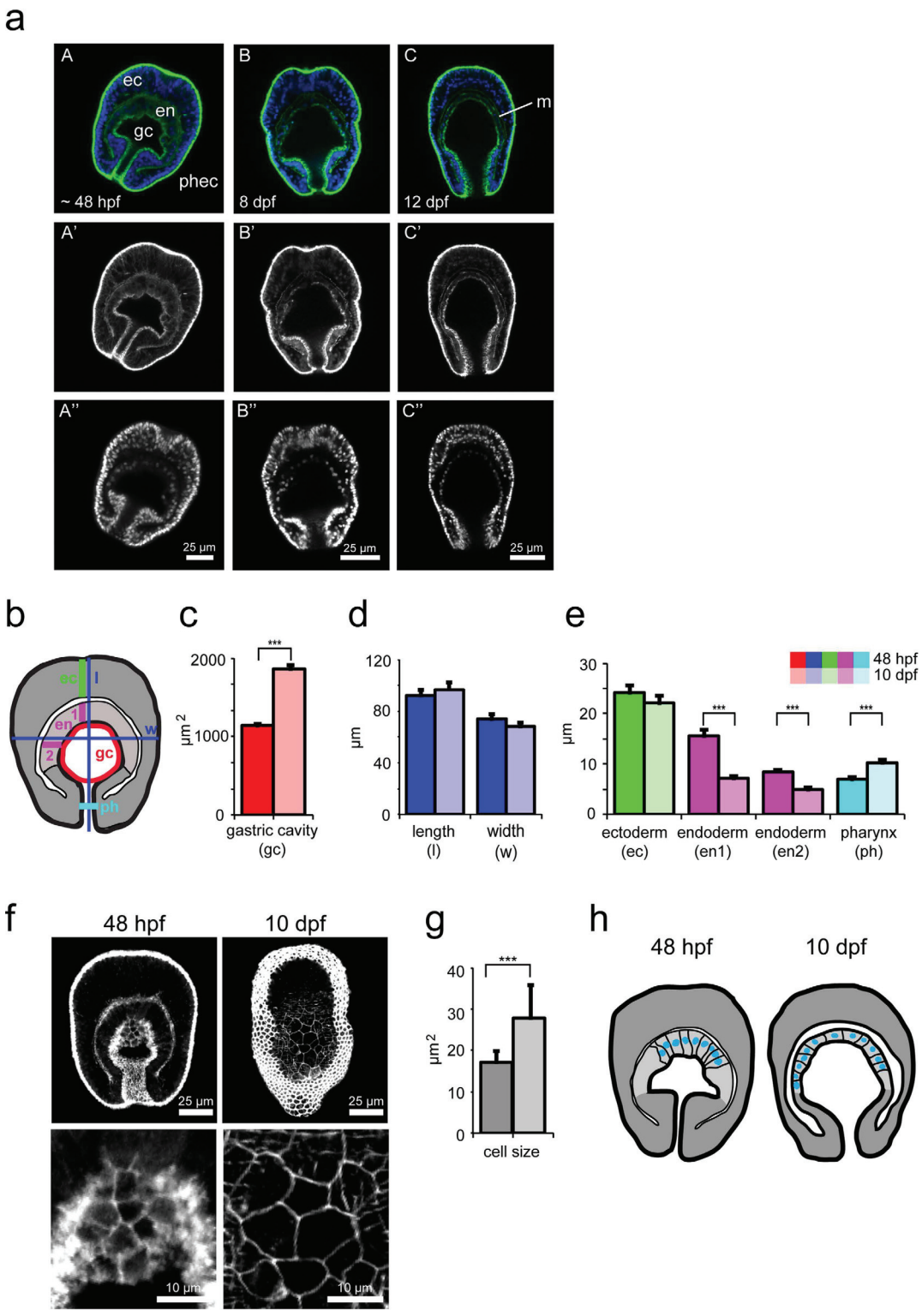

Figure 2. Morphological changes of the larval endoderm during development. (**a**) Representative confocal microscopy images of *Aiptasia* larvae 48 hpf (A–A"), 8 dpf (B–B"), and 12 dpf (C–C"). The upper row (A–C) shows merged images of Hoechst-stained nuclei (blue) and phalloidin-stained F-actin (green), the middle row (A'–C') only actin, and the lower row (A"–C") only nuclei. The endoderm (en), ectoderm (ec), gastric cavity (gc), pharyngeal ectoderm (phec), and mesoglea (m) are indicated. (**b**) Schematic of larva with colored lines indicating positions of measurement of morphological features in (**c–e**). $n = 23$ for larvae 48 hpf and $n = 22$ for larvae 10 dpf. (**c**) Quantification of change in gastric cavity area between larvae 48 hpf and 10 dpf. Error bars are SEM, $^{***}p < 0.001$ as determined by Student's *t*-test for unpaired data. (**d**) Quantification of change in larval length and width between larvae 48 hpf and 10 dpf. Error bars are SEM. (**e**) Quantification of change in thickness of the ectoderm (ec), endoderm (en1, en2), and pharyngeal width (ph) between larvae 48 hpf and

10 dpf. Error bars are SEM, $***p < 0.001$ as determined by Student's *t*-test for unpaired data. (**f**) Representative confocal microscopy images of *Aiptasia* larvae 48 hpf and 10 dpf showing phalloidin-stained F-actin to mark the cell outlines. Each image comprises z-projections of multiple planes of the endoderm. Below are corresponding higher-magnification images of endodermal cells. (**g**) Quantification of endodermal cell sizes of larvae 48 hpf and 10 dpf from images as shown in (**f**). Error bars are SEM, $***p < 0.001$ as determined by Student's *t*-test for unpaired data, $n = 56$ cells for larvae 48 hpf (5 larvae) and $n = 82$ cells for larvae 10 dpf (5 larvae). (**h**) Schematic of larvae summarizing morphological changes: younger larvae (48 hpf) have a small gastric cavity, a thick endoderm with columnar cells, and a pronounced pharyngeal ectoderm when compared to older larvae (10 dpf), which have a bigger gastric cavity, flattened endodermal cells, smaller pharyngeal ectoderm, and more pronounced mesoglea.

(Fig. 3a). Algae were first detected in larvae between 1 and 2 dpf (Fig. 3a); by this time, the mouth had formed and the endodermal and ectodermal tissue layers were clearly distinguishable. However, infection was very low (~3%), suggesting only a recent ability of the larvae to acquire algae, likely largely due to recent mouth formation. Infection increased over time to ~20–25% as larvae matured (we did not distinguish between algae inside the gastric cavity and those integrated into the endodermal tissue) (Fig. 3a).

We next analyzed symbiont uptake efficiencies in older larvae by monitoring over longer periods of time. To this end, we incubated larvae with a constant environmental supply of *Symbiodinium* strain SSB01 (again 10,000 algae/ml) for incremental four-day windows, beginning with larvae 48 hpf, and then measured the infection efficiencies at the end of each of these four-day windows. Between 2 and 14 dpf, ~25–30% of *Aiptasia* larvae take up symbionts from the environment; however, at 15–16 dpf, symbiont uptake by larvae is drastically decreased (Fig. 3b). Taken together, these experiments indicate that larval competency for symbiosis establishment peaks in middle-aged larvae, with young larvae (48 hpf) just gaining competency and older larvae (over 16 dpf) losing competency.

Through similar experiments as above (larvae 6–7 dpf exposed to *Symbiodinium* for four days), we find that symbiont uptake efficiency increases with algal concentration: at 100,000 algae/ml, more larvae (>70%) take up symbionts than at 10,000 algae/ml (~40%) and at 1,000 algae/ml (~10%). However, infection efficiency does not further increase at 200,000 algae/ml, indicating saturation (Fig. 3c). After four days exposure at non-saturating algal concentrations (10,000 algae/ml), SSB01 symbionts are taken up by larvae 4 dpf more efficiently than inert fluorescent beads, a proxy for food particles[14] of similar size (~7 μm) (Fig. 3d). These data indicate that *Aiptasia* larvae may distinguish between SSB01 algae and inert particles, preferentially taking up the former, and that this uptake may depend on the frequency of encounters between larvae and algae.

To visualize the cellular architecture of symbionts housed within larval host cells during symbiosis establishment, we again used confocal microscopy to visualize nuclei (Hoechst staining), cell boundaries (phalloidin staining of F-actin), and symbionts (endogenous algal chlorophyll autofluorescence). Anthozoan endodermal cells have been shown to be rather small (i.e. 10 μm × 25 μm) when compared to symbiont sizes (~7–10 μm in diameter), yet they typically house one or two (and sometimes up to twelve) symbiont cells[21,40,41]. As such, we observe that phagocytosed symbionts occupy a major portion of their host cells in *Aiptasia* larvae (Fig. 3e). When observed at the tissue level, this tight cell-within-cell arrangement and its consequent effects on endodermal organization become more apparent: the endodermal tissue containing symbionts consistently bulges out into the gastric cavity (Fig. 3f).

Changes in endodermal localization of symbionts during development. We then sought to connect the observed endodermal changes during regular development with the endodermal remodeling seen during symbiosis establishment, in order to address the question of how these changes may affect symbiosis establishment. To this end, we incubated non-symbiotic larvae 48 hpf or 10 dpf with a constant supply of *Symbiodinium* strain SSB01 algae at 100,000 algae/ml for 24 h, after which larvae were fixed and three parameters were measured: infection efficiency (measured in percent of larvae containing one or more algal cells), exact number of algal cells per larva, and localization of the algae within the larvae. We found that symbiont uptake efficiency does not differ markedly between larvae 48 hpf and 10 dpf, with approximately 50%–60% of larvae containing algae (Fig. 4a). Likewise, the average number of algae in each larva remained essentially constant between the younger and older larvae, with most larvae containing three or four algal cells (Fig. 4a).

In contrast, when we analyzed how symbiont phagocytosis is spatially regulated within the endodermal tissue, we observed a striking difference between younger and older larvae. In younger larvae, algal cells are located primarily in the aboral endoderm, whereas in older larvae, algal cells are distributed throughout both the aboral and oral regions of the endoderm (Fig. 4b). Quantification of this phenomenon further emphasized this difference: nearly 90% of the algal cells in larvae 48 hpf were in the aboral endoderm, whereas in larvae 10 dpf, only around 60% of algal cells were in the aboral endoderm, with the remainder appearing in the oral endoderm (Fig. 4c).

Discussion

Here we provide the first overview of *Aiptasia* embryogenesis and key morphological features of *Aiptasia* planula larvae as well as a quantification of vital aspects of symbiosis establishment in relation to *Aiptasia* development. Similar to many anthozoans, *Aiptasia* embryos undergo stereotypic and holoblastic cleavages to form a ciliated blastula before gastrulation gives rise to the characteristic diploblastic anthozoan planula larva with an open blastopore, defined gastric cavity, and apical tuft[8,31]. However, we also found differences between embryonic/larval development of *Aiptasia* and that of other anthozoan systems such as *Nematostella* or corals. For example, we never observe prawn chip stages preceding blastula formation[30,42]. Neither do we observe mesentery formation

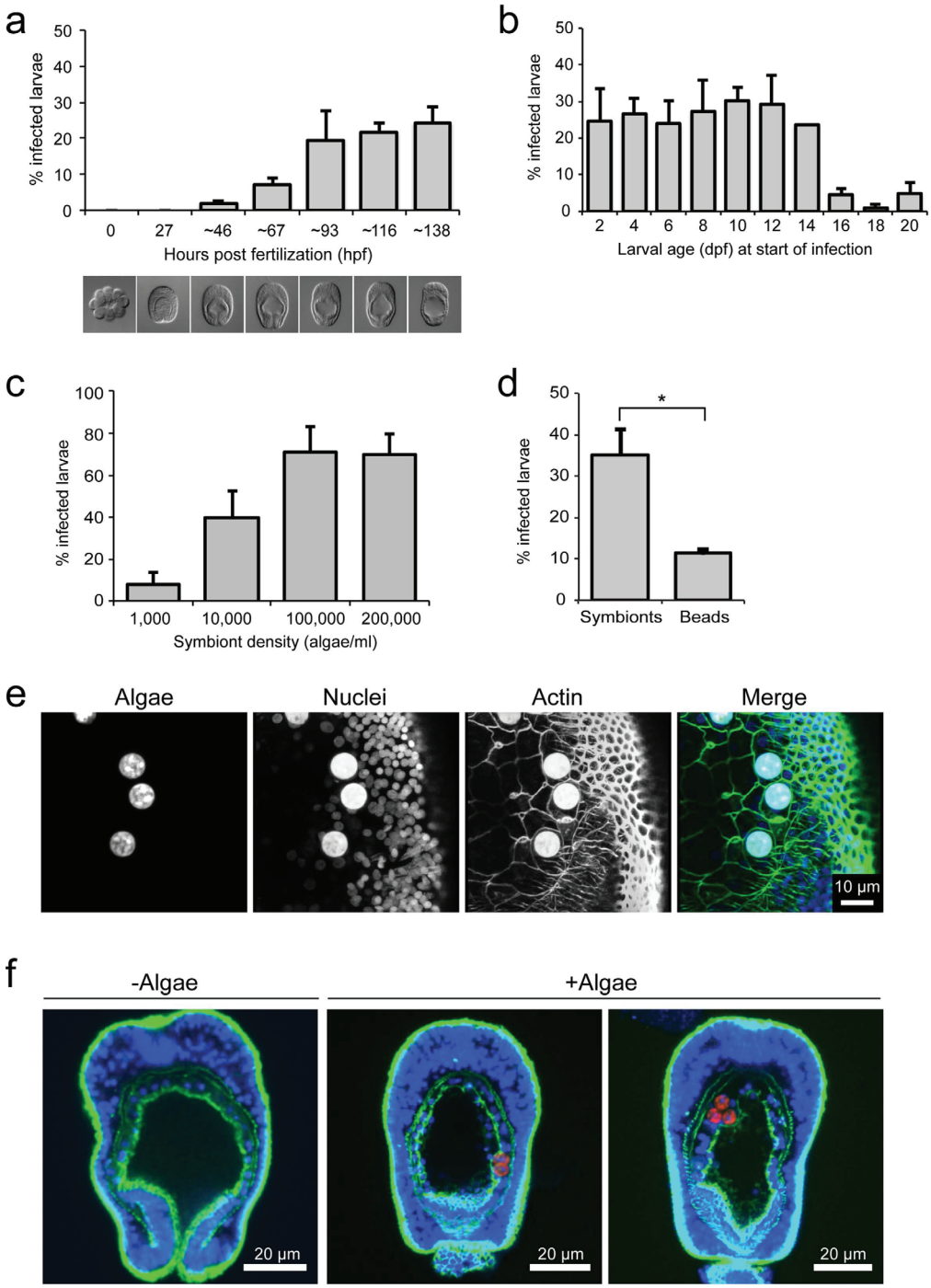

Figure 3. Symbiosis establishment during larval development. (**a**) Quantification of symbiont uptake efficiencies in *Aiptasia* embryos and early planula larvae: early (<32-cell-stage) embryos were exposed to a constant environmental supply of *Symbiodinium* strain SSB01[21] (10,000 algae/ml) and subsets were sampled at the times indicated (hpf) to assess infection efficiency. Representative DIC images are shown below each timepoint. Error bars are SEM, $n = 3$ replicate experiments. (**b**) Quantification of symbiont uptake efficiencies for larvae between 2 and 20 dpf: larvae at the ages indicated (dpf) were incubated with *Symbiodinium* strain SSB01 (10,000 algae/ml) for four days, after which infection efficiency was assessed. Error bars are SEM, $n = 3$ replicate experiments. (**c**) Quantification of symbiont uptake efficiencies after four days exposure for larvae 6–7 dpf at increasing algal concentrations. Error bars are SEM, $n = 3$ replicate experiments. (**d**) Quantification of comparison of uptake efficiency between SSB01 algae and inert fluorescent beads for larvae 4 dpf after four days exposure. Error bars are SEM, $^{***}p < 0.001$ as determined by Student's *t*-test for unpaired data, $n = 3$ replicate experiments. (**e**) Representative fluorescence microscopy images of phagocytosed symbionts in endodermal cells of larvae 8 dpf. Hoechst-stained nuclei are shown in blue, phalloidin-stained F-actin to mark cell outlines in green, and endogenous autofluorescence of algal chlorophyll in red. Note that algae exhibit strong autofluorescence in all channels. (**f**) Representative confocal microscopy images of larvae 10 dpf with or without symbionts. Fluorescence channels are as in (**e**).

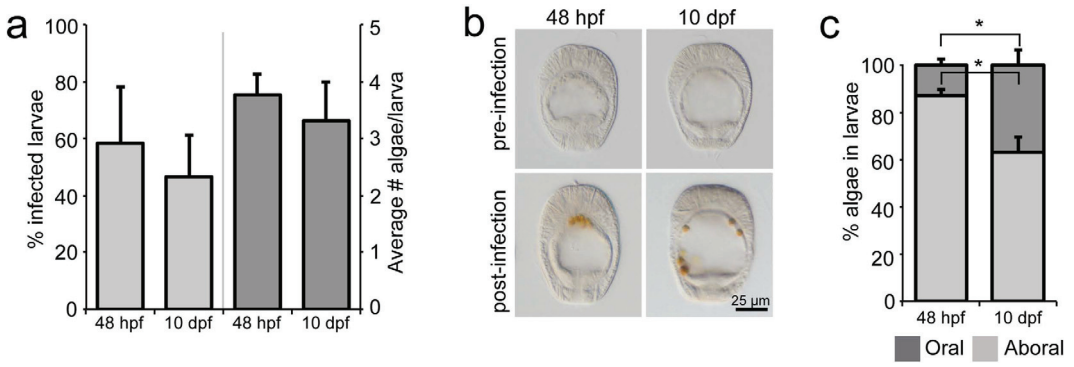

Figure 4. Change in localization of symbiosis establishment during development. (**a–c**) After 24 h exposure to symbionts (100,000 algal cells/ml), larvae 48 hpf and 10 dpf were scored for infection efficiency and average number of algal cells per larva. $n = 3$ replicate experiments (**a**). Additionally, the localization of the algal cells in the aboral or oral endoderm in each larva was recorded: representative DIC microscopy images are shown in (**b**) and quantification in (**c**). $n = 3$ replicate experiments, ≥ 30 larvae per experiment. Error bars are SEM, $^{*}p < 0.05$ as determined by Student's *t*-test for unpaired data.

within *Aiptasia* larvae as reported for late larval stages in *Nematostella*[43,44]. This difference is likely due to the fact that *Nematostella* larvae spontaneously initiate metamorphosis and settlement under laboratory conditions, while *Aiptasia* larvae have not yet been reported to metamorphose or settle spontaneously under laboratory conditions. This suggests that *Aiptasia* larvae, similar to corals, may need specific cues that induce neuropeptide expression to exit larval stages and proceed with development into the polyp stage[45]. As mesentery formation might mark the beginning of metamorphosis, we therefore expect it to be observed in *Aiptasia* larvae once these metamorphosis cues have been identified. The identification of these specific cues to promote progression of *Aiptasia* development, thus closing the life cycle in the laboratory, is an important step for the *Aiptasia* laboratory model system. More broadly, the overview of *Aiptasia* early development together with the *in situ* hybridization protocol to analyze gene expression patterns presented here now opens the door for comparative molecular analyses of *Aiptasia* development to that of other cnidarian larvae, especially *Nematostella*, to dissect the similarities and differences between two distinct representatives of anthozoan larval forms.

To study phagocytosis of symbionts by endodermal cells during horizontal transmission at the molecular level, detailed knowledge of the temporal and spatial regulation of symbiont uptake in *Aiptasia* larvae is essential. We found that *Aiptasia* does not take up symbionts during embryogenesis as suggested for solitary non-colonial corals (e.g. *Fungia scutaria*)[16] but rather resembles the majority of colonial coral species tested to date in that the formation of an open mouth and a developed gastric cavity are prerequisites for symbiont uptake[15]. *Aiptasia* larvae phagocytose symbionts with similar efficiency between 48 hpf and ~16 dpf, after which uptake decreases in these conditions. However, we currently cannot distinguish whether this is an inherent characteristic of larvae or whether it was because no food was provided in these experiments, possibly causing starvation and the consequent inability to phagocytose symbionts. Indeed, many anthozoan larvae appear to be planktotrophic[8,11] and recent experiments showed that *Nematostella* larvae may assimilate certain types of dissolved organic matter (DOM)[46]. Thus, the time window for symbiont uptake in *Aiptasia* larvae may even be larger in nature, where food can be assimilated from the environment. It will therefore be interesting to test whether food supply can extend the window of symbiont uptake competency in *Aiptasia* larvae in the future. Moreover, it will be important to analyze if and how energy derived through food uptake and photosynthetically active symbionts affects the survival of *Aiptasia* larvae. Both may be important factors in extending larval lifetime and hence dispersal, both of which have profound effects on species biogeography. This is particularly important for sessile symbiotic anthozoans, including *Aiptasia* and corals, which depend upon favorable environmental conditions (e.g. temperature and light) for a thriving symbiotic partnership and consequent survival in their nutrient-poor environment.

Harii and colleagues hypothesized that the enlargement of the gastric cavity in coral larvae, which may be accompanied by the development of functional, ciliated gastrodermal cells, may enhance acquisition of symbionts by late developmental stages[15]. Indeed, in *Aiptasia* larvae we also find an enlargement of the gastric cavity as a result of the widening of the pharynx and the flattening of the endodermal tissue layer when comparing younger larvae to older larvae. However, such changes do not seem to drastically affect symbiont uptake efficiency of larvae or the total number of symbionts acquired, indicating that the observed changes may simply be developmentally associated and unrelated to symbiosis *per se*. However, we do observe a prominent difference in the spatial distribution of symbiont phagocytosis within the endoderm between younger and older larvae: younger larvae take up symbionts primarily in the aboral region, whereas older larvae efficiently take up symbionts in both the aboral and the oral region of the endoderm. It may be that the distribution of endodermal cells capable of phagocytosing symbionts changes and expands over time, potentially defining predominant symbiont uptake regions within the endoderm. A similar effect has been observed in larvae of the coral *Fungia scutaria*, in which the equatorial region of the endoderm was principally involved in phagocytosis of appropriate symbionts[14], supporting the idea of functional differences of endodermal cells in corals that may change over time. However, it remains unclear whether the endoderm of anthozoan larvae is differentiated into distinct cell types and, if so, when during

Brachyury F	5′ - AACCATATCCTTCAAGCCGCA - 3′
Brachyury R	5′ - AGATCCGCGCGCTTGTAATA - 3′
Forkhead F	5′ - AAGGCGCGCCGATCCCTCGCAAAACCCTCA - 3′
Forkhead R	5′ - AATTAATTAAGCAATTCGCCGCTGTAAACA - 3′
β-catenin F	5′ - AAGGCGCGCCTGGACACTGCGTAACCTGTC - 3′
β-catenin R	5′ - TTTTAATTAAGTTGTGTCGCGTTTTCAGCT - 3′
Chordin F	5′ - AAGGCGCGCCTCAGGCGCCATTCACAGATT - 3′
Chordin R	5′ - TTTTAATTAACACTTGGGTACGTCACGACA - 3′
Wnt2 F	5′ - AAGGCGCGCCGGTTGAATTCCAAATGAATAACAA - 3′
Wnt2 R	5′ - TTTTAATTAACAACACCAATAAAACTTACAGTAGCA - 3′
OtxA F	5′ - AAGGCGCGCCTGACTCCTCCAAACATTGATTTCT - 3′
OtxA R	5′ - TTTTAATTAAGGGATTGCCTATCTGTGACGA - 3′

Table 1. Primers used to generate *in situ* hybridization probes.

development this differentiation occurs. To this end, an important goal of future research is to determine which cellular features (e.g. cilia development, digestive properties, or expression of symbiont-uptake receptors) are responsible for rendering endodermal cells capable of symbiont acquisition and how these relate to larval endodermal development. Additionally, it will be particularly interesting to uncover the molecular mechanisms of when and how cnidarian larvae distinguish between symbionts and inert beads (as a proxy for food particles) ([14] and this study, Fig. 3d).

Our analyses presented here generate the framework for such future investigations by providing a thorough description of *Aiptasia* early development in relation to symbiosis establishment as well as essential tools including *in situ* hybridization and confocal microscopy. Together with the recently published *Aiptasia* genome and a robust spawning protocol as important resources[23,24], the field is now well positioned to begin dissecting the mechanisms of symbiont phagocytosis, integration, and maintenance in the cnidarian host cells at the cell and molecular levels, using *Aiptasia* larvae as a model system. The study of endosymbiosis between cnidarians and their symbionts as the foundation of coral reef ecosystems is of broad interest in cell biology as well as of high ecological and evolutionary relevance. Moreover, *Aiptasia* may also help to uncover common principles as well as differences of photosymbiosis, a diverse and complex phenomenon that has been found throughout the tree of life ranging from cnidarians to mollusks (e.g. giant clams and sea slugs) to vertebrates (e.g. salamanders)[47–49].

Methods

***Aiptasia* culture conditions and spawning induction.** *Aiptasia* strains CC7 and F003 were cultured and induced to produce larvae as previously described[23]. Larvae were collected and filtered as previously described[23] and kept in Intellus Ultra Controller Incubators (Model I-36LL4LX, Percival) at 26 °C on a diurnal 12L:12D cycle (12 h light:12 h dark) under white fluorescent bulbs with an intensity of ~20–25 μmol m^{-2} s^{-1} of photosynthetically active radiation (PAR), as measured with an Apogee PAR quantum meter (MQ-200, Apogee).

***Symbiodinium* culture conditions.** Clonal and axenic cultures of *Symbiodinium* strain SSB01[21] were maintained in IMK medium[50] at 26 °C and 20–25 μmol $m^{-2}s^{-1}$ of photosynthetically active radiation (PAR) as previously described[21]. To determine the approximate algal density of inocula in larval infection experiments, a Neubauer chamber was used for direct microscopic counts.

Brightfield microscopy of *Aiptasia* embryos and larvae. Embryos and larvae were collected and fixed for 30 min in 3.7% formaldehyde in filter-sterilized artificial seawater (FASW). Specimens were washed three times in PBS-0.2% Triton X-100 (PBT) and then washed into PBS, after which they were mounted in 1:1 glycerol:PBS on glass slides with glass coverslips. Embryos and larvae were imaged with a Nikon Eclipse 80i microscope using Differential Interference Contrast (DIC), a Nikon Plan Fluor 20× dry lens, and a Digital Sight DS-1QM camera (Nikon Instruments).

***In situ* hybridization of *Aiptasia* embryos and larvae.** Probes for *in situ* hybridization of *Aiptasia Forkhead*, *Brachyury*, *β-catenin*, *Chordin*, *Wnt2*, and *OtxA* were designed by using the according *Nematostella vectensis* gene sequences to locate the sequences in the *Aiptasia* genome[24]. Fragments of the genes were amplified from *Aiptasia* CC7[25] genomic DNA or larval first-strand cDNA via PCR (primer sequences in Table 1). PCR reactions of 50 μl contained 2U Phusion polymerase, 0.1 μM of each primer, 200 μM dNTPs, 1X Phusion HF Buffer (#B0518S, NEB), and 50–150 ng template DNA. Amplification conditions were as follows: initial denaturation at 98 °C for 2 min; 35 cycles of denaturation at 98 °C for 15 s, annealing at 60–63 °C for 30 s, extension at 72 °C for 1 min; final extension at 70 °C for 10 min. Fragments of the expected size were then cloned into the pCRII TOPO-TA Dual Promoter vector (#45-0640, Qiagen) and sequenced with M13F and M13R standard primers to confirm their identity. Digoxygenin-labeled riboprobes were synthesized using the SP6/T7 Transcription Kit (#10999644001, Roche) according to the manufacturer's instructions.

The following *in situ* hybridization protocol is based on that previously described for *Nematostella*[51], with modifications. Larvae were fixed for 1 h in 4% formaldehyde in FASW, washed twice in PBT, and then stored in 100% methanol at −20 °C until further use. Fixed larvae were rehydrated by sequential washes in: 100% methanol; 60% methanol/40% PBS-0.1% Tween-20 (PTW); 30% methanol/70% PTW; 100% PTW. Larvae were then

permeabilized with 10 μg/ml proteinase K in PTW for 8 min. This was followed by two washes in 2 mg/ml glycine in PTW, one wash in 1% triethanolamine in PTW, and two washes each in 0.3% and 0.6% acetic anhydride/1% triethanolamine in PTW respectively. Larvae were then washed twice in PTW and post-fixed in 4% formaldehyde in PTW for 30 min. After five PTW washes, larvae were transferred into hybridization solution consisting of: 50% formamide, 4X SSC pH 4.5, 50 μg/ml Heparin, 0.25% Tween-20, 1% SDS, 50 μg/ml salmon sperm DNA (#15632-011, Invitrogen). Pre-hybridization was performed first at room temperature (RT) for 10 min, after which the hybridization solution was exchanged and pre-hybridization continued for 1 h at 61 °C. Full hybridization was then carried out at 61 °C for approximately 36 h with 1 ng/ul final probe concentration. Unbound probe was removed by washing twice in hybridization solution, and then larvae were transferred to 2X SSC by sequential washing at 61 °C in the following proportions of hybridization buffer/2X SSC: 100% hybridization solution; 75%/25%; 50%/50%; 25%/75%; 100% 2X SSC. Larvae were then washed twice in 0.05X SSC at 61 °C. Larvae were then transferred to PTW by sequential washing at RT in the following proportions of 0.05X SSC/PTW: 100% 0.05X SSC; 75%/25%; 50%/50%; 25%/75%; 100% PTW. Samples were then blocked in 1X blocking solution (#11096176001, Roche) diluted in maleic acid buffer (0.1 M maleic acid, 0.05 M NaCl) for 30 min at RT. Probe detection was achieved by incubation with an anti-DIG alkaline-phosphatase-conjugated antibody (#11093274910, Roche) diluted 1:5000 in blocking solution overnight at 4 °C. After 10 washes in PBT, larvae were washed twice in AP buffer (0.1 M Tris-HCl pH 9.5, 0.1 M NaCl, 0.1% Tween 20) without $MgCl_2$ and twice in AP buffer with 0.05 M $MgCl_2$. Probe detection was performed with NBT/BCIP (#11681451001, Roche) diluted 1:50 in buffer (0.1 M Tris-HCl pH 9.5, 0.1 M NaCl). Detection was stopped with several rinses in 100% ethanol, and larvae were mounted in 1:1 glycerol:PBS on glass slides with glass coverslips Specimens were imaged with a Nikon Eclipse 80i microscope using Differential Interference Contrast (DIC), a Nikon Plan Fluor 20× dry lens, and a Digital Sight DS-U1 color camera (Nikon Instruments).

Symbiosis establishment in *Aiptasia* larvae. For infections, larvae were counted as previously described[23] and distributed in 6-well plates with 300–500 larvae in 5 ml FASW per well. Infection with *Symbiodinium* strain SSB01[21] was performed by adding algae to each well at a final concentration of 1,000, 10,000, or 100,000 algal cells/ml, as indicated in the text. After addition of algae, each well was mixed by gently pipetting up and down. Infection experiments with inert polystyrene fluorescent beads (#C36950, Life Technologies) were carried out identically; FASW was used as a negative control. Larvae were then fixed for 1 h in 4% formaldehyde in FASW, washed three times in PBT, washed into PBS, and then mounted in 1:1 glycerol:PBS on glass slides with glass coverslips. Slides were analyzed using a Nikon Eclipse 80i microscope with a Nikon Plan Fluor 20× dry lens. A minimum of 70 larvae per slide were scored per condition per time-point.

Confocal microscopy of *Aiptasia* embryos and larvae. For confocal imaging, embryos and larvae were fixed in 3.7% formaldehyde in FASW for 30 min, washed three times in PBT, and washed once in PBS. Approximately 50–100 larvae were transferred to PCR tubes and permeabilized with 10 μg/ml proteinase K in PBS for 8 min. Permeabilization was stopped by washing twice for 5 min in 2 mg/ml glycine in PBT. Larvae were post-fixed in 3.7% formaldehyde in PBT, then washed twice for 10 min in PBT and twice for 10 min in PBS. Larvae were incubated with AlexaFluor-488 phalloidin (#A12379, Invitrogen) diluted 1:300 in PBS for 1 h at RT on a rotor (Intelli mixer #7-0045, NeoLab) at a speed of 20 rpm. Larvae were then washed twice for 15 min in PBT and incubated with 10 μg/ml Hoechst in buffer (Tris-buffered saline, pH 7.4, 0.1% Triton X-100, 2% bovine serum albumin, 0.1% sodium azide) for 15 min. Final washes were carried out in PBT three times each for 15 min. Samples were mounted in 87% glycerol in PBS containing 2.5 mg/ml DABCO (1,4-Diazabicyclo[2.2.2]octan, #D27802, Sigma Aldrich). Images of embryos and larvae in Figs. 2 and 3f were acquired using a Nikon A1 confocal microscope with a Nikon Plan Fluor 40× oil immersion objective and Nikon Elements Software. Images of intracellular algae in Fig. 3c were acquired using a Leica TCS SP5II confocal microscope with a Leica HCX PL APO lambda blue 63.0 × 2.10 UV water immersion objective and Leica Application Suite Advanced Fluorescence software. Image processing and maximum projections of Z-stacks was performed using Fiji[52].

References

1. Muscatine, L. The role of symbiotic algae in carbon and energy flux in coral reefs In *Coral Reefs* (ed. Zubinsky, Z.) 75–87 (Elsevier, 1990).
2. Pochon, X. & Gates, R. D. A new *Symbiodinium* clade (Dinophyceae) from soritid foraminifera in Hawai'i. *Mol. Phylogenet. Evol.* **56,** 492–497 (2010).
3. Rowan, R. Coral bleaching: thermal adaptation in reef coral symbionts. *Nature* **430,** 742 (2004).
4. Jones, A. M., Berkelmans, R., van Oppen, M. J. H., Mieog, J. C. & Sinclair, W. A community change in the algal endosymbionts of a scleractinian coral following a natural bleaching event: field evidence of acclimatization. *Proc. Biol. Sci.* **275,** 1359–1365 (2008).
5. Sampayo, E. M., Ridgway, T., Bongaerts, P. & Hoegh-Guldberg, O. Bleaching susceptibility and mortality of corals are determined by fine-scale differences in symbiont type. *Proc. Natl. Acad. Sci. USA* **105,** 10444–10449 (2008).
6. Fadlallah, Y. H. Sexual reproduction, development and larval biology in scleractinian corals. *Coral Reefs* **2,** 129–150 (1983).
7. Harrison, P. L. Sexual reproduction of scleractinian corals In *Coral Reefs: an Ecosystem in Transition* (eds. Zubinsky, Z. & Stambler, N.) 59–85 (Springer, 2011).
8. Brusca, R. C. & Brusca, G. J. In *Invertebrates* 2nd edn, Ch. 8, 253–260 (Sinauer Associates, 2003).
9. Fritzenwanker, J. H., Saina, M. & Technau, U. Analysis of *forkhead* and *snail* expression reveals epithelial-mesenchymal transitions during embryonic and larval development of *Nematostella vectensis*. *Dev. Biol.* **275,** 389–402 (2004).
10. Magie, C. R., Daly, M. & Martindale, M. Q. Gastrulation in the cnidarian *Nematostella vectensis* occurs via invagination not ingression. *Dev. Biol.* **305,** 483–497 (2007).
11. Schwarz, J. A., Krupp, D. A. & Weis, V. M. Late larval development and onset of symbiosis in the scleractinian coral *Fungia scutaria*. *Biol. Bull.* **196,** 70–79 (1999).
12. van Oppen, M. *In vitro* establishment of symbiosis in *Acropora millepora* planulae. *Coral Reefs* **20,** 200 (2001).
13. Baird, A. H. *et al.* Environmental controls on the establishment and development of algal symbiosis in corals. *Proc. 11th Int. Coral Reef Symp.* **5,** 108–112 (2008).

14. Rodriguez-Lanetty, M., Wood-Charlson, E. M., Hollingsworth, L. L., Krupp, D. A. & Weis, V. M. Temporal and spatial infection dynamics indicate recognition events in the early hours of a dinoflagellate/coral symbiosis. *Mar. Biol.* **149,** 713–719 (2006).
15. Harii, S., Yasuda, N., Rodriguez-Lanetty, M., Irie, T. & Hidaka, M. Onset of symbiosis and distribution patterns of symbiotic dinoflagellates in the larvae of scleractinian corals. *Mar. Biol.* **156,** 1203–1212 (2009).
16. Marlow, H. Q. & Martindale, M. Q. Embryonic development in two species of scleractinian coral embryos: *Symbiodinium* localization and mode of gastrulation. *Evol. Dev.* **9,** 355–367 (2007).
17. Babcock, R. C. *et al.* Synchronous spawnings of 105 scleractinian coral species on the Great Barrier Reef. *Mar. Biol.* **90,** 379–394 (1986).
18. Houliston, E., Momose, T. & Manuel, M. *Clytia hemisphaerica*: a jellyfish cousin joins the laboratory. *Trends Genet.* **26,** 159–167 (2010).
19. Kraus, Y. *et al.* The embryonic development of the cnidarian *Hydractinia echinata*. *Evol. Dev.* **16,** 323–338 (2014).
20. Weis, V. M., Davy, S. K., Hoegh-Guldberg, O., Rodriguez-Lanetty, M. & Pringle, J. R. Cell biology in model systems as the key to understanding corals. *Trends Ecol. Evol.* **7,** 369–376 (2008).
21. Xiang, T., Hambleton, E. A., DeNofrio, J. C., Pringle, J. R. & Grossman, A. R. Isolation of clonal axenic strains of the symbiotic dinoflagellate *Symbiodinium* and their growth and host specificity. *J. Phycol.* **49,** 447–458 (2013).
22. Hambleton, E. A., Guse, A. & Pringle, J. R. Similar specificities of symbiont uptake by adults and larvae in an anemone model system for coral biology. *J. Exp. Biol.* **217,** 1613–1619 (2014).
23. Grawunder, D. *et al.* Induction of gametogenesis in the cnidarian endosymbiosis model *Aiptasia* sp. *Sci. Rep*. **5,** 15677 (2015).
24. Baumgarten, S. *et al.* The genome of *Aiptasia*, a sea anemone model for coral symbiosis. *Proc. Natl. Acad. Sci. USA* **112,** 11893–11898 (2015).
25. Sunagawa, S. *et al.* Generation and analysis of transcriptomic resources for a model system on the rise: the sea anemone *Aiptasia pallida* and its dinoflagellate endosymbiont. *BMC Genomics* **10,** 258 (2009).
26. Lehnert, E. M. *et al.* Extensive differences in gene expression between symbiotic and aposymbiotic cnidarians. *G3 (Bethesda)* **4,** 277–295. (2014).
27. Bayer, T. *et al. Symbiodinium* transcriptomes: genome insights into the dinoflagellate symbionts of reef-building corals. *PLoS ONE* **7,** e35269 (2012).
28. Shoguchi, E. *et al.* Draft assembly of the *Symbiodinium minutum* nuclear genome reveals dinoflagellate gene structure. *Curr. Biol.* **23,** 1399–1408 (2013).
29. Xiang, T., Nelson, W., Rodriguez, J., Tolleter, D. & Grossman, A. R. *Symbiodinium* transcriptome and global responses of cells to immediate changes in light intensity when grown under autotrophic or mixotrophic conditions. *Plant J.* **82,** 67–80 (2015).
30. Fritzenwanker, J. H., Genikhovich, G., Kraus, Y. & Technau, U. Early development and axis specification in the sea anemone *Nematostella vectensis*. *Dev. Biol.* **310,** 264–279 (2007).
31. Hand, C. & Uhlinger, K. R. The culture, sexual and asexual reproduction, and growth of the sea anemone *Nematostella vectensis*. *Biol. Bull.* **182,** 169–176 (1992).
32. Sinigaglia, C., Busengdal, H., Lerner, A., Oliveri, P. & Rentzsch, F. Molecular characterization of the apical organ of the anthozoan *Nematostella vectensis*. *Dev. Biol.* **398,** 120–133 (2015).
33. Scholz, C. B. & Technau, U. The ancestral role of *Brachyury*: expression of *NemBra1* in the basal cnidarian *Nematostella vectensis* (Anthozoa). *Dev. Genes Evol.* **212,** 563–570. (2003).
34. Wikramanayake, A. H. *et al.* An ancient role for nuclear beta-catenin in the evolution of axial polarity and germ layer segregation. *Nature* **426,** 446–450 (2003).
35. Saina, M., Genikhovich, G., Renfer, E. & Technau, U. BMPs and Chordin regulate patterning of the directive axis in a sea anemone. *Proc. Natl. Acad. Sci. USA* **106,** 18592–18597 (2009).
36. Rentzsch, F. *et al.* Asymmetric expression of the BMP antagonists *chordin* and *gremlin* in the sea anemone *Nematostella vectensis*: implications for the evolution of axial patterning. *Dev. Biol.* **296,** 375–387 (2006).
37. Kusserow, A. *et al.* Unexpected complexity of the *Wnt* gene family in a sea anemone. *Nature* **433,** 156–160 (2005).
38. Mazza, M. E., Pang, K., Martindale, M. Q. & Finnerty, J. R. Genomic organization, gene structure, and developmental expression of three clustered *otx* genes in the sea anemone *Nematostella vectensis*. *J. Exp. Zool. B. Mol. Dev. Evol.* **308,** 494–506 (2007).
39. Colley, N. J. & Trench, R. K. Cellular events in the reestablishment of a symbiosis between a marine dinoflagellate and a coelenterate. *Cell Tissue Res.* **239,** 93–103 (1985).
40. Muscatine, L. *et al.* Cell-specific density of symbiotic dinoflagellates in tropical anthozoans. *Coral Reefs* **17,** 329–337 (1998).
41. Gates, R. D. & Muscatine, L. Three methods for isolating viable anthozoan endoderm cells with their intracellular symbiotic dinoflagellates. *Coral Reefs* **11,** 143–154 (1992).
42. Okubo, N. *et al.* Comparative embryology of eleven species of stony corals (Scleractinia). *PLoS One.* **8,** e84115 (2013).
43. Leclère, L. & Rentzsch, F. RGM regulates BMP-mediated secondary axis formation in the sea anemone *Nematostella vectensis*. *Cell Rep*. **9,** 1921–1930 (2014).
44. Nakanishi, N., Renfer, E., Technau, U. & Rentzsch, F. Nervous systems of the sea anemone *Nematostella vectensis* are generated by ectoderm and endoderm and shaped by distinct mechanisms. *Development* **139,** 347–357 (2012).
45. Iwao, K., Fujisawa, T. & Hatta, M. A cnidarian neuropeptide of the GLWamide family induces metamorphosis of reef-building corals in the genus *Acropora*. *Coral Reefs* **21,** 127–129 (2002).
46. Jeackle, W. & Smith, A. K. Feeding modes of larvae of *Nematostella vectensis* (Cnidaria: Anthozoa), *Students' Professional Presentations and Publications*. Paper 2 (2013).
47. Rumpho, M. E., Pelletreau, K. N., Moustafa, A. & Bhattacharya, D. The making of a photosynthetic animal. *J. Exp. Biol.* **214,** 303–311 (2011).
48. de Vries, J., Christa, G. & Gould, S. B. Plastid survival in the cytosol of animal cells. *Trends Plant Sci.* **19,** 347–350 (2014).
49. Graham, E. R., Fay, S. A., Davey, A. & Sanders, R. W. Intracapsular algae provide fixed carbon to developing embryos of the salamander *Ambystoma maculatum*. *J. Exp. Biol.* **216,** 452–459 (2013).
50. Ishikura, M. *et al.* Isolation of new *Symbiodinium* strains from Tridacnid giant clam (*Tridacna crocea*) and sea slug (*Pteraeolidia ianthina*) using culture medium containing giant clam tissue homogenate. *Mar. Biotechnol.* **6,** 378–385 (2004).
51. Genikhovich, G. & Technau, U. *In situ* hybridization of starlet sea anemone (*Nematostella vectensis*) embryos, larvae, and polyps. *Cold Spring Harb. Protoc. 2009* **4,** 1–5 (2009).
52. Schindelin, J. *et al.* Fiji: an open-source platform for biological-image analysis. *Nature Methods* **9,** 676–682 (2012).

Acknowledgements

Funding was provided to A.G. by the Emmy-Noether-Programme of the German Research Foundation (DFG) (grant no. GU 1128/3-1) and by a Marie Curie Career Integration Grant (CIG) under the FP7-PEOPLE-2013-CIG program, European Commission; to I.W. by a PhD fellowship from the Foundation for Science and Technology (FCT, Portugal); and to P.A.V. by a PhD fellowship from the Baden-Württemberg Landesgraduiertenförderung Program. We thank Steffen Lemke, Thomas Holstein, and Suat Özbek for advice, comments, and sharing reagents and equipment; Falco Krüger and Karin Schumacher for Leica confocal microscopy and advice; and Natascha Bechtoldt for technical help with experiments.

Author Contributions

M.B., I.W., P.A.V. and A.G. designed the experiments; M.B., I.W. and P.A.V. performed the experiments. M.B., E.A.H. and A.G. wrote the manuscript. All authors reviewed the manuscript.

Additional Information

Competing financial interests: The authors declare no competing financial interests.

How to cite this article: Bucher, M. *et al.* Development and symbiosis establishment in the cnidarian endosymbiosis model *Aiptasia* sp. *Sci. Rep.* **6**, 19867; doi: 10.1038/srep19867 (2016).

Publication 3: "*Aiptasia* sp. larvae as a model to reveal mechanisms of symbiont selection in cnidarians"

Highlights

In this publication a comparative study between *Aiptasia* and two broadcasting coral species reveals many similarities between these organisms. The highlights of the following publication are:

- *Aiptasia* and *Acropora* larvae show common patterns of symbiont selection at initial life stages: three *Symbiodinium* types are positively selected (SSB01, SSA02 and CCMP2556) and one type (SSE01) is negatively selected;
- The so-far thought non-symbiotic/"free-living" *Symbiodinium* SSE01 is found internalized by endodermal cells in *Aiptasia* larvae;
- *Aiptasia* larvae positively selects symbionts pre- and post-phagocytosis;
- RNA-Seq of *Aiptasia* larvae shows clear differences of differentially expressed genes before and after symbiosis establishment opening new avenues of future investigation.

Author contribution

I am the first author of this publication and designed, performed and analyzed the experiments in Figures 1 and 2. I also collected the data in Supplementary Figures S1 and S2, Supplementary Tables S2 and S3.

This is an "Open access" publication.

SCIENTIFIC REPORTS

OPEN

Aiptasia sp. larvae as a model to reveal mechanisms of symbiont selection in cnidarians

Received: 26 April 2016
Accepted: 08 August 2016
Published: 01 September 2016

Iliona Wolfowicz[1,2], Sebastian Baumgarten[3,*,†], Philipp A. Voss[1,*], Elizabeth A. Hambleton[1], Christian R. Voolstra[3], Masayuki Hatta[4] & Annika Guse[1]

Symbiosis, defined as the persistent association between two distinct species, is an evolutionary and ecologically critical phenomenon facilitating survival of both partners in diverse habitats. The biodiversity of coral reef ecosystems depends on a functional symbiosis with photosynthetic dinoflagellates of the highly diverse genus *Symbiodinium*, which reside in coral host cells and continuously support their nutrition. The mechanisms underlying symbiont selection to establish a stable endosymbiosis in non-symbiotic juvenile corals are unclear. Here we show for the first time that symbiont selection patterns for larvae of two *Acropora* coral species and the model anemone *Aiptasia* are similar under controlled conditions. We find that *Aiptasia* larvae distinguish between compatible and incompatible symbionts during uptake into the gastric cavity and phagocytosis. Using RNA-Seq, we identify a set of candidate genes potentially involved in symbiosis establishment. Together, our data complement existing molecular resources to mechanistically dissect symbiont phagocytosis in cnidarians under controlled conditions, thereby strengthening the role of *Aiptasia* larvae as a powerful model for cnidarian endosymbiosis establishment.

Coral reefs, the most biodiverse marine ecosystem on earth, depend on a functional symbiosis between corals and dinoflagellate algae to survive in nutrient poor waters. Intracellular dinoflagellates from the genus *Symbiodinium* transfer photosynthetic products to the coral host, thereby greatly contributing to corals' nutrition in tropical habitats[1]. The genus *Symbiodinium* is very diverse[2] and it has been known for decades that symbiont/host combinations are not random: corals establish symbiosis with some *Symbiodinium* types but not others, termed "symbiosis specificity"[3,4]. In the face of climate change, this phenomenon has attracted increasing attention because certain symbiont types may allow their host to cope with changing environments better than others[5–9]. Despite this ecological importance, the fundamental mechanisms underlying "symbiosis specificity" remain poorly understood.

Symbiont selectivity may be in part governed during early life stages: many coral species produce symbiont-free offspring that acquire symbionts from the environment[10,11], and coral larvae often appear to favor homologous symbionts (i.e. those found in parents) over heterologous types[5,12,13]. Similar to other endosymbiotic relationships, establishment of coral symbiosis is thought to follow a "winnowing process"[14,15] comprising a series of steps, each of which is crucial for a stable, specific symbiotic interaction. In coral larvae and juvenile polyps, the following steps are involved in symbiosis establishment: symbiont entrance into the gastric cavity, symbiont phagocytosis by endodermal host cells, symbiont integration into the host cells, initiation of nutrient transfer, and symbiont proliferation throughout the endodermal tissue of the host. Because adult corals may not be capable of continuously acquiring new symbionts from the environment, the symbiont population integrated during early life stages is most likely important for a functional interplay between symbionts and host cells[4,16].

The molecular mechanisms underlying the steps in symbiont selection in juvenile corals are poorly understood. Likewise, how long-term hosting of foreign organisms affects host and symbiont cell physiologies,

[1]Centre for Organismal Studies (COS), Heidelberg University, Heidelberg 69120, Germany. [2]Graduate Program in Areas of Basic and Applied Biology (GABBA), University of Porto, Porto 4200-465, Portugal. [3]Red Sea Research Center, Division of Biological and Environmental Science and Engineering, King Abdullah University of Science and Technology (KAUST), Thuwal 23955-6900, Saudi Arabia. [4]Graduate School of Humanities and Sciences, Ochanomizu University, Tokyo 112-8610, Japan. [†]Present address: Biology of Host-Parasite Interactions Unit, Institut Pasteur, Paris 75015, France. [*]These authors contributed equally to this work. Correspondence and requests for materials should be addressed to A.G. (email: annika.guse@cos.uni-heidelberg.de)

including gene expression, nutrient transfer, cell organization, and cell division, is largely unclear. Progress in understanding these processes mechanistically has been, and still is, slow because molecular tools for corals and their larvae are sparse. For example, the identification of key players involved in symbiosis establishment is still in its infancy: previous comparative transcriptomics in coral larvae were unable to find many candidates. One reason may be presumably low symbiont-to-host-cell ratios that masked signals from symbiont-carrying endodermal tissue[17–19]. Furthermore, many corals spawn only once annually, severely limiting larvae access and optimization of experiments.

The small sea anemone *Aiptasia* is an emerging model for coral symbiosis[20]. Similar to corals, *Aiptasia* produces symbiont-free offspring that then establish symbiosis with various *Symbiodinium* strains but not others, suggesting that "symbiosis specificity" is a common, lineage-independent phenomenon among symbiotic cnidarians[21,22]. Importantly, defined clonal lines are available for *Aiptasia* and for *Symbiodinium*, including axenic strains representing four of the nine described major *Symbiodinium* clades A-I[2,21,23].

We recently established a robust protocol to induce *Aiptasia* spawning in the laboratory[23]. We then described when and where during larval development symbionts are phagocytosed by endodermal cells, defining reproducible experimental conditions for analyzing symbiont acquisition, and developed a set of experimental tools[24]. These resources, in conjunction with various transcriptomic, proteomic, and genomic resources for *Aiptasia*, *Symbiodinium*, and corals (for comparative analyses)[25–32], provide the foundation to use *Aiptasia* larvae as a platform to study the molecular mechanisms of symbiosis establishment in cnidarians.

Here we further develop the *Aiptasia* larval system as a model for uncovering fundamental aspects of cnidarian symbiont selection at the molecular level. We directly compared symbiont selection patterns between larvae of *Aiptasia* and of two major reef-building coral species: *Acropora digitifera* and *Acropora tenuis*. We found that the overall patterns of "symbiosis specificity" are maintained between lineages, suggesting common underlying mechanisms of symbiont selection in *Aiptasia* and corals. Using *Aiptasia* larvae as a model, we find that both uptake into the gastric cavity and phagocytosis into the endoderm play a role in distinguishing between compatible and incompatible symbionts, and we identified a set of genes likely involved in symbiosis establishment by RNA-Seq. We conclude that *Aiptasia* is a powerful system to dissect the complex molecular mechanisms underlying initial symbiont selection.

Results

Symbiosis patterns are similar in *Aiptasia* and *Acropora*. To date, a direct comparison of symbiosis establishment patterns between *Aiptasia* and corals is missing. To assess similarities and differences between *Aiptasia* and two major reef-building corals of the genus *Acropora*, *A. tenuis* and *A. digitifera*, we compared symbiont selection at early life stages using defined *Symbiodinium* strains. We incubated *Aiptasia* and coral larvae with four clonal, axenic *Symbiodinium* strains – SSA01, SSA02 (both clade A), SSB01 (clade B), SSE01 (clade E)[21,23] – and the non-clonal, non-axenic strain CCMP2556 (clade D)[33,34] for 10 days. We found that the strains SSA02, SSB01, and CCMP2556 efficiently infected hosts, whereas strain SSE01 was found in lower proportions of the larval populations (Fig. 1a–c). Strain SSA01[23–25] was able to efficiently establish symbiosis with *Aiptasia* larvae but was rarely found in *Acropora* larvae (Fig. 1b–d). In line with the observation that the *Symbiodinium* strains SSA02, SSB01, and CCMP2556 efficiently infect coral larvae, microscopic analysis shows that many *Symbiodinium* cells were taken up per larva, especially when compared to strains SSE01 and SSA01 (Fig. 1d; Supplementary Fig. S1).

Symbiosis establishment patterns are maintained between larva and polyp stages in *Aiptasia*[22]; to test whether such similarities hold true for *Acropora* larvae and juvenile polyps, we exposed juvenile *Acropora* polyps to the five different *Symbiodinium* strains for four days, after which algae were removed from the environment; progression of infection was monitored for six additional days (Fig. 2; Supplementary Fig. S2). We found that, as in conspecific larvae, polyps were efficiently infected by the *Symbiodinium* strains SSB01, SSA02, and CCMP2556 within the monitored time period (Fig. 2a). Symbiosis establishment occurred rapidly, with most polyps hosting algae after only 5 days and comparably robust populations after 10 days (Fig. 2a). Residential algal populations increased after the removal of environmental algae, indicating *in hospite* symbiont proliferation (Fig. 2a). *Symbiodinium* strains SSA01 and SSE01 failed to effectively infect polyps of either coral species, as these algae were nearly undetectable in polyps (Fig. 2; Supplementary Fig. S2).

Symbiosis patterns established during early life stages may change over longer time periods[4,8]. Therefore, we tested whether the two symbiont types that infect *Acropora* most effectively, SSB01 and CCMP2556, were maintained over longer time periods in polyps under laboratory conditions. We exposed *A. tenuis* and *A. digitifera* larvae to either *Symbiodinium* strain for nine days, induced metamorphosis, and monitored the *in hospite* algal populations in the polyps with light microscopy 2, 23, and 49 days post-metamorphosis (dpm). At 2 dpm, the majority of polyps hosted symbionts: for *A. tenuis*, 35 of 35 polyps had SSB01 and 34 of 34 had CCMP2556; for *A. digitifera*, 12 of 16 had SSB01 and 26 of 27 had CCMP2556. At 23 dpm, 100% of the polyps were infected. At 49 dpm, 100% of polyps remained infected, although polyp budding and mortality led to different polyp numbers: for *A. tenuis*, 43 polyps with SSB01 and 41 with CCMP2556; for *A. digitifera*, 25 polyps with SSB01 and 18 with CCMP2556. Although all polyps were infected in the duration of the experiment, the populations of both CCMP2556 and SSB01 appeared to decrease during the monitored time period, SSB01 apparently more drastically than CCMP2556 (Fig. 3).

Early acquisition steps are more efficient for compatible symbionts than incompatible symbionts. Our comparative analysis showed striking similarities in symbiont selection between *A. tenuis, A. digitifera*, and *Aiptasia*, with high compatibility of SSB01 and low compatibility of SSE01. To better understand the common principles underlying the broad preference for SSB01 over SSE01, we used *Aiptasia* larvae as a model and compared two distinct steps during the early phase of symbiosis establishment: uptake of symbionts into the

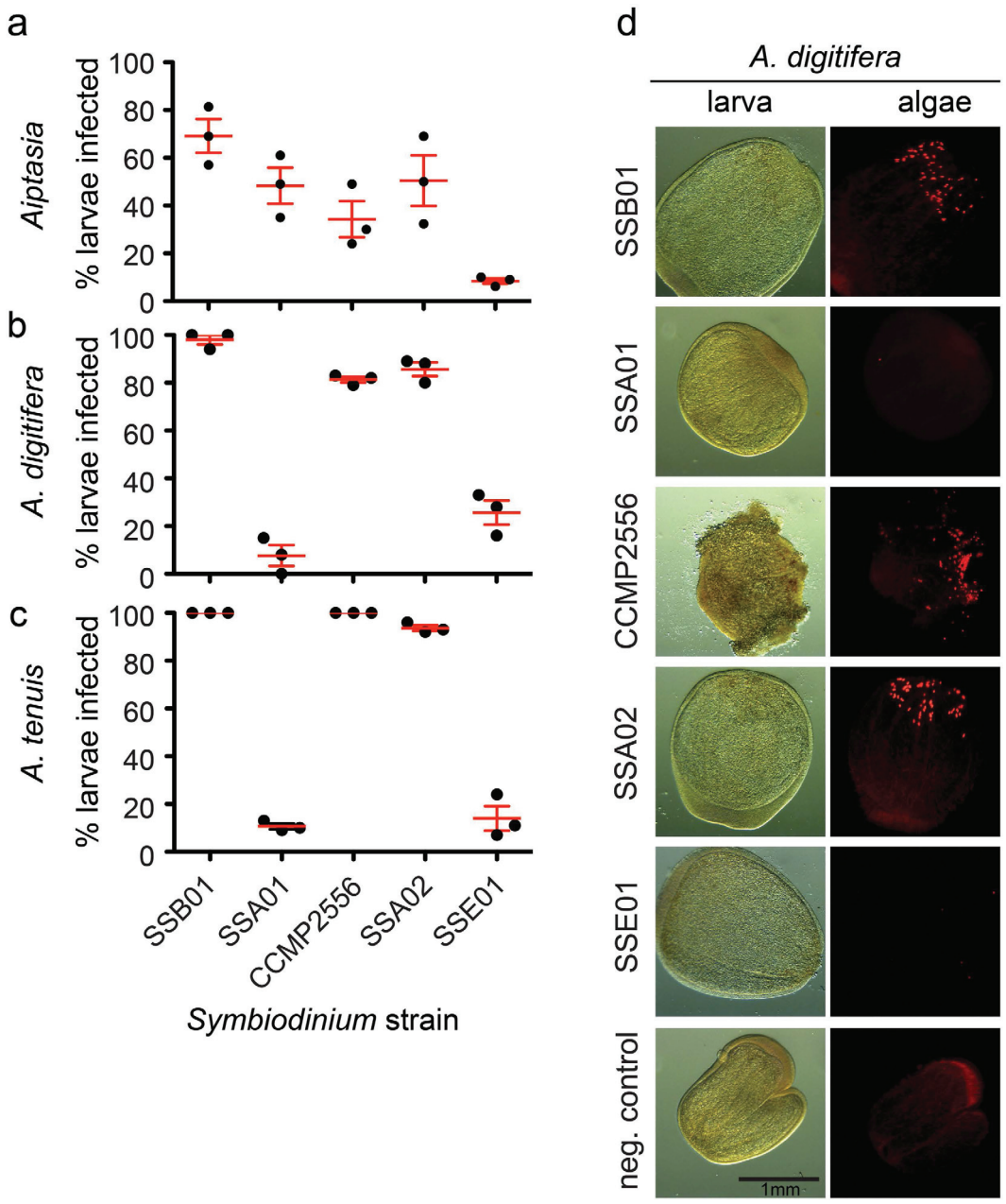

Figure 1. Symbiosis patterns are similar between *Aiptasia* and *Acropora*. (**a**–**c**) Percentage of infected larvae of *Aiptasia* (**a**) and the corals *Acropora digitifera* (**b**) and *Acropora tenuis* (**c**) after exposure to the indicated *Symbiodinium* strains at 10,000 algal cells/ml for 10 days. Strains used in this study are SSB01 (clade B), SSA01 (clade A), CCMP2556 (clade D), SSA02 (clade A), and SSE01 (clade E). Infected larvae contain one or more algal cells. Error bars are SEM of 3 replicate experiments. (**d**) Representative images of *Symbiodinium* infections in *A. digitifera* larvae. Left panels are brightfield images, right panels are red autofluorescence of algal photosynthetic pigments. Note the diffuse weak autofluorescence of larvae that is distinct from the bright puncta of the algae.

gastric cavity and phagocytosis of symbionts into the endodermal tissue. We infected *Aiptasia* larvae 6–7 days post-fertilization (dpf) for four days with either SSB01, SSE01, or inert fluorescent polystyrene beads (7 μm diameter) and again found that SSB01 was taken up more efficiently by *Aiptasia* larvae (an average 65% of larvae contained one or more symbionts) than SSE01 and inert beads (19% and 10%, respectively) (Fig. 4a). When distinguishing the localization of algae inside larvae (Fig. 4b), we found that the majority of SSB01 algae appeared to be integrated in the endoderm (63%; 1072/1693), compared to only 33% (65/198) of SSE01 algae (Fig. 4c). Interestingly, of the beads that were taken up by larvae, a higher proportion (49%; 48/98) than SSE01 were found in the endoderm (Fig. 4c). Because SSE01 has been thought to be free-living[21,33,35], its endodermal localization was surprising. We therefore imaged larvae at the tissue and cellular level using confocal microscopy to demonstrate that, indeed, SSB01 and SSE01 are found intracellularly in the endodermal cells (Fig. 4d,e).

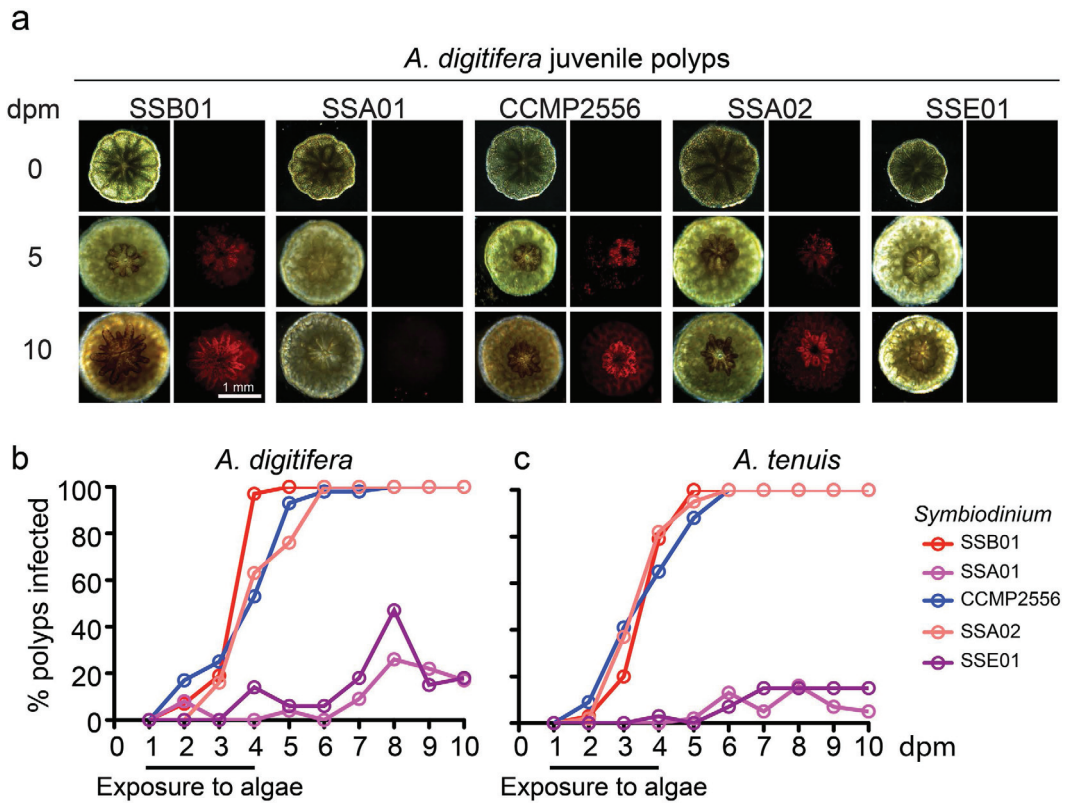

Figure 2. Symbiosis patterns are maintained between *Acropora* larvae and juvenile polyps. (**a**) Representative images of *Symbiodinium* infections in *A. digitifera* polyps. Left panels are brightfield images, right panels are red autofluorescence of algal photosynthetic pigments. dpm = days post-metamorphosis. (**b**,**c**) Percentage of infected juvenile polyps of *A. digitifera* (**b**) and *A. tenuis* (**c**) after exposure to the indicated *Symbiodinium* strains at 10,000 algal cells/ml for 4 days. Infected polyps contained visible algal cells.

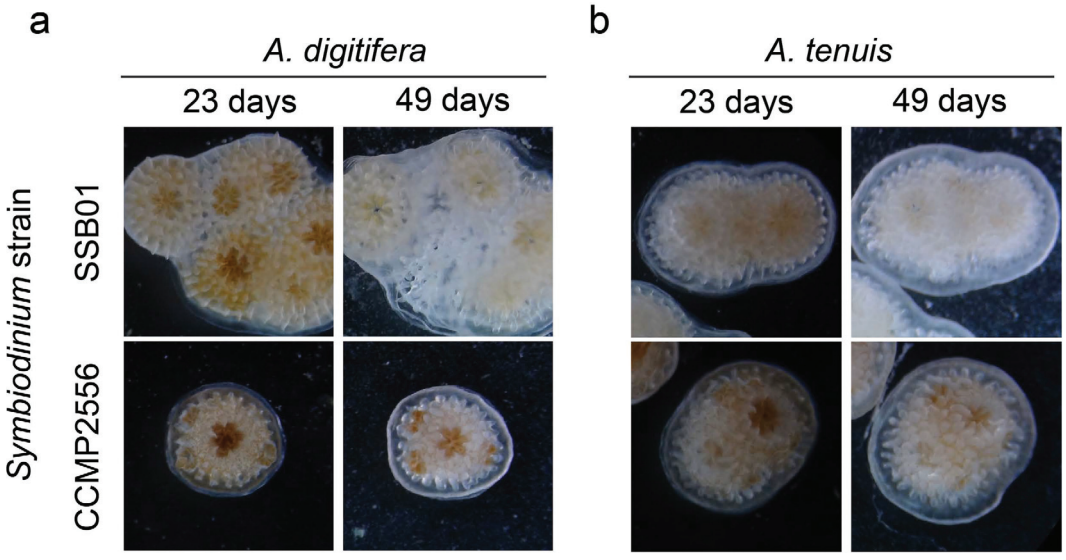

Figure 3. Long-term symbiosis patterns in juvenile *Acropora* polyps. Representative brightfield images of changes in residential *Symbiodinium* populations (brown coloration) over time in juvenile polyps of *A. digitifera* (**a**) and *A. tenuis* polyps (**b**) monitored for 49 days under laboratory conditions.

In other systems, phagocytosis efficiency is dependent on size and shape of the phagocytosed particle, with larger particles being phagocytosed less efficiently than smaller ones[36]. As noted previously, SSE01 cells

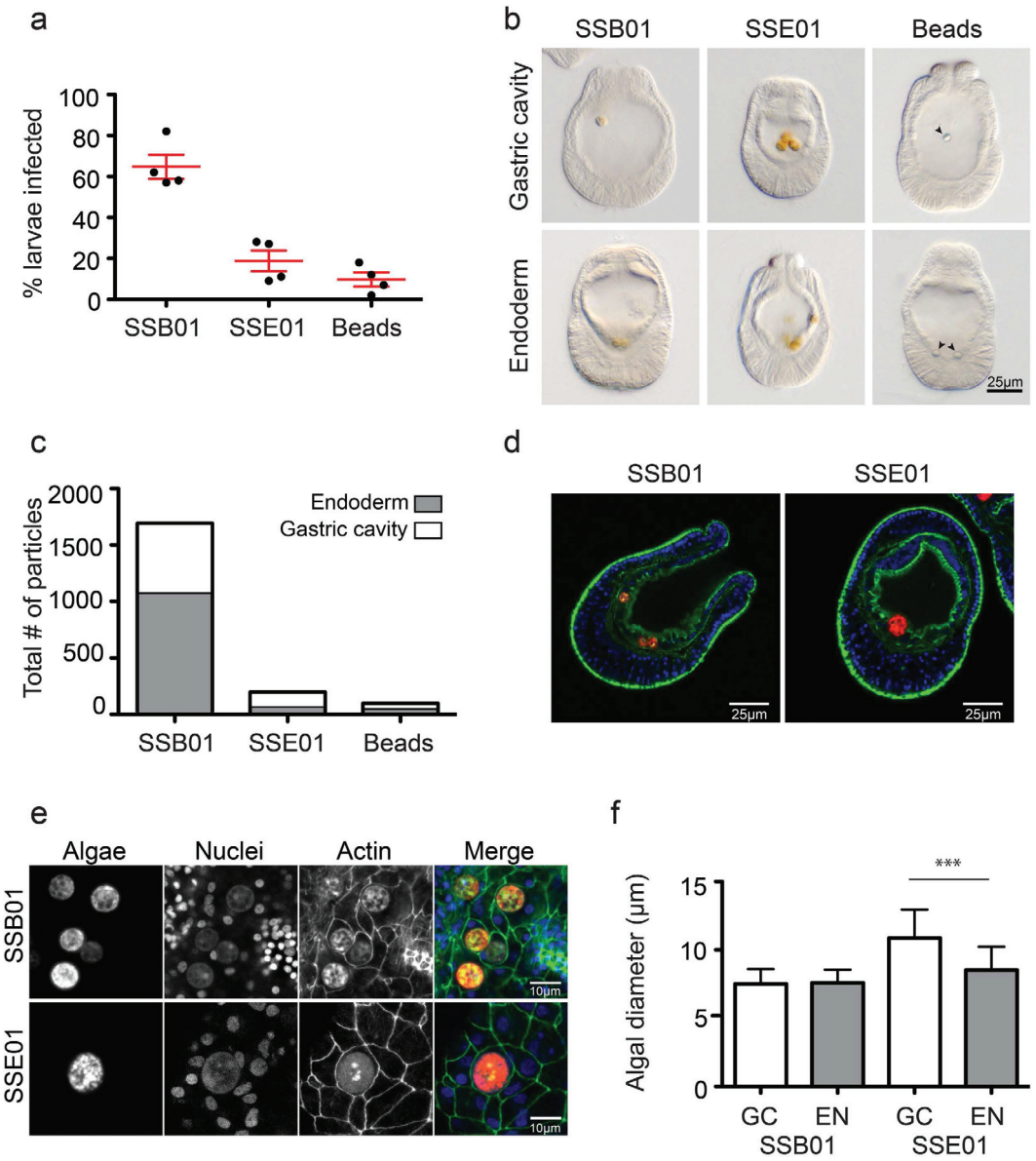

Figure 4. Early acquisition steps are more efficient for compatible symbionts than incompatible symbionts. (**a**) Percentage of *Aiptasia* larvae infected after exposure to the *Symbiodinium* strains SSB01 or SSE01 or inert polystyrene beads at 100,000 particles/ml for 4 or 5 days. Error bars are SEM of 4 replicate experiments. (**b**) Representative brightfield images of larvae from experiments in (**a**) used to distinguish between algae/beads in the gastric cavity or in the endoderm. Algae appear golden brown; arrows show beads. (**c**) Quantification of intra-larval localization of algae/beads in larvae from (**a**,**b**). (**d**) Representative confocal images of SSB01 and SSE01 algae integrated into the endodermal tissue. Colors are: autofluorescence of algal photosynthetic pigment (red), Hoechst-stained nuclei (blue), phalloidin-stained F-actin (green). (**e**) Representative confocal images of intracellular SSB01 and SSE01 algae. Colors of the merge are: autofluorescence of algal photosynthetic pigment (red), Hoechst-stained nuclei (blue), phalloidin-stained F-actin (green). (**f**) Quantification of cell sizes of SSB01 and SSE01 in the gastric cavity (GC) or in the endoderm (EN). Error bars are SEM, $^{***}p < 0.0001$ as determined by Student's two-tailed unpaired *t*-test.

are relatively large, especially compared to SSB01 cells[33,37] (Fig. 4b). To ask whether the cell size of SSE01 may correlate with phagocytosis efficiency, we compared cell sizes of these algae found in the gastric cavity and in the endoderm. SSE01 cells in the endoderm were significantly smaller than algae in the gastric cavity (8.5 µm vs. 11 µm), whereas such a difference could not be detected for SSB01 cells (Fig. 4f). Together, our results indicate that the compatible symbiont strain SSB01 is more efficiently taken up into the gastric cavity and phagocytosed into the endoderm, with the latter process potentially influenced by algal cell size.

Identification of candidate genes involved in symbiosis by RNA-Seq. Identification and functional characterization of key players involved in symbiosis establishment and selection during larval stages is crucial

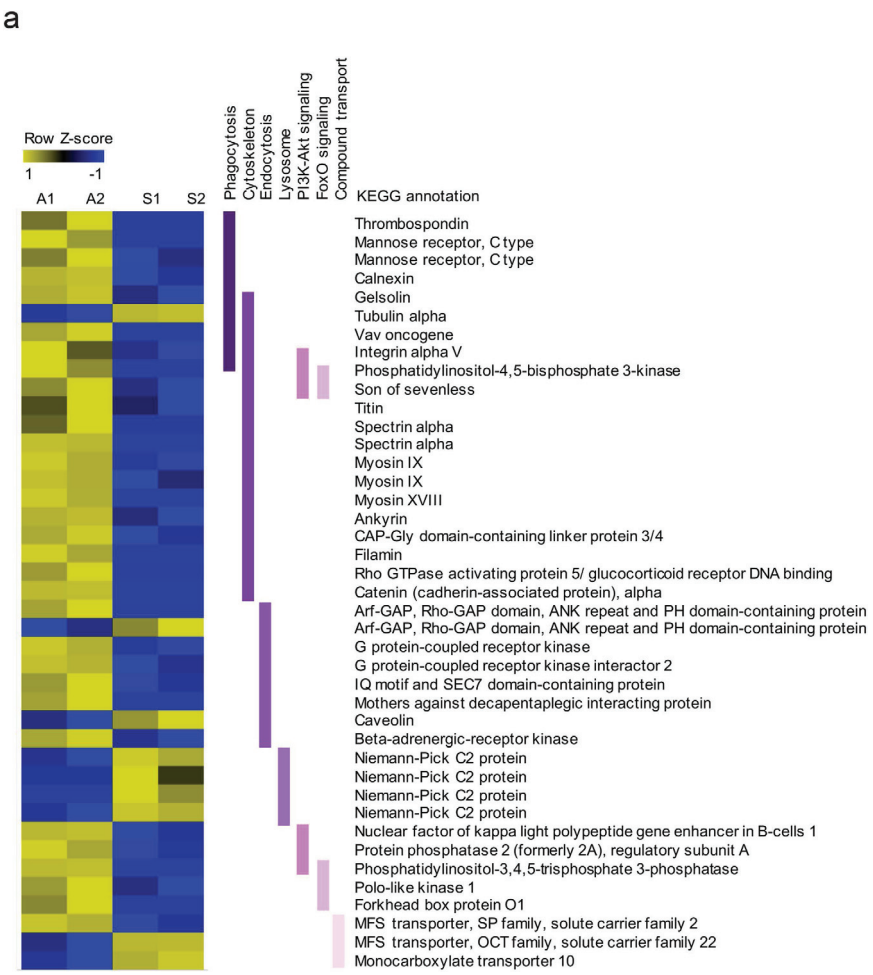

Figure 5. Differential expression of genes putatively involved in symbiosis establishment in *Aiptasia* larvae. Heatmap of 41 significantly differentially expressed genes. Gene expression was calculated over two replicates of aposymbiotic (A1, A2) and symbiotic (S1, S2) samples each. Up-regulation of gene expression is shown in yellow, down-regulation in blue. Genes were categorized by KEGG pathway annotations (purple bars) potentially involved in symbiosis establishment: Phagocytosis (ko04145: Phagosome, ko04666: Fc-gamma mediated phagocytosis), Cytoskeleton (ko04812: Eukaryotic cytoskeleton proteins, ko04810: Regulation of actin cytoskeleton), Endocytosis (ko04144), Lysosome (ko04142), PI3K-Akt signaling (ko04151), FoxO signaling (ko04068) and Compound transport. KEGG annotation was automated based on homology.

to understand these processes at the molecular level. We therefore used RNA-Seq to compare gene expression between symbiotic and non-symbiotic *Aiptasia* larvae. *Aiptasia* larvae (5 dpf) were either infected with SSB01 or kept non-symbiotic as a control for five days[29]. We identified 19,771 genes (of a total of 26,039 genomic gene models) expressed in at least one of the four replicates (two symbiotic and two non-symbiotic samples) with an FPKM value over 0 (Fragments Per Kilobase reference per Million mapped reads). Of these genes, the difference in expression levels were significant for 351 genes between the two states (False Discovery Rate ≤ 0.1). The majority of differentially expressed genes ($n = 219$) are down-regulated in the symbiotic state, resulting in an average log2 fold change of -2.3. However, the log2 fold changes ranged from -10.9 to 10.8. (Supplementary Table S1). To assess and illustrate clustering and variation between replicates, gene expression data was plotted as a multidimensional scaling plot (MDS plot) (Supplementary Fig. S3).

Recent transcriptomic and proteomic approaches in different systems have identified a set of symbiosis-specific candidate genes, and we found many similar genes among our list of differentially expressed genes (DEG); for example, the lysosomal Niemann-Pick disease type C2 (NPC2) protein[28,38]; transmembrane receptors that may play a role in symbiont recognition[29,39,40]; and small GTPases potentially involved in endocytotic vesicle transport during phagocytosis[41–43] (Fig. 5). However, our dataset also identified many new genes encoding factors potentially involved in symbiosis establishment. Using the functional annotations of the Kyoto Encyclopedia of Genes and Genomes (KEGG)[44], we found in total 41 DEGs related to phagocytosis, endocytosis, lysosomes, signaling pathways, cytoskeletal reorganization, and transport of compounds between partners. Among these genes, 9 genes are up- and 32 are down-regulated in the symbiotic state (Fig. 5). Thus, RNA-Seq of whole larvae is sufficiently sensitive to identify many genes putatively involved in symbiosis establishment.

Discussion

"Symbiosis specificity", defined as non-random host/symbiont combinations, may have broad ecological implications for coral reef ecosystems; however, this remains a matter of debate, with interpretations of the symbiosis ranging from specific and evolutionarily fixed to largely random and highly adaptive (e.g. during environmental change)[7,45–53]. Reaching a unified understanding of fundamental principles is difficult because of the complexity of the phenomenon: it is likely influenced by coral taxa, developmental stage, varying microhabitats of corals and symbionts, and local availability of symbionts. These factors, together with limited experiments under controlled laboratory conditions to standardize experimental design and replication, slow the progress of directly testing influences of host and symbiont. The molecular mechanisms underlying "symbiosis specificity" are likewise unclear and remain impossible to dissect without molecular tools and approaches.

To dissect "symbiosis specificity" using *Aiptasia* larvae as a model, we provide here the first direct comparison of symbiont uptake specificity in *Aiptasia* and *Acropora* under laboratory conditions using defined *Symbiodinium* strains. We tested two strains (SSB01 and SSA01) originating from *Aiptasia*[21,23,25], two strains (SSA02 and CCMP2556) isolated from corals[21], and the presumably free-living strain SSE01[21,33,35]. We find that patterns of symbiont selectivity are very similar between these taxa, indicating low lineage-constrained selectivity for *Symbiodinium* during early development stages (larval and juvenile polyp) independent of whether the algal strain originated from *Aiptasia* or a coral host. Of the *Symbiodinium* strains tested, three (SSB01, SSA02 and CCMP2556) are positively selected and one (SSE01) is negatively selected by *Aiptasia* and both Acroporids, even when the latter strain is present at high concentrations. This indicates that fundamental mechanisms of positive and negative symbiont selection are generally conserved between *Aiptasia* and *Acropora* during early life stages. SSA01 is a notable exception: it is efficiently acquired by progeny of its original host (*Aiptasia*) but rejected by both *Acropora* species tested. This comparative dataset is an important step towards dissecting fundamental and conserved principles (as well as differences) underlying host/symbiont compatibility and incompatibility in cnidarians.

Symbiosis establishment is a complex process comprising multiple steps, including symbiont uptake into the gastric cavity, phagocytosis by host cells, integration into host cell function, long-term persistence, and proliferation[15]. Each step, alone or in conjunction with others, may play a role during the establishment of suitable host/symbiont combinations. Further, each step may be influenced by specific molecular mechanisms as well as physical factors ([36,54], this study). In the first step, encounter efficiency may be important for initial uptake into the gastric cavity; for example, we have previously shown that symbiont uptake efficiency is concentration-dependent in *Aiptasia* larvae[24]. However, symbionts are presumably sparse in the natural environment and direct chemical attraction may facilitate host/symbiont meeting[54]. Once inside the gastric cavity, algae and host cell-cell contact is important to trigger phagocytosis. To date, it is unclear whether symbiont phagocytosis is restricted to certain cells with distinct receptors or whether it is an unspecific, evolutionarily conserved feeding mechanism in nutritive cells[15,55]. Many cell types are capable of engulfing particles, but phagocytosis requires fundamental changes in cell shape and architecture and, accordingly, particle size and shape directly influence cells' phagocytosis efficiencies[36]. Despite having entered host cells, symbionts may still fail to populate hosts; various examples indicate that coral larvae initially take up heterologous symbionts that are ultimately not maintained over longer time periods[12,13] (Fig. 3). It is unknown whether this lack of long-term compatibility is due to symbiont expulsion, digestion, or a lack of proliferation capacities.

Indeed, our analyses in *Aiptasia* larvae directly comparing the broadly compatible symbiont strain SSB01 and the incompatible strain SSE01 confirm the collective influence of multiple steps for the efficiency of symbiont acquisition. Despite our observation that SSE01 cells are phagocytosed into *Aiptasia* larvae endodermal cells, we repeatedly find virtually no larvae stably infected with SSE01 under the tested conditions. This failure stands in contrast to the consistent high infection rates of SSB01 symbionts in larvae. SSB01 is taken up into the gastric cavity more efficiently than SSE01 (alternatively, the SSE01 expulsion rate may be higher); phagocytosis of SSB01 is more efficient than that of SSE01; and while the number of SSB01 algae inside larvae increases over time, SSE01 fail to persist in larvae at detectable levels ([22]; this study). Phagocytosis efficiency may be directly related to symbiont size, as SSE01 is phagocytosed at the lowest rates, yet our comparison of SSB01, SSE01, and small inert beads indicates that entering or persisting in the gastric cavity is not (Fig. 4a,c). It is noteworthy that SSE01, similar to other *Symbiodinium* types in Clade E, is thought to be free-living[21,33,35]. Our data suggest that the inability of SSE01 to establish stable symbiosis in cnidarians is not governed by the inhibition of phagocytosis into host cells, but may rather be a consequence of the inability of the two partners to initiate a functional molecular cross-talk after intracellularization. The direct involvement of more complex molecular mechanisms during symbiont selection is supported by our observation that SSA01 acceptance by cnidarian hosts is opposite for *Aiptasia* and Acroporids: *Aiptasia* larvae take up SSA01 cells with high efficiency, but *Acropora tenuis* and *Acropora digitifera* do not (Fig. 1).

In the future, it will be also interesting to extend the analysis of changes in "symbiosis specificity" over longer time periods. Other studies have shown that juvenile *A. tenuis* larvae exhibit different specificity throughout ontogeny, with nonhomolgous symbiont types (in clade D) being taken up first and replaced only after several months/years by the homologous symbionts (in clade C) that dominate adult colonies[5,34,56]. Our observations that populations of nonhomologous symbiont strains SSB01 (clade B) and CCMP2556 (clade D) declined over time in *Acroprora* polyps are consistent with this phenomenon (Fig. 3). However, *Acropora* polyps are notoriously difficult to keep in the laboratory, and the polyps we monitored under laboratory conditions suffered substantial mortality. Further, the low number of polyps in our experiment prevents us from drawing hard conclusions: additional experiments are needed under controlled and optimized growth conditions for juvenile *Acropora*. Alternatively, similar long-term experiments could be done with *Aiptasia* and defined *Symbiodinium* strains under controlled conditions, which would greatly increase reproducibility and comparability and further reveal the complex dynamics of symbiosis specificity over time. Likewise, *Aiptasia* may help reveal the influence of

environmental factors (e.g. elevated temperature) on symbiosis specificity, further highlighting the need for a laboratory-based model system to dissect "symbiosis specificity" in a systematic, controlled way.

To dissect distinct molecular mechanisms involved in "symbiosis specificity" and symbiosis establishment in general, the identification of key players is crucial. Here we used RNA-Seq as a proof-of-concept to identify symbiosis-specific genes in *Aiptasia* larvae, and we found over 300 genes that are differentially expressed in symbiotic versus non-symbiotic larvae. Notably, a suite of those genes are involved in pathways and biological processes that were previously identified to play a role in the cnidarian-dinoflagellate endosymbiosis, validating this approach[28,29,32,39–43]. RNA-Seq is an easy, rapid, and cost-effective technique, and in the future it can be combined with cell biological analyses to reveal the functions of identified candidates in the symbiosis.

We propose that *Aiptasia* larvae, together with the suite of compatible and incompatible symbiont strains, constitute a powerful platform to elucidate fundamental mechanisms of the distinct steps involved in symbiosis establishment in cnidarians. We envision exploiting the *Aiptasia* larvae model by taking advantage of the easily controllable laboratory system and available molecular and cell biological tools, including RNA-Seq, to mechanistically dissect how stable host/symbiont combinations are established. Moreover, we can begin to dissect the various contributions of environmental conditions, host and symbiont genotype, and ontogeny to the phenomenon of "symbiosis specificity". Ultimately, such laboratory experiments may also help to better understand and predict the potential of certain symbiotic associations for the resilience and adaptive capacities of coral reefs to environmental change.

Methods

Collection and maintenance of *Acropora* planula larvae. Colonies of *Acropora digitifera* and *Acropora tenuis* were collected with permission by the Okinawa prefecture (#27-1) at Sesoko Island (26°37'41"N, 127°51'38"E, Okinawa, Japan). Corals were kept in tanks with running natural seawater and under partially shaded natural light at Sesoko Marine Station (University of Ryukyus, Okinawa, Japan). After spawning on May 31 2015, bundles of symbiont-free gametes from multiple colonies of each coral species were mixed and the resulting planula larvae were maintained in plastic bowls at approximately 1000 larvae/L in 10 μm-filtered natural seawater (FNSW). FNSW was exchanged daily.

***Aiptasia* culture conditions and spawning induction.** Spawning of *Aiptasia* clonal lines CC7 and F003 (for symbiosis establishment studies) and clonal lines CC7 and H2 (for transcriptomic comparisons) was induced as previously described[23]. *Aiptasia* larvae were kept in filter-sterilized artificial seawater (FASW) in glass beakers at 26 °C on a 12 h light:12 h dark (12L:12D) cycle.

***Symbiodinium* cultures and conditions.** For infection of cnidarian hosts, we used the following clonal and axenic *Symbiodinium* strains: SSB01 (clade B), SSA01 (clade A), SSA02 (clade A), and SSE01 (clade E)[21,23] as well as the non-clonal, non-axenic *Symbiodinium* culture CCMP2556 (clade D) from the scleractinian coral *Orbicella faveolata* (formerly *Montastrea faveolata*)[33] purchased from the National Center for Marine Algae and Microbiota (NCMA, Bigelow Laboratory for Ocean Sciences, Maine, USA). All cultures were grown in cell culture flasks in IMK medium[57] at 26 °C on a 12L:12D cycle under 20–25 μmol m^{-2} s^{-1} of photosynthetically active radiation (PAR), as measured with an Apogee PAR quantum meter (MQ-200; Apogee, Logan, USA).

Symbiosis establishment experiments in *Acropora* and *Aiptasia*. *Aiptasia larvae.* For infection experiments, *Aiptasia* larvae 2 days post-fertilization (dpf) were distributed into 6-well plates at 300 larvae in 5 ml of FASW per well. *Symbiodinium* cells were added to each well at a final concentration of 10,000 algal cells/ml; FASW was used as a negative control. Three biological replicates (e.g. spawning crosses) were used per algae/host combination. Plates were kept in incubators at 26 °C under white fluorescent bulbs at 20–25 μmol m^{-2} s^{-1} on a 12L:12D cycle with regular exchange of FASW; *Symbiodinium* cells were re-added after each wash. After ten days of exposure to *Symbiodinium*, larvae were fixed for 30 min in 4% formaldehyde in seawater, washed 3 times in PBS, and mounted in 87% glycerol in PBS for analysis. Over 45 *Aiptasia* larvae were counted per algae/host replicate.

The experiments in Fig. 4 were carried out with the following changes: larvae were 6–7 dpf at start of infection; *Symbiodinium* cells of strains SSB01 and SSE01 and inert polysterene fluorescent beads (#C36950, Thermo Fisher Scientific) were added at a final concentration of 100,000 particles/ml; larvae were fixed for analysis after 4–5 days of exposure to algal cells. Over 85 *Aiptasia* larvae were counted per algae/host replicate.

Acropora larvae. At 4 dpf, *Acropora* larvae of either coral species were distributed into 24-well cell culture plates, with 30 larvae in 2 ml FNSW per well. *Symbiodinium* cells were added to each well at a final concentration of 10,000 algal cells/ml; FNSW was used as a negative control. Three technical replicates (i.e. wells) were used per algae/host combination. Plates were kept at ~25 °C under ambient room light (~9–12 μmol m^{-2} s^{-1}) on an approximate 12L:12D cycle. Larvae were washed with FNSW every one or two days as appropriate; *Symbiodinium* cells were re-added after each wash. After ten days of exposure to *Symbiodinium*, larvae were mounted in FNSW on glass slides with glass coverslips for analysis. An average of 22 larvae were counted per technical triplicate; for details, see Supplementary Table S2.

Acropora polyps: short-term exposure. At 6 dpf, larvae of either species were induced to metamorphose and settle in 6-well plates through overnight incubation in 5 ml FNSW supplemented with 1 μM Hym-248 neuropeptide[58]. The following day, 30–60 polyps had metamorphosed and settled per plate (~5–10 polyps in per well). *Symbiodinium* cells were added to each well at a final concentration of 10,000 algal cells/ml; FNSW was used as a negative control. Plates were kept at ~25 °C under ambient light (~9–12 μmol m^{-2} s^{-1}) on an

approximate 12L:12D cycle with daily exchanges of FNSW; *Symbiodinium* cells were re-added after each wash. *Symbiodinium* exposure proceeded for four days, after which environmental algae were removed by exchanging FNSW without re-addition of *Symbiodinium*. Polyps were monitored daily for 10 days total by microscopy. An average of 41 polyps were counted per host/algae combination; for details, see Supplementary Table S3.

Acropora polyps: long-term exposure. At 5 dpf, larvae of either species were distributed into plastic bowls at 250 larvae per 200 ml FNSW. *Symbiodinium* cells of strains SSB01 or CCMP2556 was added to each bowl at a final concentration of 10,000 algae cells/ml; FNSW was used as a negative control. Bowls were kept on the bench at ~25 °C under ambient light (~9–12 μmol m^{-2} s^{-1}) on an approximate 12L:12D cycle. At 12 dpf larvae were package at a density of ~1000 larvae/L in 50 ml conical tubes and overnight shipped to the Hatta lab, Tokyo. At 14 dpf, environmental algae were removed by exchanging FNSW without re-addition of algae and metamorphosis was induced as described above. Polyps that had successfully metamorphosed and settled by the following day were included in subsequent monitoring: for *A. tenuis*, 35 polyps exposed to SSB01 and 34 polyps exposed to CCMP2556; for *A. digitifera*, 15 polyps exposed to SSB01 and 27 polyps exposed to CCMP2556. The polyps were then washed with daily exchange of seawater, which was a 50%/50% mixture of FNSW sterilized at 105 °C for 3 min and artificial seawater (Coral Pro, RedSea). Polyps were qualitatively assessed as hosting symbionts by light microscopy and photography at 2, 23, and 49 days post-metamorphosis (dpm). At 23 dpm, polyp numbers were those from the initial metamorphosis; at 49 dpm, budding and mortality led to new population sizes: for *A. tenuis*, 43 polyps with SSB01 and 41 with CCMP2556; for *A. digitifera*, 25 polyps with SSB01 and 18 with CCMP2556.

Microscopy. *Acropora* larvae and polyps were analyzed using a Leica S8APO stereoscope equipped with a Leica MC170 HD color camera. Endogenous autofluorescence of *Symbiodinium* photosynthetic pigments was visualized using the Leica S8APO stereoscope in combination with a Stereomicroscope Fluorescence Adapter kit (#SFA-LFS-Green, NightSea, USA). Microscopic analysis of *Aiptasia* larvae was carried out with a Nikon Eclipse Ti inverted microscope using Differential Interference Contrast (DIC) and a Nikon Plan Fluor 20x dry lens. Microscopic images of *Aiptasia* larvae were captured with a Nikon Eclipse 80i microscope using DIC and a Digital Sight DS-U1 color camera (Nikon Instruments).

For confocal imaging, *Aiptasia* larvae 4 dpf were infected for 4 days and then fixed in 4% formaldehyde in FASW for 30 min, followed by three washes in PBS containing 0.2% Triton X-100 (PBT). Approximately 50–100 larvae were transferred to 0.2 ml reaction tubes and permeabilized in 0.01 mg/ml Proteinase K (#03115879001, Roche Diagnostics) in 1x PBS for 8 min. Permeabilization was stopped by washing larvae in 2 mg/ml glycine in PBT twice for 15 min each. Larvae were post-fixed in 4% formaldehyde in PBT for 20 min and then washed twice in PBT and twice in PBS, 15 min per wash. Larvae were incubated in Phalloidin-Atto 565 (#94072, Sigma-Aldrich) diluted 1:200 in PBS for 60 min on a rotor (Intelli mixer #7-0045, NeoLab) at 20 rpm. Larvae were washed twice in PBT before incubation in 10 μg/ml Hoechst in buffer (Tris-buffered saline, pH 7.4; 0.1% Triton X-100; 2% bovine serum albumin; 0.1% sodium azide) for 15 min. After three washes in PBT for 15 min each, larvae were mounted in 87% glycerol in PBS containing 2.5 mg/ml DABCO (1,4-Diazabicyclo[2.2.2]octan, #D27802, Sigma-Aldrich). Confocal images were acquired using a Nikon A1R confocal microscope with a Nikon Plan Apo 60x oil immersion objective (NA = 1.4) and Nikon Elements Software. Image processing and maximum projections of Z-stacks were performed using Fiji[59].

Analysis of differential gene expression. *RNA isolation and sequencing.* For the analysis of differentially expressed genes, the *Aiptasia* larval RNA-Seq datasets described in Baumgarten *et al.*[29] were obtained from the NCBI SRA database, with two replicates for aposymbiotic (accession no.: SRX757531) and symbiotic (accession no.: SRX757532) larvae each. Briefly, larvae 3–4 dpf were infected with *Symbiodinium* strain SSB01 at a concentration of 2.5–5 × 10^4 algae/ml for 5–6 days (FASW as negative control). Two separate crosses were used for duplicate pairs, with cross 1 containing 6,500 larvae per treatment and cross 2 containing 8,400 larvae per treatment. For all samples, total RNA was extracted using TriZol (#15596, Thermo Fisher Scientific) and the mRNA was purified using Dynabeads oligo(dT)25 (#61002, Thermo Fisher Scientific). The sequencing libraries were prepared with the NEBNext Ultra Directional RNA Library Prep Kit (#E7420, NEB) with 180 bp insert sizes and sequenced on an Illumina HiSeq2000 at 2 × 101 bp read length. As a mapping reference for the calculation of transcript abundances, we used the *Aiptasia* genomic gene set (NCBI Genome ID: 40858, Accession: LJWW01000000).

Sequencing adaptors and low quality reads were trimmed and filtered from the sequence reads using Trimmomatic[60]. The reads were mapped to the reference genomic gene set using bowtie2[61] with settings "-a -t -X 500–no-unal–rdg 6,5–rfg 6,5–score-min L,-.6,-.4–no-discordant–no-mixed–phred33". Read count abundances were calculated using eXpress[62] with settings "–rf-stranded" and a read count table was generated using a custom perl script.

Statistical analysis. Significantly differentially expressed genes (DEGs) were subsequently calculated in R[63] using the package edgeR[64]. Specifically, to test for differential expression of genes between symbiotic and aposymbiotic *Aiptasia* larvae, first the variation of gene expression between replicates was determined. Two types of variation contribute to the total variation in RNA-Seq experiments and are expressed as follows: 1) technical coefficient of variation, which describes the measurement error derived from the uncertainty with which the abundance of every gene is estimated from the sequencing platform. This variation decreases with increasing total counts for each gene in an RNA sample and can be distinguished from 2) the biological coefficient of variation (BCV). The latter denotes the variation of the true, unknown expression of each gene among biological replicates, which remains even at indefinite sequencing depth[65]. This represents the most important source of variation in RNA-Seq experiments and is calculated from the biological replication prior to the test of differential expression between

treatments[66]. Although higher confidence estimates of BCV might be obtained with higher numbers of biological replicates, both the common dispersion (i.e. BCV^2) as well as the gene-specific dispersion could be calculated robustly among the four biological replicates (i.e. $n = 2$ for both aposymbiotic and symbiotic larvae) using the functions "estimateCommonDisp()" and "estimateTagwiseDisp()" using the package edgeR, respectively. Differential expression was subsequently calculated using the function "exactTest()" within the edgeR package and a multidimensional scaling (MDS) plot of differentially expressed genes (FDR $\leq = 0.1$) was plotted using the function "plotMDS()". The distances between pairs of RNA samples in the MDS plot correspond to the leading log2 fold changes, which is the average (root mean square) of the largest absolute log2 fold changes[64].

Gene annotation. KEGG pathway identifiers of the differentially expressed genes were obtained from the gene annotations. To sort DEGs into higher level biological processes, we used the automated KEGG pathway annotations for *Aiptasia*[29]. DEGs were sorted by their KEGG annotations into the processes 'Phagocytosis' (ko04145: Phagosome, ko04666: Fc-gamma mediated phagocytosis), 'Cytoskeleton' (ko04812: Eukaryotic cytoskeleton proteins, ko04810: Regulation of actin cytoskeleton), 'Endocytosis' (ko04144), 'Lysosome' (ko04142), 'PI3K-Akt signaling' (ko04151), 'FoxO' (ko04068) as well as 'Compound transport'. The log2 fold changes of DEGs belonging to either of these groups were calculated with the predFC function in edgeR, normalized to Z-scores following the formula $z = (x-u)/s$ ($z = Z$ score; $x =$ fold change; $u =$ mean fold change across all replicates; $s =$ standard deviation across all replicates) and visualized as a heatmap in MeV[67].

References

1. Muscatine, L. The role of symbiotic algae in carbon and energy flux in coral reefs in *Coral Reefs* (ed. Zubinsky, Z.) 75–87 (Elsevier, 1990).
2. Pochon, X. & Gates, R. D. A new *Symbiodinium* clade (Dinophyceae) from soritid foraminifera in Hawai'i. *Mol. Phylogenet. Evol.* **56,** 492–497 (2010).
3. LaJeunesse, T. C. *et al.* Diversity and host specificity observed among symbiotic dinoflagellates in reef coral communities from Hawaii. *Coral Reefs* **23,** 596–603 (2004).
4. Coffroth, M. A., Poland, D. M., Petrou, E. L., Brazeau, D. A. & Holmberg, J. C. Environmental symbiont acquisition may not be the solution to warming seas for reef-building corals. *PLoS ONE* **5,** e13258 (2010).
5. Little, A. F., van Oppen, M. J. H. & Willis, B. L. Flexibility in algal endosymbioses shapes growth in reef corals. *Science* **304,** 1492–1494 (2004).
6. Rowan, R. Coral bleaching: thermal adaptation in reef coral symbionts. *Nature* **430,** 742 (2004).
7. Jones, A. M., Berkelmans, R., van Oppen, M. J. H., Mieog, J. C. & Sinclair, W. A. A community change in the algal endosymbionts of a scleractinian coral following a natural bleaching event: field evidence of acclimatization. *Proc. R. Soc. B* **275,** 1359–1365 (2008).
8. Sampayo, E. M., Ridgway, T., Bongaerts, P. & Hoegh-Guldberg, O. Bleaching susceptibility and mortality of corals are determined by fine-scale differences in symbiont type. *Proc. Natl. Acad. Sci. USA* **105,** 10444–10449 (2008).
9. DeSalvo *et al.* Coral host transcriptomic states are correlated with *Symbiodinium* genotypes. *Mol. Ecol.* **19,** 1174–1186 (2010).
10. van Oppen, M. *In vitro* establishment of symbiosis in *Acropora millepora* planulae. *Coral Reefs* **20,** 200 (2001).
11. Harii, S., Yasuda, N., Rodriguez-Lanetty, M., Irie, T. & Hidaka, M. Onset of symbiosis and distribution patterns of symbiotic dinoflagellates in the larvae of scleractinian corals. *Mar. Biol.* **156,** 1203–1212 (2009).
12. Weis, V. M., Reynolds, W. S., deBoer, M. D. & Krupp, D. A. Host-symbiont specificity during onset of symbiosis between the dinoflagellates *Symbiodinium* spp. and planula larvae of the scleractinian coral *Fungia scutaria*. *Coral Reefs* **20,** 301–308 (2001).
13. Rodriguez-Lanetty, M., Wood-Charlson, E. M., Hollingsworth, L. L., Krupp, D. A. & Weis, V. M. Temporal and spatial infection dynamics indicate recognition events in the early hours of a dinoflagellate/coral symbiosis. *Mar. Biol.* **149,** 713–719 (2006).
14. Nyholm, S. V. & McFall-Ngai, M. The winnowing: establishing the squid-*Vibrio* symbiosis. *Nat. Rev. Microbiol.* **2,** 632–642 (2004).
15. Davy, S. K., Allemand, D. & Weis, V. M. Cell biology of cnidarian-dinoflagellate symbiosis. *Microbiol. Mol. Biol. Rev.* **76,** 229–261 (2012).
16. Lewis, C. L. & Coffroth, M. A. The acquisition of exogenous algal symbionts by an octocoral after bleaching. *Science* **304,** 1490–1492 (2004).
17. deBoer, M. L., Krupp, D. A. & Weis, V. M. Proteomic and transcriptional analyses of coral larvae newly engaged in symbiosis with dinoflagellates. *Comp. Biochem. Phys. D* **2,** 63–73 (2007).
18. Voolstra, C. R. *et al.* The host transcriptome remains unaltered during the establishment of coral-algal symbioses. *Mol. Ecol.* **18,** 1823–1833 (2009).
19. Schnitzler, C. E. & Weis, V. M. Coral larvae exhibit few measurable transcriptional changes during the onset of coral-dinoflagellate endosymbiosis. *Mar. Genomics* **3,** 107–116 (2010).
20. Weis, V. M., Davy, S. K., Hoegh-Guldberg, O., Rodriguez-Lanetty, M. & Pringle, J. R. Cell biology in model systems as the key to understanding corals. *Trends Ecol. Evol.* **23,** 369–376 (2008).
21. Xiang, T., Hambleton, E. A., DeNofrio, J. C., Pringle, J. R. & Grossman, A. R. Isolation of clonal axenic strains of the symbiotic dinoflagellate *Symbiodinium* and their growth and host specificity. *J. Phycol.* **49,** 447–458 (2013).
22. Hambleton, E. A., Guse, A. & Pringle, J. R. Similar specificities of symbiont uptake by adults and larvae in an anemone model system for coral biology. *J. Exp. Biol.* **217,** 1613–1619 (2014).
23. Grawunder, D. *et al.* Induction of gametogenesis in the cnidarian endosymbiosis model *Aiptasia* sp. *Sci. Rep.* **5,** 15677 (2015).
24. Bucher, M., Wolfowicz, I., Voss, P. A., Hambleton, E. A. & Guse, A. Development and symbiosis establishment in the cnidarian endosymbiosis model *Aiptasia* sp. *Sci. Rep.* **6,** 19867 (2016).
25. Sunagawa, S. *et al.* Generation and analysis of transcriptomic resources for a model system on the rise: the sea anemone *Aiptasia pallida* and its dinoflagellate endosymbiont. *BMC Genomics* **10,** 258 (2009).
26. Bayer, T. *et al. Symbiodinium* transcriptomes: genome insights into the dinoflagellate symbionts of reef-building corals. *PLoS ONE* **7,** e35269 (2012).
27. Shoguchi, E. *et al.* Draft assembly of the *Symbiodinium minutum* nuclear genome reveals dinoflagellate gene structure. *Curr. Biol.* **23,** 1399–1408 (2013).
28. Lehnert, E. M. *et al.* Extensive differences in gene expression between symbiotic and aposymbiotic cnidarians. *G3* (*Bethesda*) **4,** 277–295 (2014).
29. Baumgarten, S. *et al.* The genome of *Aiptasia*, a sea anemone model for coral symbiosis. *Proc. Natl. Acad. Sci. USA* **112,** 11893–11898 (2015).
30. Lin, S. *et al.* The *Symbiodinium kawagutii* genome illuminates dinoflagellate gene expression and coral symbiosis. *Science* **350,** 691–694 (2015).
31. Xiang, T., Nelson, W., Rodriguez, J., Tolleter, D. & Grossman, A. R. *Symbiodinium* transcriptome and global responses of cells to immediate changes in light intensity when grown under autotrophic or mixotrophic conditions. *Plant J.* **82,** 67–80 (2015).

32. Oakley, C. A., Ameismeier, M. F., Peng, L., Weis, V. M., Grossman, A. R. & Davy, S. K. Symbiosis induces widespread changes in the proteome of the model cnidarian *Aiptasia*. *Cell. Microbiol.* **18,** 1009–1023 (2016).
33. Yamashita, H. & Koike, K. Genetic identity of free-living *Symbiodinium* obtained over a broad latitudinal range in the Japanese coast. *Phycol. Res.* **61,** 68–80 (2013).
34. Yuyama, I. & Higuchi, T. Comparing the effects of symbiotic algae (*Symbiodinium*) clades C1 and D on early growth stages of *Acropora tenuis*. *PLoS ONE* **9,** e98999 (2014).
35. Jeong, H. J. *et al.* Genetics and morphology characterize the dinoflagellate *Symbiodinium voratum*, n. sp., (Dinophyceae) as the sole representative of *Symbiodinium* clade E. *J. Eukaryot. Microbiol.* **61,** 75–94 (2014).
36. Paul, D. *et al.* Phagocytosis dynamics depends on target shape. *Biophys. J.* **105,** 1143–1150 (2013).
37. LaJeunesse, T. C., Parkinson, J. E. & Reimer, J. D. A genetics-based description of *Symbiodinium minutum* nov. and *S. psygmophilum* sp. nov. (Dinophyceae), two dinoflagellates symbiotic with Cnidaria. *J. Phycol.* **48,** 1380–1391 (2012).
38. Dani, V., Ganot, P., Priouzeau, F., Furla, P. & Sabourault, C. Are Niemann-Pick type C proteins key players in cnidarian-dinoflagellate endosymbioses? *Mol. Ecol.* **23,** 4527–4540 (2014).
39. Wood-Charlson, E. M., Hollingsworth, L. L., Krupp, D. A. & Weis, V. M. Lectin/glycan interactions play a role in recognition in a coral/dinoflagellate symbiosis. *Cell. Microbiol.* **8,** 1985–1993 (2006).
40. Kvennefors, E. C. E. *et al.* Analysis of evolutionarily conserved innate immune components in coral links immunity and symbiosis. *Dev. Comp. Immunol.* **34,** 1219–1229 (2010).
41. Chen, M.-C., Cheng, Y.-M., Hong, M.-C. & Fang, L.-S. Molecular cloning of Rab5 (ApRab5) in *Aiptasia pulchella* and its retention in phagosomes harboring live zooxanthellae. *Biochem. Biophys. Res. Commun.* **324,** 1024–1033 (2004).
42. Chen, M.-C. *et al.* Cloning and characterization of the first cnidarian ADP-ribosylation factor, and its involvement in the *Aiptasia-Symbiodinium* endosymbiosis. *Mar. Biotechnol.* **6,** 138–147 (2004).
43. Chen, M.-C. *et al.* ApRab11, a cnidarian homologue of the recycling regulatory protein Rab11, is involved in the establishment and maintenance of the *Aiptasia-Symbiodinium* endosymbiosis. *Biochem. Biophys. Res. Commun.* **338,** 1607–1616 (2005).
44. Kanehisa, M. & Goto, S. KEGG: Kyoto Encyclopedia of Genes and Genomes. *Nucleic Acids Res.* **28,** 27–30 (2000).
45. Buddemeier, R. W. & Fautin, D. G. Coral bleaching as an adaptive mechanism. *BioScience* **43,** 320–326 (1993).
46. Baker, A. C. Ecosystems: reef corals bleach to survive change. *Nature* **411,** 765–766 (2001).
47. Baker, A. C. Flexibility and specificity in coral-algal symbiosis: diversity, ecology, and biogeography of *Symbiodinium*. *Annu. Rev. Ecol. Evol. S.* **34,** 661–689 (2003).
48. Baker, A. C., Starger, C. J., McClanahan, T. R. & Glynn, P. W. Coral reefs: corals' adaptive response to climate change. *Nature* **12,** 741 (2004).
49. Berkelmans, R. & van Oppen, M. J. The role of zooxanthellae in the thermal tolerance of corals: a 'nugget of hope' for coral reefs in an era of climate change. *Proc. R. Soc. B* **22,** 2305–2312 (2006).
50. Goulet, T. Most corals may not change their symbionts. *MEPS* **321,** 1–7 (2006).
51. Baird, A. & Maynard, J. A. Coral adaptation in the face of climate change. *Science* **18,** 315–316 (2008).
52. Baskett, M. L., Gaines, S. D. & Nisbet, R. M. Symbiont diversity may help coral reefs survive moderate climate change. *Ecol. Appl.* **19,** 3–17 (2009).
53. Silverstein, R. S., Correa, A. M. & Baker, A. C. Specificity is rarely absolute in coral-algal symbiosis: implications for coral response to climate change. *Proc. R. Soc. B* **7,** 2609–2618 (2012).
54. Hagedorn, M. *et al.* Trehalose is a chemical attractant in the establishment of coral symbiosis. *PLoS ONE* **28,** e0117087 (2015).
55. Bowers, B. & Olszewski, T. E. Acanthamoeba discriminates internally between digestible and indigestible particles. *J. Cell Biol.* **97,** 317–322 (1983).
56. Abrego, D., van Oppen, M. J. H. & Willis, B. L. Onset of algal endosymbiont specificity varies among closely related species of *Acropora* corals during early ontogeny. *Mol. Ecol.* **18,** 3532–3543 (2009).
57. Ishikura, M. *et al.* Isolation of new *Symbiodinium* strains from Tridacnid giant clam (*Tridacna crocea*) and sea slug (*Pteraeolidia ianthina*) using culture medium containing giant clam tissue homogenate. *Mar. Biotechnol.* **6,** 378–385 (2004).
58. Iwao, K., Fujisawa, T. & Hatta, M. A cnidarian neuropeptide of the GLWamide family induces metamorphosis of reef-building corals in the genus *Acropora*. *Coral Reefs* **21,** 127–129 (2002).
59. Schindelin, J. *et al.* Fiji: an open-source platform for biological-image analysis. *Nat. Methods* **9,** 676–682 (2012).
60. Bolger, A. M., Lohse, M. & Usadel, B. Trimmomatic: a flexible trimmer for Illumina sequence data. *Bioinformatics* **30,** 2114–2120. (2014).
61. Langmead, B. & Salzberg, S. L. Fast gapped-read alignment with Bowtie 2. *Nat. Methods* **9,** 357–359 (2012).
62. Roberts, A. & Pachter, L. Streaming fragment assignment for real-time analysis of sequencing experiments. *Nat. Methods* **10,** 71–73 (2013).
63. R Development Core Team. R: A language and environment for statistical computing (R Foundation for Statistical Computing, Vienna, Austria) (2012).
64. Robinson, M. D., McCarthy, D. J. & Smyth, G. K. edgeR: a Bioconductor package for differential expression analysis of digital gene expression data. *Bioinformatics* **26,** 139–140 (2010).
65. Parkinson, J. E. *et al.* Gene expression variation resolves species and individual strains among coral-associated dinoflagellates within the genus *Symbiodinium*. *Genome Biol. Evol.* **8,** 665–680 (2016).
66. McCarthy, D. J., Chen, Y. & Smyth, G. K. Differential expression analysis of multifactor RNA-Seq experiments with respect to biological variation. *Nucleic Acids Res.* **40,** 4288–4297 (2012).
67. Howe, E. A., Sinha, R., Schlauch, D. & Quackenbush, J. RNA-Seq analysis in MeV. *Bioinformatics* **27,** 209–210 (2011).

Acknowledgements

Funding was provided to A.G. by the Emmy-Noether-Programme of the German Research Foundation (DFG) (grant no. GU 1128/3-1), by a Marie Curie Career Integration Grant (CIG) under the FP7-PEOPLE-2013-CIG program, European Commission, and with financial support through funds for the future concept of Heidelberg University within the Excellence Initiative by German federal and state governments; to I.W. by a PhD fellowship from the Foundation for Science and Technology (FCT, Portugal); and to P.A.V. by a PhD fellowship from the Baden-Württemberg Landesgraduiertenförderung Program. Research reported in this publication was supported by King Abdullah University of Science and Technology (KAUST). We thank Steffen Lemke, Thomas Holstein, and Suat Özbek for advice, comments, and sharing reagents and equipment; and Natascha Bechtoldt and Madeline Bucher for technical help with experiments. We thank the Nikon Imaging Center at the University of Heidelberg, especially Nico Dross for help with microscopy. We also thank members of the Jun Minagawa and Naoto Ueno groups for help with coral larvae collection and maintenance at Sesoko as well as for sharing expertise, equipment, and reagents.

Author Contributions

I.W., P.A.V., E.A.H. and A.G. designed the experiments; I.W., P.A.V. and M.H. performed the experiments. S.B. and C.R.V. analyzed gene expression data. C.R.V., M.H. and A.G. provided materials, reagents and tools. I.W., S.B., P.A.V., E.A.H. and A.G. wrote the manuscript. All authors reviewed the manuscript.

Additional Information

Supplementary information accompanies this paper at http://www.nature.com/srep

Competing financial interests: The authors declare no competing financial interests.

How to cite this article: Wolfowicz, I. *et al. Aiptasia* sp. larvae as a model to reveal mechanisms of symbiont selection in cnidarians. *Sci. Rep.* **6**, 32366; doi: 10.1038/srep32366 (2016).

SUPPLEMENTARY INFORMATION
Aiptasia sp. larvae as a model to reveal mechanisms of symbiont selection in cnidarians
Authors: I. Wolfowicz, S. Baumgarten, P.A. Voss, E.A. Hambleton, C.R. Voolstra, M. Hatta, A. Guse

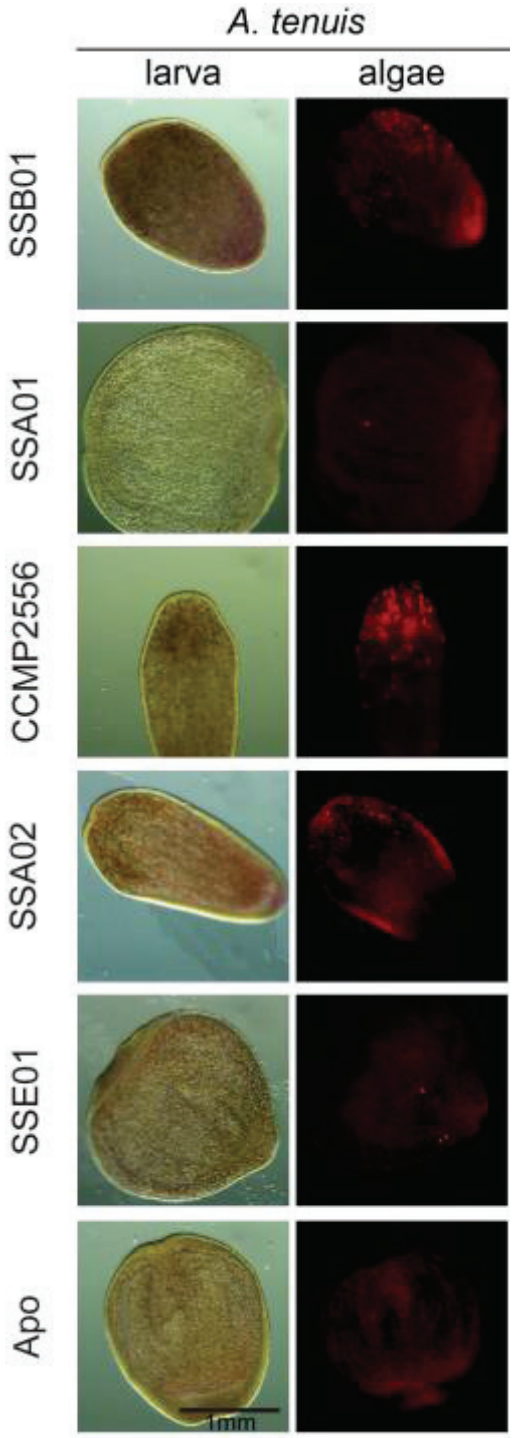

Supplementary Figure S1: Representative images of *Symbiodinium* infections in *A. tenuis* larvae with *Symbiodinium* strains SSB01, SSA01, CCMP2556, SSA02, SSE01 and the aposymbiotic control. Left panels are brightfield images, right panels are red autofluorescence of algal photosynthetic pigments. Note the diffuse weak autofluorescence of larvae that is distinct from the bright puncta of the algae.

SUPPLEMENTARY INFORMATION
Aiptasia sp. larvae as a model to reveal mechanisms of symbiont selection in cnidarians
Authors: I. Wolfowicz, S. Baumgarten, P.A. Voss, E.A. Hambleton, C.R. Voolstra, M. Hatta, A. Guse

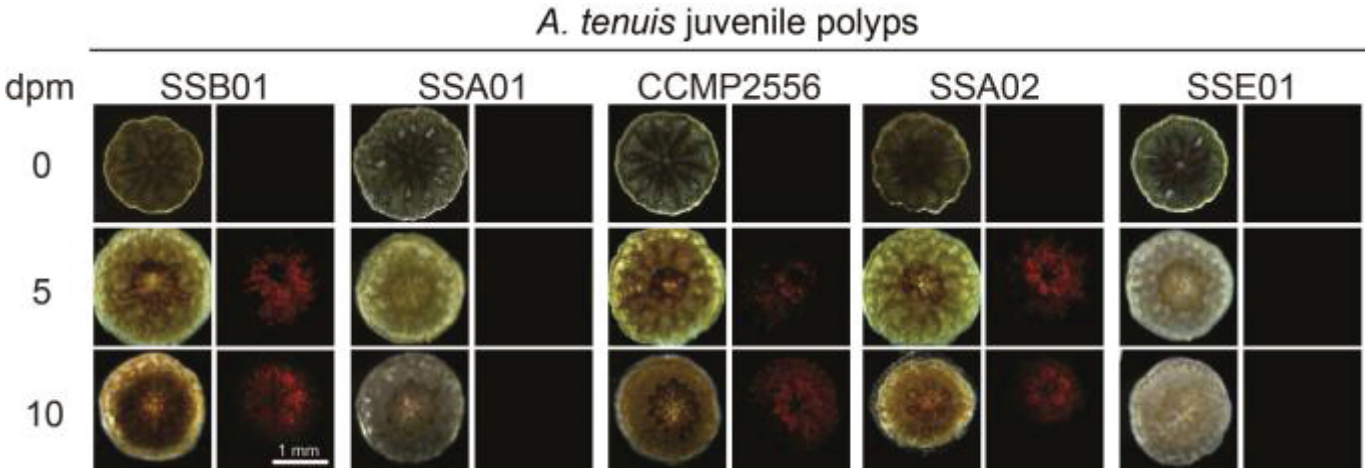

Supplementary Figure S2: Representative images of *Symbiodinium* infections in *A. tenuis* polyps. Left panels are brightfield images, right panels are red autofluorescence of algal photosynthetic pigments. dpm = days post-metamorphosis.

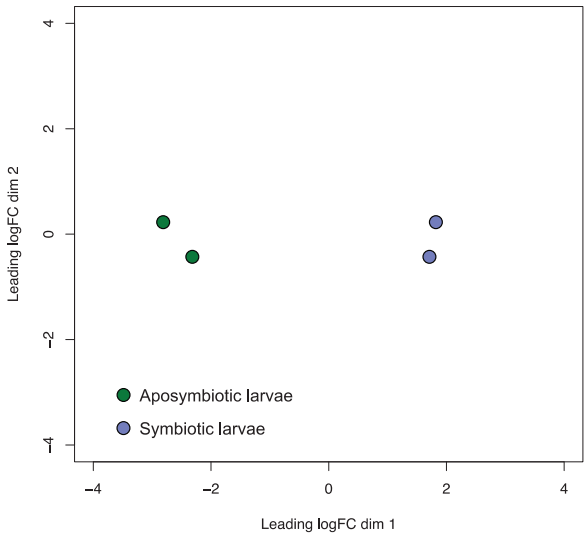

Supplementary Figure S3: Multidimensional scaling plot showing the replicate clustering along the primary and secondary leading log2 fold change (LFC) axes of differentially expressed genes (n= 351, FDR ≤ 0.1).

SUPPLEMENTARY INFORMATION
Aiptasia sp. larvae as a model to reveal mechanisms of symbiont selection in cnidarians
Authors: I. Wolfowicz, S. Baumgarten, P.A. Voss, E.A. Hambleton, C.R. Voolstra, M. Hatta, A. Guse

Supplementary Table S2: Quantification of *Acropora* larvae infections with SSB01, SSA01, SSA02, SSE01, CCMP2556 and the aposymbiotic control.

A. tenuis	Triplicate #	# Larvae	# Larvae infected	% Larvae infected
SSB01	1	26	26	100
	2	25	25	100
	3	24	24	100

A. digitifera	Triplicate #	# Larvae	# Larvae infected	% Larvae infected
SSB01	1	13	13	100
	2	16	16	100
	3	17	16	94

A. tenuis	Triplicate #	# Larvae	# Larvae infected	% Larvae infected
SSA01	1	23	3	13
	2	30	3	10
	3	22	2	9

A. digitifera	Triplicate #	# Larvae	# Larvae infected	% Larvae infected
SSA01	1	20	3	15
	2	12	1	8
	3	14	0	0

A. tenuis	Triplicate #	# Larvae	# Larvae infected	% Larvae infected
SSA02	1	27	25	93
	2	26	24	92
	3	24	23	96

A. digitifera	Triplicate #	# Larvae	# Larvae infected	% Larvae infected
SSA02	1	16	14	88
	2	18	16	89
	3	10	8	80

A. tenuis	Triplicate #	# Larvae	# Larvae infected	% Larvae infected
SSE01	1	28	3	11
	2	28	2	7
	3	21	5	24

A. digitifera	Triplicate #	# Larvae	# Larvae infected	% Larvae infected
SSE01	1	18	6	33
	2	19	3	16
	3	18	5	28

A. tenuis	Triplicate #	# Larvae	# Larvae infected	% Larvae infected
CCMP 2556	1	29	29	100
	2	18	18	100
	3	31	31	100

A. digitifera	Triplicate #	# Larvae	# Larvae infected	% Larvae infected
CCMP 2556	1	29	24	83
	2	28	23	82
	3	28	22	79

A. tenuis	Triplicate #	# Larvae	# Larvae infected	% Larvae infected
Apo	1	27	0	0
	2	22	0	0
	3	22	0	0

A. digitifera	Triplicate #	# Larvae	# Larvae infected	% Larvae infected
Apo	1	18	0	0
	2	22	0	0
	3	25	0	0

SUPPLEMENTARY INFORMATION
Aiptasia sp. larvae as a model to reveal mechanisms of symbiont selection in cnidarians
Authors: I. Wolfowicz, S. Baumgarten, P.A. Voss, E.A. Hambleton, C.R. Voolstra, M. Hatta, A. Guse

Supplementary Table S3: Quantification of *Acropora* polyps infections with SSB01, SSA01, SSA02, SSE01, CCMP2556 and the aposymbiotic control. dpm = days post-metamorphosis.

A. tenuis	dpm	# polyps	# polyps infected	% polyps infected
SSB01	1	66	0	0
	2	66	2	3
	3	60	12	20
	4	58	46	79
	5	58	58	100
	6	57	57	100
	7	57	57	100
	8	53	53	100
	9	53	53	100
	10	53	53	100

A. digitifera	dpm	# polyps	# polyps infected	% polyps infected
SSB01	1	44	0	0
	2	44	3	7
	3	43	8	19
	4	33	32	97
	5	33	33	100
	6	32	32	100
	7	32	32	100
	8	32	32	100
	9	32	32	100
	10	32	32	100

A. tenuis	dpm	# polyps	# polyps infected	% polyps infected
SSA01	1	56	0	0
	2	56	0	0
	3	56	0	0
	4	56	0	0
	5	56	1	2
	6	56	7	13
	7	55	3	5
	8	55	9	16
	9	55	4	7
	10	55	3	5

A. digitifera	dpm	# polyps	# polyps infected	% polyps infected
SSA01	1	36	0	0
	2	36	3	8
	3	30	0	0
	4	26	0	0
	5	23	1	4
	6	23	0	0
	7	23	2	9
	8	23	6	26
	9	23	5	22
	10	23	4	17

A. tenuis	dpm	# polyps	# polyps infected	% polyps infected
SSA02	1	59	0	0
	2	59	1	2
	3	57	21	37
	4	56	46	82
	5	56	53	95
	6	56	56	100
	7	55	55	100
	8	55	55	100
	9	55	55	100
	10	55	55	100

A. digitifera	dpm	# polyps	# polyps infected	% polyps infected
SSA02	1	35	0	0
	2	35	0	0
	3	31	5	16
	4	30	19	63
	5	29	22	76
	6	14	14	100
	7	11	11	100
	8	9	9	100
	9	9	9	100
	10	9	9	100

Supplementary Table S3 (continued): Quantification of *Acropora* polyps infections with SSB01, SSA01, SSA02, SSE01, CCMP2556 and the aposymbiotic control. dpm = days post-metamorphosis.

A. tenuis	dpm	# polyps	# polyps infected	% polyps infected
SSE01	1	41	0	0
	2	41	0	0
	3	32	0	0
	4	32	1	3
	5	27	0	0
	6	27	2	7
	7	27	4	15
	8	27	4	15
	9	27	4	15
	10	27	4	15

A. digitifera	dpm	# polyps	# polyps infected	% polyps infected
SSE01	1	37	0	0
	2	37	0	0
	3	35	0	0
	4	35	5	14
	5	35	2	6
	6	35	2	6
	7	34	6	18
	8	34	16	47
	9	34	5	15
	10	34	6	18

A. tenuis	dpm	# polyps	# polyps infected	% polyps infected
CCMP 2556	1	54	0	0
	2	54	5	9
	3	51	21	41
	4	48	31	65
	5	48	42	88
	6	48	48	100
	7	48	48	100
	8	48	48	100
	9	48	48	100
	10	48	48	100

A. digitifera	dpm	# polyps	# polyps infected	% polyps infected
CCMP 2556	1	42	0	0
	2	42	7	17
	3	40	10	25
	4	40	21	53
	5	40	37	93
	6	40	39	98
	7	40	39	98
	8	40	40	100
	9	40	40	100
	10	40	40	100

A. tenuis	dpm	# polyps	# polyps infected	% polyps infected
Apo	1	50	0	0
	2	50	0	0
	3	49	0	0
	4	49	0	0
	5	48	0	0
	6	48	0	0
	7	44	0	0
	8	44	0	0
	9	41	0	0
	10	41	0	0

A. digitifera	dpm	# polyps	# polyps infected	% polyps infected
Apo	1	39	0	0
	2	39	0	0
	3	38	0	0
	4	38	0	0
	5	38	0	0
	6	38	0	0
	7	38	0	0
	8	38	0	0
	9	38	0	0
	10	38	0	0

A complete list of detected differentially expressed genes can be found under “Supplementary Dataset S1” in:

http://www.nature.com/articles/srep32366#supplementary-information

Unpublished data

1. Lysosome distribution in *Aiptasia* sp. larva

To date it is unclear how symbionts avoid phagolysosomal digestion by the host cells. The prevailing belief in the field is that symbionts actively manipulate phagolysosomal maturation to avoid fusion with lysosomes (Davy et al. 2012, Chen et al., 2004 Chen et al. 2003, Chen et al. 2005, Hill & Hill 2012, Hill 2014). This hypothesis is in line with the finding that symbionts co-localize with Rab5, a marker for early phagosomes (Chen et al. 2004). However, in contrast to this, some evidence indicates that symbiosomes indeed resemble digestive lysosomes in the way that they are highly acidic (pH ~ 4, Barott et al. 2015). Thus, the molecular mechanism underlying symbiosome formation is controversial. In the last part of my thesis, I aimed to characterize the molecular composition of symbiosomes by using molecular dyes and establishing immunofluorescence for various molecular markers as the first step towards a mechanistic understanding on how symbionts avoid digestion by the host cell to stably integrate into host cell function.

1. 1 Lysosomal distribution in *Aiptasia* larvae during development

To characterize the post-phagocytic compartment in which intracellular symbionts reside, and in particular to determine whether these vesicles have lysosomal characteristics (as reported for corals in Barott et al.), I first sought to assess the distribution of lysosomes at the organismal and cellular levels in steady state (i.e. non-symbiotic) *Aiptasia* larvae during their development using two classical lysosomal markers.

1.1.1 Lysosome distribution at the organismal level

To map lysosomal distribution in developing larvae at the organismal level, I used confocal microscopy of larvae at 2 and 10 dpf to visualize lysosomes stained with either: (a) the acidotropic Lysotracker, a small basic amine molecule with fluorescent acidotropic properties that is trapped and accumulates in

compartments with low pH; or (b) the protease activity marker DQ-Green, a protease substrate that gets unquenched upon cleavage over a wide pH range, i.e. pH 3 to pH 11 (Kasper et al. 2014, Reis et al. 1998, Salao et al. 2016).

The pattern of lysosome distribution revealed by the different dyes may indicate areas with (high) digestive properties (Figure 5a and Figure 5b). Lysotracker detects mostly lysosomes in the aboral endoderm (Figure 5a, Lysotracker) whereas DQ-Green more evidently stains well-defined puncta, likely lysosomes, in the pharynx (Figure 5b, DQ-Green). DQ-Green shows a consistent staining in the pharynx and mouth aperture (Figure 5b, 2dpf) accompanied with labeling of clusters in the endoderm but not as well-defined spherical vesicles as observed with Lysotracker labelling. Observed puncta possibly indicate the presence of mucus or mucus granules in the oral region of *Aiptasia* – a feature previously described in other marine larvae (Huvard & Holland 1986, Schwarz et al. 1999).

In early development (2dpf), larvae preferentially take up symbionts in the aboral endoderm. In contrast, at later development (10dpf), symbionts show a wider distribution (i.e., aboral and oral) through the endoderm (Bucher et al. 2016). However, it is unclear whether gaining of digestive properties by endodermal cells influences the distribution of symbionts in the endoderm. Interestingly, the staining pattern of each dye alone varied between larvae at 2 dpf and 10 dpf. While young larvae displayed in the endoderm individual spherical vesicles that were homogeneously distributed (Figure 5a, 2dpf), older larvae showed additional prominent clusters (defined as at least 8 spherical vesicles) in the endoderm (Figure 5a, 10dpf). The difference in number of clusters was quantified and numbers are represented in Figure 5c. We find that larvae at 2dpf contain on average of 7 clusters/larva and larvae at 10 dpf an average of 15 clusters/larva (Figure 5c).

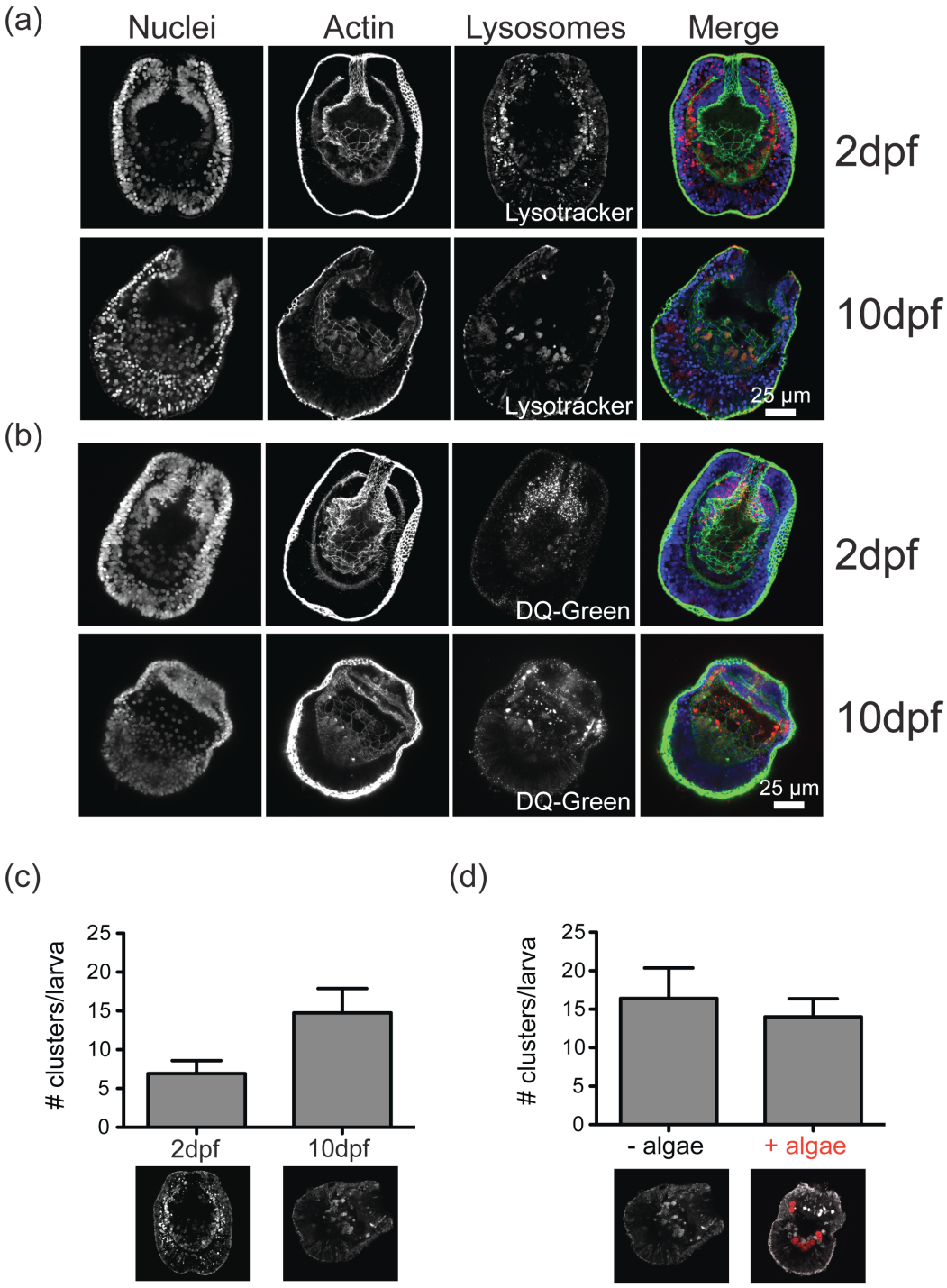

Figure 5 Lysosomal distribution during development in *Aiptasia* larvae at the organismal level. Representative fluorescence confocal microscopy images of lysosomes at developmental stages 2dpf and 10dpf. Hoechst-stained nuclei are shown in blue, phalloidin-stained F-actin to mark cell outlines in green and Lysotracker-stained (a) or DQ-Green-stained lysosomes (b) shown in red. (c) Quantification of changes in number of lysosomal clusters in young (2dpf) and old (10dpf) larvae. Error bars are SEM, *n* = 15 for 2 dpf larvae and 10 dpf larvae; (d) Quantification of

changes in number of lysosomal clusters in symbiotic and symbiont-free larvae at 10 dpf. Error bars are SEM, *n* = 15 for symbiont-free and symbiotic larvae.

Symbionts transfer photosynthetic products thereby altering the nutritional status of their host (Muscatine 1990). In many other systems, the lysosomal distribution changes during starvation (lysosomes cluster close to the nucleus) when compared to lysosomal localization close to the plasma membrane during nutrient uptake (Korolchuck et al. 2011, Dodson et al. 2012, Pu et al. 2015). I investigated global lysosomal localization in response to nutrient input from symbionts.

To test whether the lysosomal distribution in larvae change upon symbiosis establishment, I quantified lysosome clusters in symbiotic and symbiont-free larvae at 10 dpf (Figure 5d). However, I find no significant correlation between symbiont presence and quantity of lysosome clusters. Taken together, the data indicate that the endodermal cells in *Aiptasia* larvae contain lysosomes, which cluster into bigger lysosomal aggregates as larvae age (Figure 5c), potentially within specific secretory cells. This process seems to be independent of whether symbionts are present or not (Figure 5d).

1.2 Characterization of lysosomal-cluster containing cells

Next I asked whether the Lysotracker and DQ-Green co-localize (Figure 6). Both dyes substantially co-localized as shown by the overlap in the endodermal clusters (Figure 6). This indicates that the clusters observed may indeed contain lysosomes.

The lysosomal clusters appear to form a bag-shaped structure with a prominent actin ring outline (possibly an aperture to the gastric cavity) towards the gastric cavity of the larva (see arrows, Figure 7a). The bag-shaped cell-outline, and the abundance of vesicles indicate that these cells may be digestive and/or secretory cells that are integrated into the larval endoderm. The larval ectodermal cells also contain many lysosomes, however no particular difference in lysosomal distribution between larvae at different developmental stages was observed (Figure 7b, and data not shown).

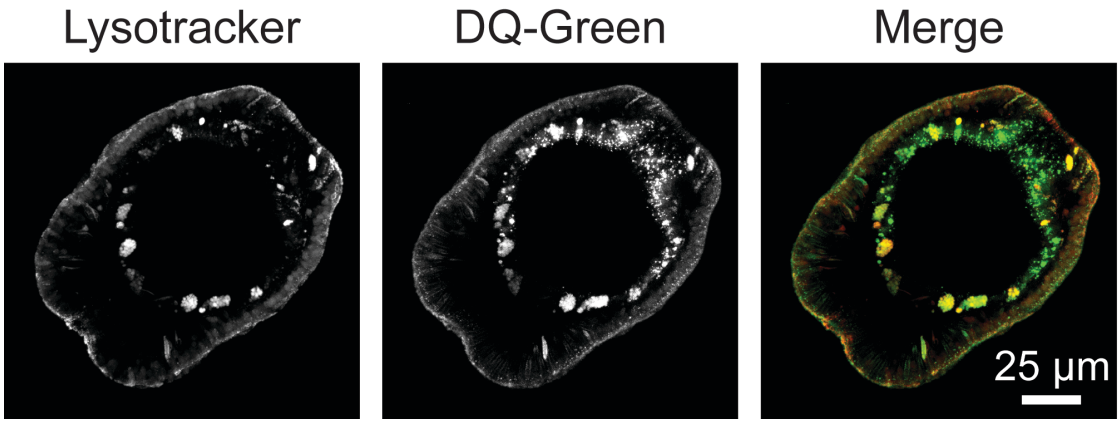

Figure 6 Co-staining of *Aiptasia* larva with lysosomal dyes. Representative fluorescence confocal microscopy images of lysosomes in *Aiptasia* larva. Lysotracker staining is shown in red and DQ-Green-stained lysosomes in green. Co-localization of both molecular markers is yellow.

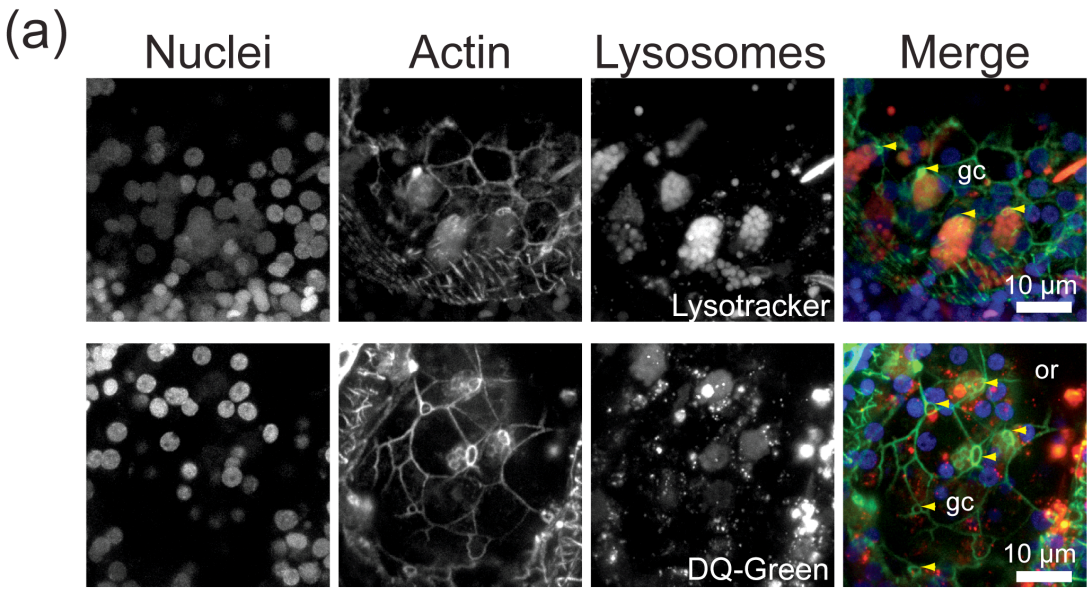

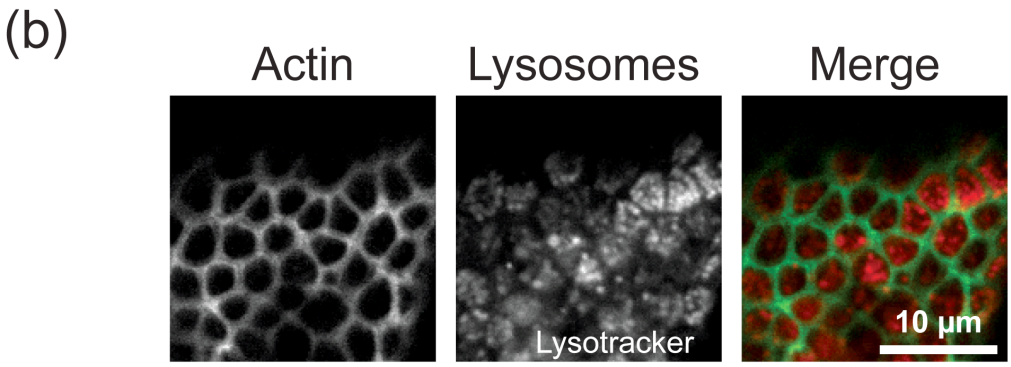

Figure 7 Distribution of lysosomes in endodermal and ectodermal cells. (a) Representative fluorescence confocal microscopy images of endodermal lysosomes of larvae at 10dpf. Hoechst-stained nuclei are shown in blue, phalloidin-stained F-actin to mark cell outlines in green and

Lysotracker-stained or DQ-Green-stained lysosomes in red. Yellow arrowheads show actin rings towards the gastric cavity of larvae. gc = gastric cavity; or = oral; (b) Representative fluorescence confocal microscopy images of ectodermal lysosomes of larvae. Phalloidin-stained F-actin to mark cell outlines in green and Lysotracker-stained lysosomes in red.

1.3 Co-localization of lysosomal dyes with symbionts

After characterizing the distribution of lysosomes in larvae, I next sought to measure the overlap of these lysosomal patterns with intracellular symbionts (Figure 8). I investigated whether symbiosomes display lysosomal characteristics indicated by co-localization with two lysosomal markers. Contrary to what was observed in symbiont-containing coral cells (Barott et al. 2015), we observe no halo of Lysotracker (Figure 8, Lysotracker) or DQ-Green (Figure 8, DQ-Green) around symbiotic algae. In this experiment it is not clear if the lack of halo around symbiotic algae is due to a technical issue or a biological result. Nevertheless, Chen and colleagues found that symbiotic algae co-localize with a non-mature phagosome marker, possibly as a strategy to avoid fusion with lysosomes (Chen et al. 2003, Chen et al. 2005).

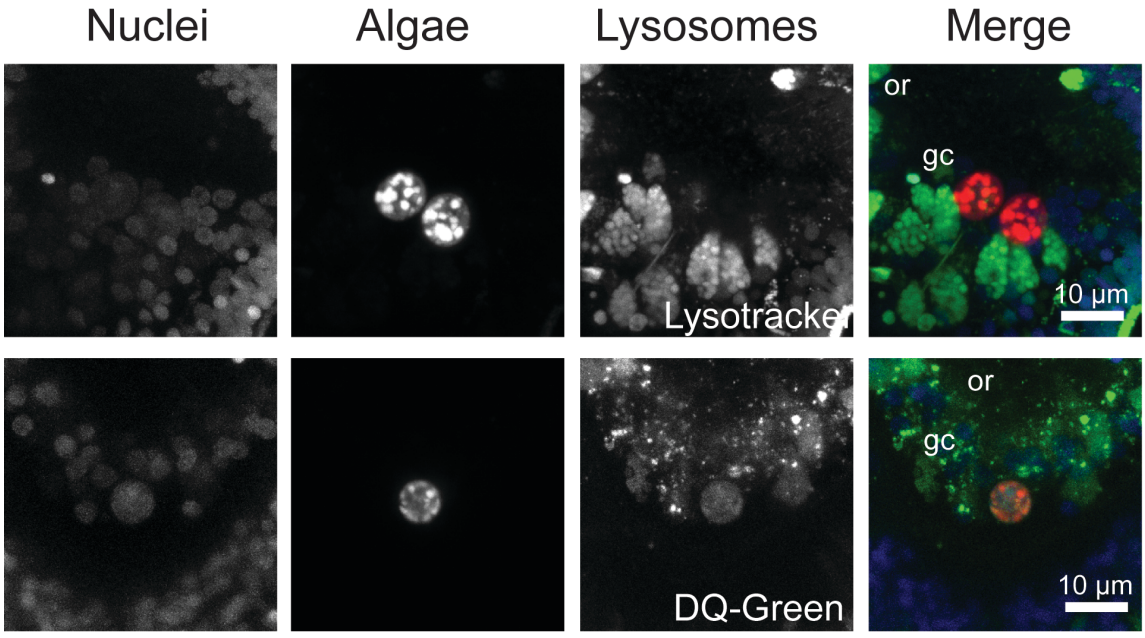

Figure 8 Co-localization of symbiotic algae with lysosomal markers in *Aiptasia* larva. Representative fluorescence confocal microscopy images of symbiotic algae in the endoderm of symbiotic *Aiptasia* larva. Hoechst-stained nuclei are shown in blue, Lysotracker-stained or DQ-Green-stained lysosomes in green; gc = gastric cavity; or = oral.

2. Immunolocalization of lysosomal proteins in *Aiptasia* sp. larva and adult tissue macerates

In the previous section I showed the distribution of lysosomes in *Aiptasia* larvae, providing a basic description of the system and a framework to further characterize the symbiosome in the larva. Using Lysotracker and DQ-Green, the symbiosome was not detected, but it was not clear if this was a technical issue or a biological result. To test it, I used other approaches: staining symbiotic cells with lysosomal markers via immunolocalization in symbiotic larva and macerated symbiotic tissue from *Aiptasia* adult.

2.1. Staining of *Aiptasia* adult symbiotic cell membrane and lysosomes

To distinguish intact isolated symbiotic cells, I used the lipophilic fluorescent tracer DiO to detect cell membranes. In the bright field image, distinct cells are observed (Figure 9, Bright-field, first row): a group of two algal cells, a group of four algal cells and a non-symbiotic cell. The host nucleus is visible in between the group of two algal cells. Possibly these two algal cells share the same host cell but, as seen in the bright-field image (Figure 9, Bright-field, first row), the host cell membrane is compromised. Besides the detection of host nucleus, the algal nucleus is detected together with an unspecific signal, possibly from a starch compartment of the alga. Algal nucleus is distinguished by its bright “dotted” structure (highlighted with a star) (Figure 9, nuclei images), due to the permanently condensed chromosomes of *Symbiodinium* (Shoguchi et al. 2013). Noteworthy, in these experiments, auto-fluorescence from the algae was detected at variable levels/intensities (Figure 9 and Figure 10, Algae column). We have observed this phenomenon multiple times in these experiments and those from others in the lab, but as yet the cause of these differences remains unclear. The DiO membrane shows a bright staining around the algae, either detecting the plasma membrane and/or the symbiosome (Figure 9, first row).

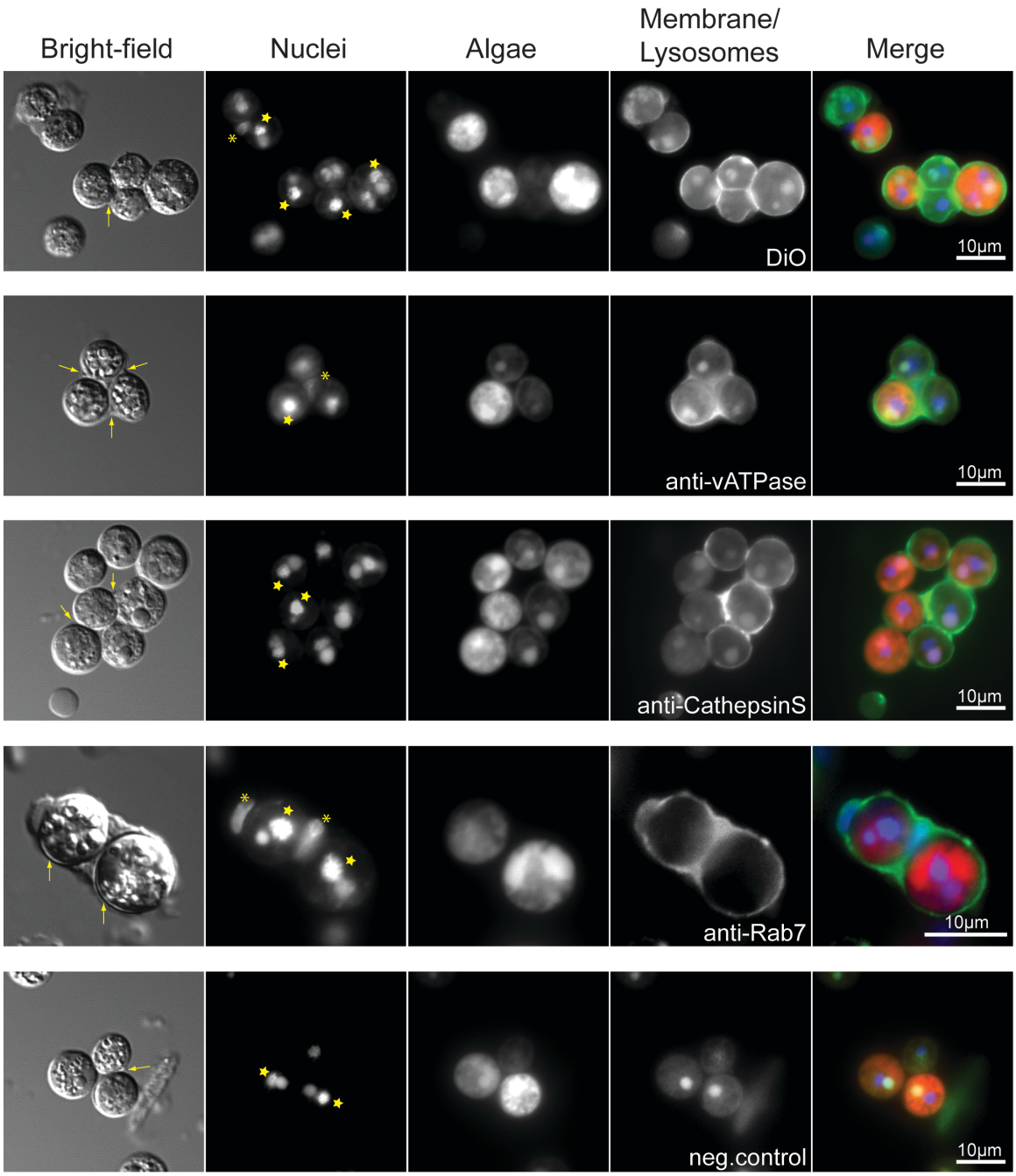

Figure 9 Fluorescence microscopy images of *Aiptasia* adult symbiotic macerated tissue and immunolocalization of lysosomal proteins. Representative fluorescence and immunofluorescence images of *Aiptasia* symbiotic tissue macerates (bright-field), Hoechst-stained nuclei are shown in blue, algae detected via algal photosynthetic pigment in red, membrane-stained and vATPase, Rab7 or Cathepsin S–stained lysosomes shown in green. Stars indicate algal nucleus, asterisks indicate host nucleus and arrows indicate membrane.

It is known that mature phagosomes, lysosomes and phagolysosomes have in their composition several proteins, such as the proton transporter vATPase, the Rab7 GTPase and the acid hydrolase Cathepsin S (Flannagan et al. 2012).

vATPase is a conserved lysosomal proton transporter, which has been shown to decorate symbiont compartments in symbiotic coral cells (Barott et al. 2015) and Rab7 is a lysosomal protein, which has been shown to decorate compartments with heat-killed symbionts and excluded from live symbiont compartments in *Aiptasia* (Chen et al. 2003). Nothing is known about Cathepsin in the context of symbiosis in cnidarians. However, Cathepsins have been detected in a proteomic analysis using *Aiptasia* anemones infected with the microorganism *Vybrio campbellii*, and suggested to be involved in pathogen destruction in the lysosome (Brown & Rodriguez-Lanetty 2015).

I tested whether these proteins constitute the symbiosome in symbiotic cells by immunofluorescence in adult symbiotic tissue macerates (Figure 9). I detected the presence of signal around the algae for the vATPase, Cathepsin S and Rab7 protein markers (Figure 9). Specifically, for the vATPase, I observed the host nucleus between the three algae (Figure 9, second row), strongly indicating that the three algal cells are symbiotic and reside in the same host cell. What is not clear in these images is if the signal is restricted to the symbiosome only. For Cathepsin S (Figure 9, third row), staining is also observed around the algae, but in this case it was not possible to distinguish the host nucleus or nuclei therefore it is difficult to guarantee that this staining is restricted to the symbiosome. In the case of Rab7 (Figure 9, fourth row), each algal cell is close to a host nucleus indicating that each of them belongs to an individual host cell. The continuous signal between the two cells could be a consequence of the integrity of the host cell membrane, which is possibly compromised in this procedure as a consequence of the maceration process and/or staining protocol. Importantly, no unspecific staining around the algae was observed in the negative control (no primary antibody added) in these experiments (Figure 9, last row). Altogether, this is a first indication that lysosomal proteins such as vATPase, Cathepsin S and Rab7 may constitute the symbiosome in symbiotic cells from adult *Aiptasia*. However, this technique does not allow us to be certain about the membrane staining observed being restricted to the symbiosome and not reflecting other structures in *Aiptasia* symbiotic cells.

I also used scanning confocal microscopy, to try to distinguish between those two possibilities (Figure 10). The vATPase staining shows signal around the

algae and in between the algal cells (Figure 10, first row), which could be an indication of staining non-restricted to the symbiosome. This is unexpected, because the vATPase is a protein pump typical of lysosome/vacuole membranes only. The Cathepsin S is mostly detected around the algae (Figure 10, middle row), thereby possibly reflecting the symbiosome only. In this case, the distribution of Cathepsin S seems to be more specific than that of the vATPase. The caveat of this trial was that no host nucleus was observed and cell membrane staining was not performed. Therefore, it is not possible to guarantee that these host cells were symbiotic. An important point is that the algal cells seem to maintain an intact symbiosome around them after tissue maceration. Rab7 staining reveals a localization pattern similar to that of the vATPase (Figure 10, lower row). In this experiment, Rab7 localizes around the individual algae, but also close to the host nucleus. As mentioned above, algae autofluorescence varies and differences in fluorescence intensity are observed. In the future, a membrane staining should be combined with the immunolocalization of lysosomal proteins for the host cell membrane to be distinguished from the symbiosome of symbiotic cells.

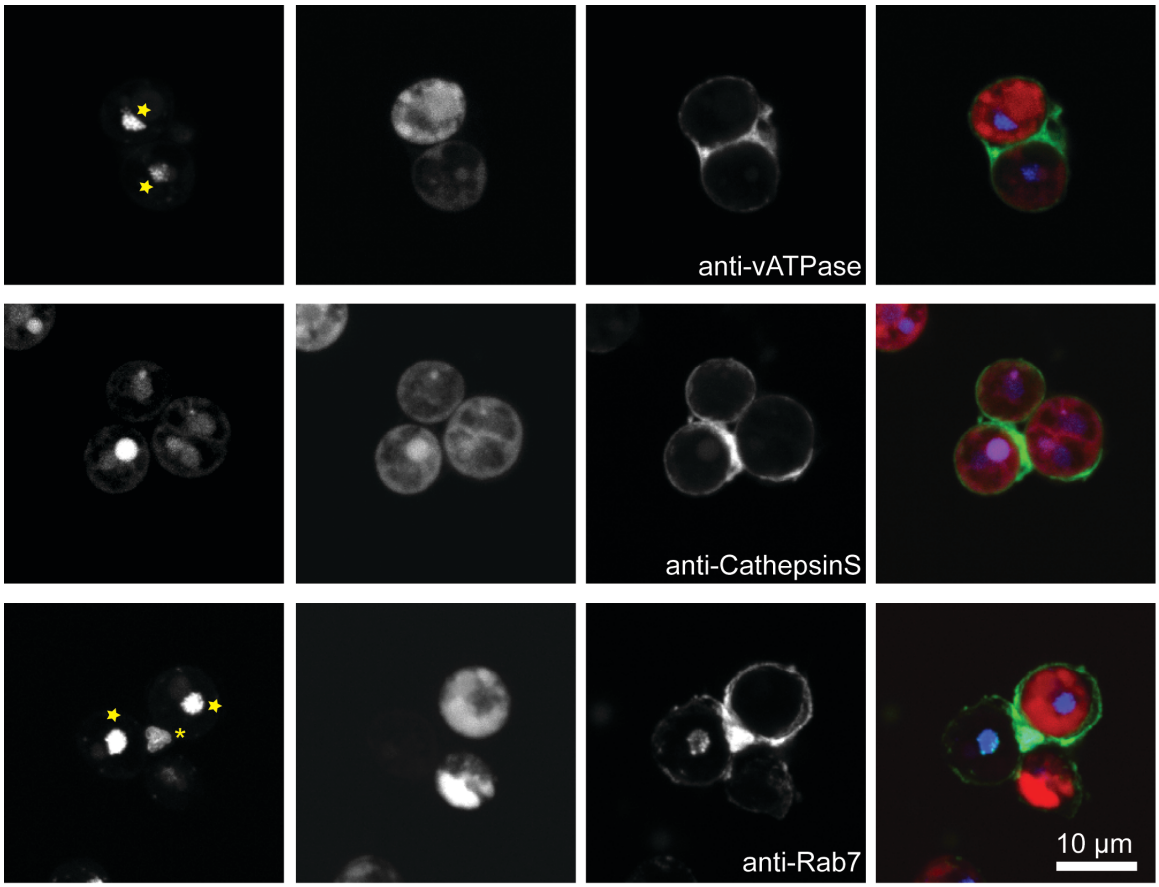

Figure 10 Immunolocalization of lysosomal proteins in *Aiptasia* adult symbiotic macerated tissue. Representative fluorescence confocal microscopy images of symbiotic cells. Hoechst-stained nuclei are shown in blue, algae detected via algal photosynthetic pigment shown in red, vATPase, Rab7 or Cathepsin S–staining shown in green. Stars indicate algal nucleus, asterisk indicates host nucleus.

2.2. Co-localization of lysosomes and intracellular symbionts

To overcome potential technical issues or artifacts associated with the preparation of macerated cells, I tested whether symbiosomes co-localize with lysosomal markers in whole *Aiptasia* larvae. In this case, both lysosomal dyes Lysotracker and DQ-Green and antibodies against vATPase and Rab7 were used. Contrary to what was observed in symbiont-containing coral cells (Barott et al. 2015), a halo of vATPase (and Rab7) around symbiotic algae was not observed (Figure 11). However, further tests will be necessary to guarantee that the antibodies used work well in *Aiptasia* larvae.

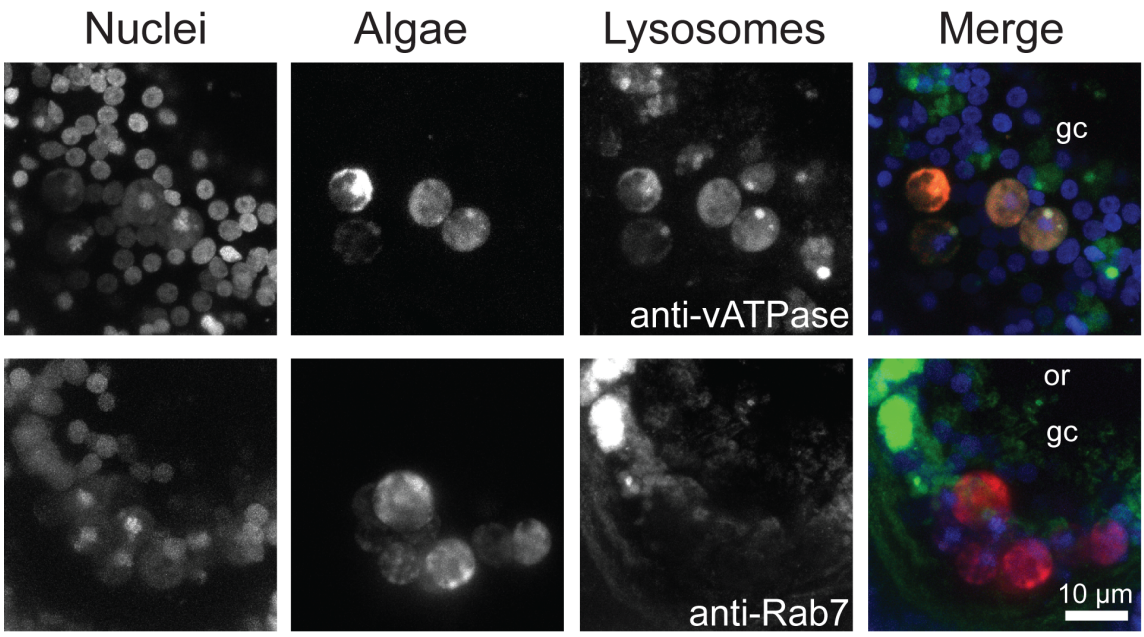

Figure 11 Co-localization of symbiotic algae with lysosomal markers in *Aiptasia* larva. Representative fluorescence confocal microscopy images of symbiotic larvae. Hoechst-stained nuclei are shown in blue, vATPase-stained or Rab7-stained lysosomes in green; gc = gastric cavity; or = oral.

2.3 Expression of vATPase and Cathepsin S in *Aiptasia*

I also tested the abundance of vATPase and Cathepsin S proteins in *Aiptasia* adult homogenates by Western Blot (Figure 12). A single band of the expected molecular weight (58 kDa) is observed with the antibody against the vATPase indicating that the antibody indeed recognizes *Aiptasia* vATPase protein. Western blots using the antibody against Cathepsin S were however not conclusive (Figure 12): *Aiptasia* Cathepsin S has a molecular weight of approximately 37 kDa and a single band of around 70 kDa was detected. Thus, it is likely that this antibody is not detecting Cathepsin S in our system.

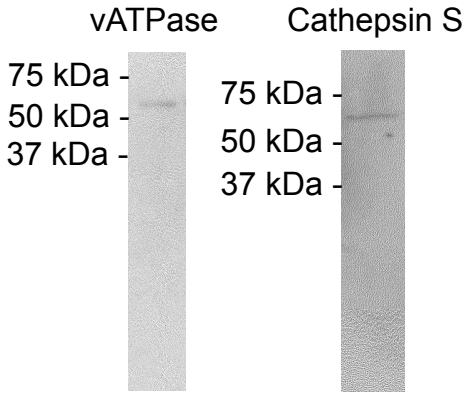

Figure 12 Western blot of vATPase and Cathepsin S in *Aiptasia* extracts. Western Blot detection of *Aiptasia* vATPase (molecular weight 58 kDa) and Cathepsin S (molecular weight 37 kDa) using anti-vATPase and anti-Cathepsin S antibodies.

3. Materials and Methods

Aiptasia culture conditions and spawning induction

Aiptasia clonal lines CC7 and F003 were cultured and induced to spawn with subsequent larvae collection, filtration and maintenance as previously described (Grawunder et al. 2015).

Symbiodinium culture conditions

The clonal and axenic cultures of *Symbiodinium* type SSB01 (Xiang et al. 2013) were kept in IMK medium (Ishikura et al. 2004) in an Intellus Ultra Controller Incubator (Model I-36LL4LX, Percival) at 26 °C and 20-25 µmol/m/s of photosynthetically active radiation (PAR) under 12h light:12h dark regime as previously described (Xiang et al. 2013). To determine the algal density, for larval infection experiments, an automated cell counter (TC20, #1450102, BioRad) was used.

Symbiosis establishment experiments in *Aiptasia* larvae

Aiptasia larvae at 2dpf were counted as previously described (Grawunder et al. 2015), and distributed in 6-well cell culture plates with 300 larvae in 5 ml of artificial seawater (ASW) per well. *Symbiodinium* type SSB01 was added to each well at 10.000 algal cells/ml for 3 or 8 days followed by gentle pipetting up and down. Larvae were stained and prepared for microscopy as described below.

Aiptasia larvae lysosomal staining

The distribution of lysosomes in *Aiptasia* larvae at 2 dpf and 10 dpf from three biological replicates was investigated using two live dyes: the acidotropic dye LysoTracker Red DND-99 (#L7528, Life Technologies) (as from now referred as Lysotracker, for simplicity) and the fluorogenic substrate for proteases DQ-Green BSA (#D12050, Life Technologies) (as from now referred as DQ-Green, for simplicity). Either Lysotracker or DQ-Green was added to a final concentration of 1µg/ml and 10µg/ml in ASW, respectively, to either symbiotic or symbiont-free larvae. Between 100-150 larvae were incubated in 1 ml of the mixture in 24-well cell culture plates for 2h (Lysotracker) or overnight (DQ-Green) protected from

light. After incubation, larvae were fixed for 30-45 minutes with 4% formaldehyde in PBS with 3 subsequent washes with PBS. If not specified differently, all incubation and washing steps occurred at room temperature (RT). Larvae samples were stained for actin with either phalloidin-alexa488 or phalloiding-atto561, and nuclei stained with Hoechst and subsequently mounted for microscopy according to Bucher et al. 2016 and Wolfowicz et al. 2016. For co-localization assessment larvae were first stained with DQ-Green at 10µg/ml overnight, directly followed by 1µg/ml of Lysotracker staining for 2h.

Aiptasia larvae immunofluorescence

For antibody staining, larvae at 5 dpf from two biological replicates were fixed with formaldehyde and washed in PBS as described above. Subsequently, approximately 100 larvae from each two biological replicates were collected in 0.2 ml reaction tubes and washed twice briefly with PBS-0.2% Triton X-100 (PBS-T). For permeabilization, larvae were subjected to PBS-T for 1h. In order to block unspecific binding, larvae were incubated in 1% BSA in PBS-0.1% Triton X-100 (blocking buffer) for 1h. Primary monoclonal antibodies were raised against a peptide from human Rab7 protein, epitope EQAFQTIARNALKQE, (mouse monoclonal, #R8779, Sigma Aldrich) with 86.7% identity (13 out of 15 residues) to the corresponding sequence of *Aiptasia* Rab7 (AIPGENE5165), and a peptide from human vATPase Subunit B2 protein, epitope AAREEVPGRRGFPGY, (rabbit monoclonal, #A00960-owl, One World Lab), with 100% identity (15 out of 15 residues) to the corresponding sequence of *Aiptasia* vATPase (AIPGENE19317). Antibodies were each centrifuged at 13 000 *xg* for 5 min prior to dilution (1:100) in blocking buffer and added to larvae overnight at 4 °C. PBS-T only was used as negative control. The next day, larvae were washed 2 times briefly in PBS-T followed by 3 washes of 15 min each with PBS-T. Secondary polyclonal antibody coupled to Alexa Fluor 488 were prepared as described above in blocking buffer at a 1:100 dilution: either goat anti-mouse polyclonal IgG (#A-11001, ThermoFischer Scientific) for anti-Rab7 detection or goat anti-rabbit polyclonal IgG (#ab150089, Abcam) for anti-vATPase detection, The samples were incubated for 2h under gently rotation at RT. Samples were then washed twice briefly with PBS-T followed by 3 washes of 15 min each with PBS-T. When lysosomes were stained with DQ-Green, actin was stained with Phalloidin-Atto561 (described in Wolfowicz et al.

2016), was excited at 561nm and DQ-Green at 488nm. To detect nuclei, samples were stained with Hoechst at 10 µg/ml in antibody dilution buffer for 15 min at RT, followed by washing twice briefly with PBS-T, twice with PBS-T for 10 min each, and 3 times briefly with PBS. Larvae were mounted between slide and coverslip as previously described in Bucher et al. 2016.

Aiptasia immunofluorescence in adult tissue macerates

To collect symbiotic cells, 3 tentacles of each 3 to 4 *Aiptasia* clonal line CC7 (oral disk diameter approx. 0.5-1.0 cm) were collected with tweezers into a 1.5 micro-centrifuge tube. Tentacles were transferred to a plastic petri dish in 200µl PBS and cute transversally to scrape off the endoderm with a scalpel. This procedure was performed under a Leica S8APO binocular (top illumination), to allow easy visualization of tentacles' tissues. To increase mechanical maceration of tissue, the samples were pipetted 3 times up and down with a 200µl pipette. A volume of 200µl was transferred to a 15ml ml tube and fixed with 4% formaldehyde for 20min at RT. To remove the fixative, 5ml of PBS was added to the mixture followed by centrifugation at 2500 rpm (GS-6R centrifuge, Beckman) for 10 min. The supernatant was removed, the pellet re-suspended in 200µl PBS and transferred to a 1.5ml micro-centrifuge tube. A Neubauer chamber was used to assess cell concentration of the suspension. In order to prepare for detection of lysosomes or cell membrane, the symbiotic tissue macerates were allowed to adhere to 10-well 6.7 mm Ø diagnostic microscope slides (ER-208B-CE24, #574572, Thermo Scientific). Between 10.000-20.000 cells were added per well in 10 to 20µl volume. The cell suspension was allowed to dry under the fume hood for 30-60 min followed by re-hydration with 20 µl deionized water for 5 min. Excess of water and subsequent excess of liquid through this protocol was removed by suction using a vacuum system connected to a 200µl pipette tip. To permeabilize cells, PBS-T was added, followed by 20 min incubation at room temperature. The excess of liquid was removed and samples were allowed to block in 1% BSA in PBS-0.1% Triton X-100 (blocking buffer) for 1h and 30min. For cell membrane staining, DiO (#D275, ThermoScientific) was dissolved in DMSO to form a stock solution of 1 mg/ml and further diluted in PBS to 0.5µg/ml for addition into cell suspension. Primary monoclonal antibodies for Rab7 (#R8779, Sigma Aldrich),

vATPase Subunit B2 (#A00960_owl, One World Lab) or Cathepsin S epitope QLKLKTGKLVSL (#bs-8558R_owl, One World Lab) with 75% identity (9 out of 12 residues) with the *Aiptasia* Cathepsin S (AIPGENE6003), was centrifuged at 11 000 *xg* for 5 min prior to 1:100 dilution in blocking buffer in a 1.5 micro-centrifuge tube with subsequent brief vortex and brief spin-down. For staining, either DiO or the correspondent antibody was added to the cells adhered. PBS-0.1% Triton X-100 was used as negative control. DiO was incubated for 1 hour at RT and antibodies were incubated overnight at 4 °C. For DiO staining, samples were washed 3 times with PBS-T followed by nuclei staining with Hoechst at 10 µg/ml in antibody dilution buffer for 15 min at RT and protected from light. This was followed by washing 2 times briefly and 2 times 10 min each time with PBS-T, followed by 3 consecutive brief washes with PBS to remove detergent. For mounting, 3µl of 87% glycerol in PBS containing 2.5 mg/ml DABCO (#D27802, Sigma Aldrich) was added per well and covered with a cover slip, which was directly sealed with transparent nail polish. After drying of the nail polish, samples were either immediately imaged or stored at 4 °C.

For primary antibody staining, incubation was performed overnight and slides were kept in a humid chamber in order to prevent evaporation and concentration effects. The next day, liquid and excess of antibody was removed by briefly washing with 20 µl of PBS-T followed by 3 subsequent washes with the same buffer for 10 min each washing step. For primary antibody-binding detection, a secondary polyclonal antibody coupled with Alexa Fluor 488 was prepared the same way as described above in a 1:100 dilution and allowed to incubate for 1h and 45 min at RT, while protected from light. For mouse anti-Rab7 detection, the goat anti-mouse IgG Alexa Fluor 488 (#A-11001, ThermoFischer Scientific) was used. For rabbit anti-vATPase and rabbit anti-Cathepsin S detection, the goat anti-rabbit IgG Alexa Fluor 488 (#ab150089, Abcam) was used instead. To protect the samples from bleaching, antibody incubation and subsequent steps were performed in the dark by using the humid chamber covered with aluminum foil. After incubation, liquid and excess of secondary antibody was removed by washing 3 times briefly and 3 times for 15 min each time with PBS-T. To detect host and symbiont nuclei, samples were allowed to incubate with Hoechst at 10

µg/ml in antibody dilution buffer for 15 min at RT, followed by mounting as described above.

Image acquisition

Confocal images of 10 *Aiptasia* larvae per biological replicate per condition were acquired using a Nikon A1R confocal scanning microscope (Nikon Imaging Centre, Heidelberg University) with a Nikon Plan Apo 60x oil immersion objective (NA = 1.4). Hoechst-stained nuclei were excited at 405nm (detector 425-475nm), DQ-Green-stained lysosomes at 488nm (detector 500-530nm), Phalloidin-stained actin at 488nm (detector 500-530nm) or at 561nm (detector 570-620nm) for Phalloidin-Atto561, Lysotracker-stained lysosomes at 561nm (detector 570-620nm) and algae autofluorescence at 640nm (detector 663-738nm). For co-localization of Lysotracker with DQ-Green, the dyes were tested to assure that these fluorochroms did not bleed through into other channels. Larvae acquired images represent optical sections of 1µm in thickness, pixel size of 0.140µm. Confocal images of 3 to 6 adult's symbiotic isolated cells were acquired using the same microscope as above mentioned and using the same Nikon Plan Apo 60x oil immersion objective (NA = 1.4). Hoechst-stained nuclei were excited at 405nm (detector 425-475nm), antibodies were detected at 488nm (detector 500-530nm) and algae autofluorescence at 640nm (detector 663-738nm). Adult symbiotic isolated cells acquired images represent optical sections of 0.5µm in thickness, pixel size of 0.140µm. All images were acquired with NIS-Elements software. Image processing and maximum projections of Z-stacks were performed using Fiji (Schindelin et al. 2012).

Fluorescence microscopy images of *Aiptasia* adult macerates were acquired with a Nikon Eclipse Ti-E inverted epifluoresecence microscope, using a Nikon Plan Apo 60X oil (NA = 1.4) or Nikon Plan Apo 100x oil (NA = 1.45) Apo Plan objectives using DAPI (#DAPI-1160B-000, Semrock), FITC (#F36-511, Semrock) and TRITC (mCherry/Texas Red Longpass #49017, Chroma) filters. Immunofluorescence of Rab7, vATPase and Cathepsin S staining in 10-20 isolated cells from 3 or 4 biological replicates were detected based on the green fluorescence from the secondary antibodies and the red auto-fluorescence of chlorophyll from *Symbiodinium*. The host cell membrane stained with DiO was

detected via its green fluorescence. For non-DiO-stained samples, bright-field was used to detect the host cell membrane. Symbiotic cells were identified by the observation of at least two *Symbiodinium* cells with a host nucleus between the symbionts surrounded by the host cell membrane.

Confirmation of vATPase and Cathepsin S protein expression

To determine antibody specificity for *Aiptasia* epitopes, 3 adult *Aiptasia* clonal line CC7 (oral disk diameter 0.1-0.4 cm) were collected into a 1.5 micro-centrifuge tube and heated up for 5 min at 95 °C in 100 µl 4% SDS in 50mM Tris-HCl pH 7.5. This was followed by homogenization using a sonicator for 20 pulses and subsequent heating for 5 min at 95 °C. Debris was separated from proteins by centrifugation at 11 000 *xg* at RT for 10 min. The supernatant was collected in a clean 1.5 micro-centrifuge tube and total protein concentration determination with a BCA assay kit (#23225, Pierce) using BSA as standard curve. Approximately 20 µg of total protein were separated by electrophoresis and transferred to a nitrocellulose membrane. Membranes were blocked with 5% BSA in PBS-T for 1.5 hours at RT followed by 10 min washing in PBS-T and incubated with primary antibody overnight at 4 °C. Non-binding antibody was removed by washing for approximately 1 hour with PBS-T at RT. Secondary antibody was added and while protected from light incubated for 1 hour, followed by 1 hour washing with PBS-T both at RT. A last wash with PBS was performed before the membrane was developed using an ECL 1:1 developing mixture and signal was detected with photographic film.

Quantification of lysosome clusters in the endoderm of *Aiptasia* larvae

In order to quantify and describe the lysosomal clustering in *Aiptasia* larvae, confocal images were acquired as described above with Lysotracker. Per experimental condition, 15 larvae with approximately 60 optical sections in *z* per larvae were analyzed. 8 or more spherical clustered vesicles forming a bag-shaped structure tightly surrounded by actin were considered a cluster.

Chapter 4 – General discussion

This thesis aimed to overcome a bottleneck in cnidarian symbiosis research by further developing *Aiptasia* as a model organism. Symbiosis is recognized to be a widespread phenomenon in nature with enormous consequences for the physiology of many organisms, specifically for the survival of coral reefs. However, despite symbiosis' importance, progress in understanding coral-algae symbiosis has been slow, mostly due to corals' intrinsic limitations as model organisms. In my thesis, I contributed to develop *Aiptasia* larvae as a model system for coral symbiosis establishment by contributing to characterizing anemone lines and symbionts, establishing a robust spawning protocol and fieldwork experiments to directly compare *Aiptasia* to corals. I revealed similarities in patterns of symbiosis establishment in *Aiptasia* and coral larvae, indicating that symbiosis mechanisms may be similar between these species and highlighting the relevance of *Aiptasia* as a model organism. Next, I participated in describing symbiosis establishment in *Aiptasia* larvae at the organismal and cellular level and in developing imaging tools as well as identifying candidate genes to move towards a mechanistic analysis. Building up on this foundational work, I finally explored fundamental questions such as which cells take up symbionts and how the symbiosome compares to related organelles. My piloting experiments suggest that the larval endoderm has distinct cells types including secretory and symbiosis-specific cells and that symbiosomes share similarities with lysosomes. In the following I will discuss my findings in a broader context and provide an outlook on promising future directions as well as remaining limitations of the system.

Symbiosis specificity

The selection of appropriate symbionts is suspected to follow a winnowing process (Nyholm & McFall Ngai 2004), but evidence on the cellular events governing it is lacking. Therefore, a direct comparison of patterns of symbiosis between *Aiptasia* and corals was essential to show that algal symbiosis patterns between the two systems are similar and to thereby endorse the *Aiptasia*-*Symbiodinium* system for the study of coral symbiont selection. Using the symbiosis establishment assay, I revealed patterns of symbiosis in *Aiptasia* larvae and larvae from two coral species of a coral genus that is ubiquitous in the reefs –

Acropora. The fact that defined algal cultures of different *Symbiodinium* types were available (Xiang et al. 2013, Grawunder et al. 2015, Yamashita & Koike 2013) was crucial for these experiments: we could compare symbiosis establishment patterns with the same defined *Symbiodinium* types. Specifically, I tested two *Symbiodinium* types originally isolated from *Aiptasia*, two from corals and one type widely regarded as non-symbiotic or "free-living" (Xiang et al. 2013, Grawunder et al. 2015, Yamashita & Koike 2013). We found that, in the conditions tested, the majority of symbiont types tested behaved similarly in *Aiptasia* and corals. Importantly, the algal type *Symbiodinium* SSB01 and SSE01, established symbiosis similarly in *Aiptasia* and in the coral species tested. After showing that symbiosis establishment appears to be similar in *Aiptasia* and corals, we used the *Aiptasia* larva system to further dissect the steps involved in symbiosis establishment, with *Symbiodinium* SSB01 being positively selected into the gastric cavity and subsequently into endodermal cells, in contrast to *Symbiodinium* SSE01 which does not populate the host tissue. Since *Symbiodinium* SSE01 is thought to be non-symbiotic, it was unexpected that it localizes inside endodermal cells. Our results therefore contradict previous findings that defend *Symbiodinium* SSE01, and more broadly the clade E, to be exclusively found as "free-living" and speculated that clade E lacked the ability to enter the host cell (Xiang et al. 2013, Yamashita and Koike 2013, Jeong et al. 2014). These findings strengthened the indication that the positive selection of symbionts can occur post-phagocytosis and that the mechanisms leading to either maintenance or digestion/expulsion are essential in the winnowing process. This is consistent with observations in coral larvae indicating enhanced success of endogenous symbionts over heterologous ones in re-infection experiments (Weis et al. 2001, Rodriguez-Lanetty et al. 2006b).

Taken together, this set of experiments provides the basis for the future molecular dissection of the winnowing process that is conserved between *Acropora* and *Aiptasia* taking advantage of the opportunities of using *Aiptasia* as a model system. The individual steps from uptake into the gastric cavity to sorting of compatible and incompatible symbionts after phagocytosis can be assessed qualitatively and quantitatively using high-resolution microscopy and, in combination with RNA-Seq experiments that compared gene expression in non-

symbiotic relative to symbiotic larvae at the whole organism level (Wolfowicz et al. 2016) genes involved in each step can be identified. Previous RNA-Seq analysis in coral larvae did not reveal any differences in gene regulation before or after symbiosis establishment (Voolstra et al. 2009, Schnitzler et al. 2010). Maybe because of an ideal ratio of symbiotic cells versus non-symbiotic cells (ectoderm and non-symbiotic endoderm) and/or suitable time of development and symbiosis establishment, we detected differentially expressed genes when we performed RNA-Seq in whole symbiotic versus non-symbiotic larvae of *Aiptasia*: interestingly, we find that approximately 62% genes are down-regulated and 38% genes are up-regulated in the symbiotic compared to the non-symbiotic state. From the total 351 differentially expressed genes detected, 41 are known to be involved in processes previously suggested to play a role in cnidarian symbiosis either by transcriptome approaches or cell biological evidence (Lehnert et al. 2014, Dani et al. 2014, Chen et al. 2004, Chen et al. 2005). Most of these genes are down-regulated and are involved in processes of phagocytosis, endocytosis and general actin and microtubule cytoskeleton dynamics. This suggests that host cells could be "shutting down" the entrance/phagocytosis of additional symbionts in order to guarantee residency of those already internalized. Reduced internalization would also prevent pathogens to enter and prevent symbiont survival. In agreement with this, a previous study revealed that genes involved in cell growth were down-regulated in symbiotic anemones, suggesting that down-regulation of the host cell cycle could be a strategy to maintain symbionts (Rodriguez-Lanetty et al. 2006a). It is interesting to notice that, from the candidate genes involved in cytoskeleton related processes, alpha-tubulin is the only gene that is up-regulated in symbiotic larvae which is interesting and worth exploring in the future. While most genes related to phagocytosis and cytoskeleton are down-regulated, genes that encode proteins that constitute lysosomes are highly expressed in symbiotic larvae. This may suggest an important role of lysosomes in symbiosis. Such genes encode for lysosome proteins called NPCs (Niemann-Pick type C proteins) known to be highly expressed in the *Aiptasia* and in other symbiotic anemones (Lehnert et al. 2014, Dani et al. 2014). Also, human NPCs are responsible for cholesterol binding and homeostasis (reviewed in Vence et al. 2011), and lipid metabolism has been previously suggested to play a role in cnidarian symbiosis (Lehnert et al. 2014). Further studies will be necessary to reveal the function and localization of NPCs

during symbiosis – this is likely to provide us with new insights into the nature/properties of the symbiosome and understand the importance of lipid metabolism. Interestingly, caveolin, another candidate that we find to be up-regulated in symbiotic larvae, is responsible for high specificity-binding between cholesterol and lipid-layered compartments (reviewed in Liu et al. 2002). It is possible that interplays between caveolin and NPC proteins promote lipid metabolism, which would highlight the contribution of symbionts to host nutrition. Another interesting candidate to consider for further studies is the aromatic amino acid transporter Monocarboxylate transporter 10, also up-regulated in symbiotic *Aiptasia* larvae. This could constitute an important transporter present in the symbiosome that mediates the exchange of aminoacids between symbiont and host. In line with this, we know that glucose is one of the compounds transferred from the symbiont to the host and, that the glucose transporter GLUT8 is highly expressed in symbiotic *Aiptasia* anemones (Lehnert et al. 2014, Burriesci et al. 2012).

It may also be interesting to specifically compare gene expression of symbiotic cells either containing *Symbiodinium* SSB01 or SSE01. Indeed the lab is currently establishing protocols to dissociate *Aiptasia* larvae and pick individual endodermal cells for subsequent single cell transcriptomics. These and other similar approaches may finally help to reveal the mechanisms through which symbionts prevent phagolysosomal digestion by the host cell (see also below).

Endodermal organization and endodermal cell types

To date, it is not clear if specific cells are responsible for algae symbiont phagocytosis in corals or in other cnidarian hosts. While we determined symbiont up-take efficiency to be constant until 14 dpf, we observed that symbionts are preferentially found in aboral areas of the endoderm at early developmental stages (2dpf), whereas at later development stages (10dpf) symbionts are equally distributed between the aboral and oral endoderm. These findings concur with studies in larvae of the coral *Fungia scutaria* (Rodriguez-Lanetty et al. 2006b), indicating a spatially restricted uptake of homologous symbionts in the endoderm potentially by symbiosis-specific cells in cnidarians. A description of the endodermal architecture and unveiling the different cell types constituting this

tissue are fundamental to test this hypothesis. Features that may be involved in symbiont acquisition include the presence of ciliated endodermal cells (Harii et al. 2009), cellular receptors and/or digestive cells. It is conceivable that the endoderm may have distinct cells that are responsible for food particle uptake and others for symbiont phagocytosis. Alternatively, both functions are carried out by the same cells. I used lysosomal markers to monitor the distribution of presumably digestive cells in *Aiptasia* larvae and to test whether or not those cells co-localize with symbionts.

In the course of those experiments, I observed a cell type that is relatively small and appears to be packed with many lysosomal-like vesicles (Figure 7a). These vesicles do not co-localize with symbionts and the function of these vesicles-containing cells is still unclear. One possibility is that the cells with the lysosomal clusters have digestive properties, and are "waiting" for food particles, another is that these correspond to secretory cells similar to what has been observed in *Xenopus* frogs (Dubaissi & Papalopulu 2011, Quigley et al. 2011, Dubaissi et al. 2014). In these higher animals secretory cells are part of epithelia and are responsible for mucus production, which is essential for protection and maintenance of a functional epithelium (Quagliata et al. 2006). For instance, the epithelium of most vertebrates has ciliated cells, goblet cells, ionocytes and small secretory cells (SSCs), a new epithelium cell-type recently identified in *Xenopus* larva (Dubaissi & Papalopulu 2011, Quigley et al. 2011, Dubaissi et al. 2014). Specifically, SSCs have 1) large apical secretory vesicles, 2) smaller size compared to the neighboring cells, 3) apical opening towards the surface and 4) a prominent actin ring. Many of those features could also be observed in my experiments in the lysosome-packed cells of the endoderm of *Aiptasia* larva. Dubaissi and colleagues demonstrated that the mucus produced by the SSCs acts as an essential protective layer, with high content in glycoproteins and lectins that detect glycans associated with microorganisms. Mucus production is observed in corals and other cnidarians, and is possibly important in the process of symbiont and/or food capture and particle digestion (Fitt & Trench 1983b, Huvard & Holland 1986, Schwarz et al. 1999, Quigley et al. 2011), supporting the presence of secretory cells in *Aiptasia*. The complement protein C3 was identified in the mucus produced by SSCs (Dubaissi et al. 2014) and, interestingly, the *Aiptasia*

complement protein C3 has been demonstrated to localize in the mouth aperture and aboral endoderm of the larva (Hambleton 2013), a similar localization to that we reveal in this study using the proteolytic activity marker DQ-Green (Figure 5a, 2dpf, DQ-Green). Thus, it is conceivable that cnidarian larvae contain some evolutionary ancient form of secretory cells that is involved in mucus production.

One step towards a better understanding of the function of those cells would be to test whether the larval endoderm is lined with mucus or not. If mucus is present, finding out its exact composition could provide information on whether and how an interaction with symbionts, microorganisms and food particles may be established. However, it is still equally likely that these vesicle-containing cells are involved in processes related to nutrient digestion and/or other functions of the endoderm. Not much is known about feeding capabilities of cnidarian larvae. However, secretory lysosomes have been observed in the worm *Caenorhabditis elegans* and the amoeba *Dictyostelium discoideum* (Ebert et al. 1990, Nonet et al. 1997). Secretory lysosomes have both the acidity and proteolytic properties of classical lysosomes and are marked with lysosomal markers such as Cathepsins (lysosomal hydrolases) and Lamp (lysosomal-associated membrane protein) proteins, but are coupled with the ability of secreting their content rich in glycosylated proteins (its low pH can rapidly dissipate when secreted towards a cavity). Preliminary studies in *Nematostella* suggest that larva take up dissolved organic matter (DOM) into their endodermal cells (Jeackle & Smith 2013), but it is not entirely clear whether particle uptake occurs and whether particle digestion serves a nutritional purpose. Interestingly, we recently found that single-celled algae from the genus *Nannochloropsis* are intracellularized into the endodermal cells of *Aiptasia* larvae, which appear to be degraded over time (our unpublished results). In the future, it will be interesting to determine whether cnidarian larvae are capable of phagocytosing food particles for nutrition and to uncover the mechanisms of intracellular food digestion in comparison to symbiont maintenance within endodermal host cells. Moreover, further cell types may be discovered within the endoderm of *Aiptasia* using e.g. single cell transcriptomics of dissociated endodermal cells (see above), which may also allow to better understand cell type evolution and endodermal differentiation.

Characterization of the symbiosome

Besides the uptake of symbionts into the host, survival of the symbiont inside the host cell is essential for the mutually beneficial partnership between both organisms. To date it is not yet understood how algae avoid digestion by lysosomes once it is inside the host cell, however two contradictory views dominate the field.

The prevailing belief in the field is that the symbionts arrest the default phagosome maturation into a digestive phagolysosome (typical for food particle digestion or microbial elimination) thereby avoiding destruction by the host. In support of this, earlier studies in cnidarians, including *Hydra-Chlorella*, *C. xamachana-Symbiodinium*, indicate that these endosymbionts avoid intracellular digestion by preventing the maturation process of the phagosome into a phagolysosome, which was not the case for phagosomes containing heat-killed algae (Fitt & Trench 1983b, Hohman et al. 1982, O'Brien 1982). Chen et al. provided further insight showing that the Rab GTPase Rab5 (a marker for non-mature phagosomes) is present while Rab7 (a marker for mature phagosomes) is absent in phagosomes containing living algae (symbiosomes). Again, the opposite is true for phagosomes containing heat-killed algae or inert beads (Chen et al. 2003, Chen et al. 2005).

However, other studies showed that the lysosomal proteins Niemann-Pick type C protein 2 (NPC2) and vATPase are associated with symbiosomes in symbiotic adult tissue from anemones and corals (Dani et al. 2014, Barott et al. 2015). In addition to this, an early study observed levels of ATPase activity associated with symbiosomes in the symbiotic anemone *Anemonia viridis* (Rands et al. 1993). Furthermore, Barott et al. have recently demonstrated that symbiotic algae in two coral species are in a symbiosome with a pH ~ 4 (Barott et al. 2015). They also postulated that the low pH of the symbiosome (lower than a classical lysosome) is not only driven by the host vATPases but also by P-type-ATPases from *Symbiodinium* (Barott et al. 2015). P-type-ATPases have been before identified and shown to express in symbiotic but not in free-living *Symbiodinium*

(Roa et al. 2014, Bertucci et al. 2010) to possibly promote photosynthesis of the algal symbiont (Venn et al. 2009, Venn et al. 2011, Barott et al. 2015).

One can look at this interaction as host- or symbiont-centered, assuming that either the host stimulates the symbiont to produce photosynthates for the host or that the symbiont releases compounds that influence the host in a way that is advantageous for the symbiont. The material translocation rate may be an important factor to mask the symbionts (intracellular phagosome mimicry) and control the residence time of live symbionts in the host cell – a strategy possibly found in other algal-invertebrate symbiosis (Hill & Hill 2012, Hill 2014). This phenomenon is known as the arrested phagosome hypothesis (APH), with the endpoint of *Symbiodinium* residing in a symbiosome that appears to have the characteristics of a digestive compartment and the symbiont constantly releasing compounds, meeting the host metabolic needs (Hill & Hill 2012, Hill 2014). Indeed, symbionts release more photosynthates *in hospite* than in culture and are strongly favored under natural selection with *Symbiodinium* residing for the longest time *in hospite* (Colley & Trench 1983). It is estimated that the residence time for *Symbiodinium* is around 70 days, after which it is either digested or released/expelled by exocytosis (Hill & Hill 2012).

A detailed characterization of the symbiosome composition and its physiology in comparison to ordinary lysosomes will help to reveal its nature and thus potential mechanisms that explain how symbionts avoid phagolysosomal digestion. Therefore, I aimed to use the lysosomal dyes to detect acidity and proteolytic activity in the symbiosomes of *Aiptasia* larva. However, with the conditions tested I did not detect signals for these dyes around symbiotic algae. One explanation may be that the perisymbiont space (space between alga cell and symbiosome membrane) is only faintly stained (i.e., few dye molecules) making it difficult to distinguish between the algae autofluorescence and the symbiosome membrane. To address this, I also tested for the presence of classical lysosomal proteins in the symbiosome but again no “halo” was observed around algae in symbiotic larvae. Therefore, I tested the presence of lysosomal proteins in symbiotic tissue macerates from adult *Aiptasia*. In this case, I was able to detect signal of the three lysosomal markers tested (Rab7, vATPase and Cathepsin S)

around the algae. These observations indicate that the expression level of these proteins in the symbiosome could be higher in the adults than in the larva and therefore, more easily detected via microscopy. To rule out that the difference observed between larvae and adults is not developmental, the staining of symbiotic cells from larval macerates could be helpful and this technique is being developed in the lab. Confocal microscopy of physical symbiotic tissue sectioning might be as well a viable approach to detect an array of molecular markers in order to understand if manipulation of the phagolysosome occurs to allow algae maintenance or if algae are resilient to the degradative properties of this compartment (Davy et al. 2012, Tang 2015). Moreover, an important addition to this is to consider positive controls to distinguish food/microbes-containing phagosomes (classical phagocytic pathway) from algae-containing phagosomes. Such controls can be inert latex beads, incompatible *Symbiodinium* types (e.g., *Symbiodinium* SSE01) or food particles.

Taken together, while literature is ambiguous regarding the exact mechanism allowing algae to live as symbionts after phagocytic uptake, it indicates that the arrested phagosome hypothesis and vATPase-dependent acidification might play a relevant role (Figure 13). Further developing the staining and imaging approaches I have established to characterize the nature and composition of the symbiosome in *Aiptasia* will be important to better understand how symbionts avoid digestion by the host to form this long-lasting, intimate partnership between two cells from distinct organisms.

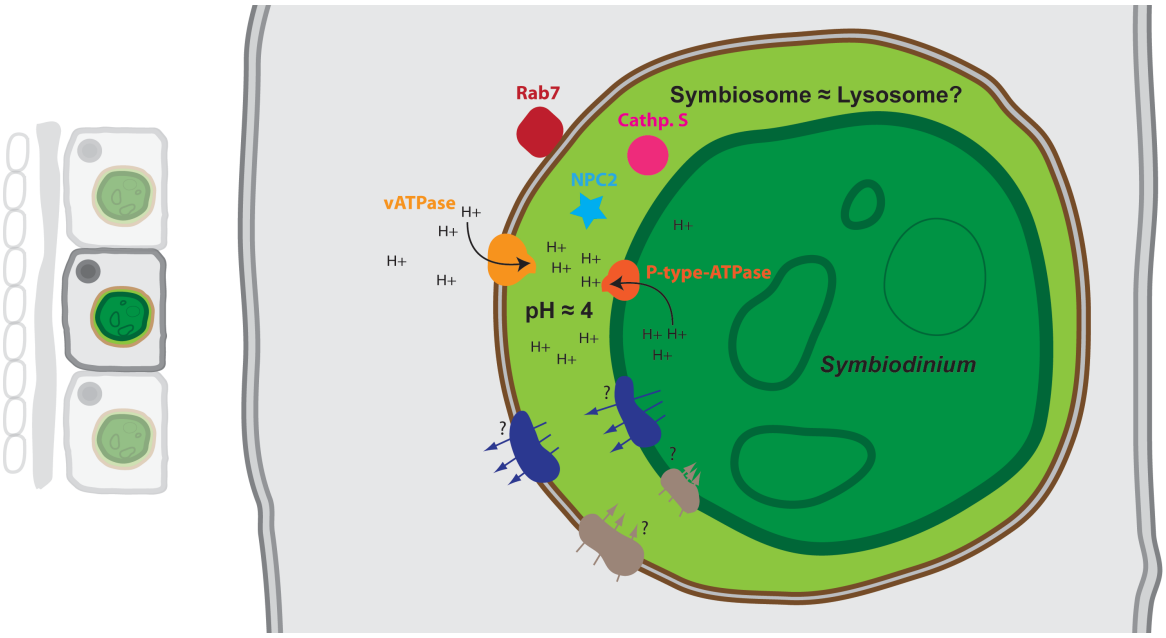

Figure 13 Proposed model of the symbiosome in cnidarian-*Symbiodinium* symbiosis. Symbionts reside inside the symbiosome, a lysosomal-like organelle, which appears to be acidic and may even have proteolytic activity. To date it is unclear how symbionts would thrive under these harsh conditions.

Aiptasia in the area of new models to dissect underexplored cell biological questions

Many well-established model organisms such as worms, flies, mice have an enormous array of experimental tools available, however many fundamental questions cannot be answered with these “traditional” model organisms (Goldstein & King 2016). The endosymbiosis between cnidarians and *Symbiodinium* is a key example (Weis et al. 2008, Goldstein & King 2016). The accessibility and cost-effectiveness of many state-of-art technologies such as high-throughput sequencing, has recently opened attractive possibilities to the use of “non-traditional” model organisms to answer specific biological questions (Goldstein & King 2016, Cook et al. 2016). The main characteristics of model organisms are a short life cycle, the ability to grow in the laboratory, high fecundity, available genetic tools, and the possibility of the use of advanced microscopy (Goldstein & King 2016).

Aiptasia is a prominent example of such a “non-traditional” model: in less than 8 years and since the first *Aiptasia* transcriptome was published (Sunagawa

et al. 2009), a relatively small community developed a powerful experimental toolbox and various biological assays anew, several of which I participated in during my thesis. By now multiple transcriptomes and sequenced genomes are available for the host and the symbionts (Baumgarten et al. 2015, Shoguchi et al. 2013, Lin et al. 2015); *Aiptasia* larvae can be generated on demand (Grawunder et al. 2015); we know exactly when and where symbionts are acquired (Bucher et al. 2016); symbiosis-specific candidate genes have been identified and the molecular and microcopy tools have been developed (Wolfowicz et al. 2016). Together, these advancements open up exciting opportunities to start dissecting the intracellular symbiosis at the molecular level.

However, some bottlenecks to reach *Aiptasia´*s full potential still remain. For example, we continue to lack the establishment of tools for functional approaches (e.g. knock-out of endogenous genes, introduction of transgenes or targeted approaches such as CRISPR/Cas9 technology). The lab has established a robust microinjection protocol that allows the efficient introduction of various molecules and dyes and microinjected mRNA is successfully translated in *Aiptasia* embryos and larvae. Thus, I believe it is just a matter of time until successful genome engineering will be achieved. A second hurdle is that the life cycle of *Aiptasia* cannot yet be closed under laboratory conditions, which impairs the generation and maintenance of stable transgenic lines by microinjection. In the future, a live imaging set-up would as well be of great aid to observe dynamic cellular events leading to establishment of symbiosis. However, due to the active swimming ability of larvae, further challenging work will be required.

Nevertheless, patience and persistence by many researchers were necessary to overcome similar difficulties with model systems that are nowadays well-established and I expect that the same will be true for *Aiptasia*.

Conclusion

During my PhD, I was decidedly involved in developing essential resources for *Aiptasia* as a powerful model system to uncover fundamental aspects of coral symbiosis. Specifically, I contributed to the development of a spawning induction protocol (Grawunder et al. 2015), the description of symbiosis establishment

during larval development (Bucher et al. 2016) and the comparison of symbiosis specificity patterns between *Aiptasia* and corals (Wolfowicz et al. 2016). Finally, I explored one of the major unresolved questions in the field: how do symbionts avoid phagolysosomal digestion by the host cell? Answering this question will provide important insight into a fundamental aspect of this ecologically and economically important symbiosis. Moreover, this information may also be integrated into what is known about related processes such as food phagocytosis and intracellular pathogenesis and thus allow to better understand the evolution of phagocytosis and innate immunity. More broadly, dissecting symbiosis establishment using *Aiptasia* as a model is an important step towards understanding how two cells from distinct organisms can form such an intimate partnership to drive the productivity of a whole ecosystem.

Bibliography

Abrego, D., van Oppen, M. J. H. & Willis, B. L. (2009). Highly infectious symbiont dominates initial uptake in coral juveniles. *Molecular Ecology*, **18**:3518-3531.

Adams, L. M., Cumbo, V. R. & Takabayashi, M. (2009). Exposure to sediment enhances primary acquisition of *Symbiodinium* by asymbiotic coral larvae. *Marine Ecology Progress Series*, **377**:149-156.

Babcock, R.C., Bull, G.D., Harrison, P.L., Heyward, A.J., Oliver, J.K., Wallace, B.L., Willis, B.L. (1986). Synchronous spawnings of 105 scleractinian coral species on the Great Barrier Reef. *Mar. Biol.*, **90**:379–94.

Baird, A. H., Guest, J. R. & Willis, B. L. (2009). Systematic and biogeographical patterns in the reproductive biology of scleractinian corals. *Annual Review of Ecology, Evolution, and Systematics*, **40**:551-571.

Baird, A.H., Gilmour, J., Kamiki, T,M., Nonaka, M., Pratchett, M.S., Yamamoyo, H.H., Yamasaki, H. (2006). Temperature tolerance of symbiotic and non-symbiotic coral larvae. *Proceedings of 10th International Coral Reef Symposium*, **1:**38-42.

Baker, A.C. (2003). Flexibility and specificity in coral-algal symbiosis: diversity, ecology and biogeography of *Symbiodinium*. *Annu. Rev. Ecol. Evol. Syst.*, **34**:661–689.

Barott, K.L., Venn, A.A., Perez, S.O., Tambutté, S., Tresguerres, M. (2015). Coral host cells acidify symbiotic algal microenvironment to promote photosynthesis. *Proc. Nat. Acad. Sciences* **112**(2): 607-612.

Baumgarten, S., Simakov, O., Esherick, L. Y., Liew, Y. J., Lehnert, E. M., Michell, C. T., Li, Y., Hambleton, E. A., Guse, A., Oates, M. E., Gough, J., Weis, V.

M., Aranda, M., Pringle, J. R., & Voolstra, C. R. (2015). The genome of *Aiptasia*, a sea anemone model for coral symbiosis. *Proc. Natl. Acad. Sci.*, **112**: 11893–11898.

Bay, L. K., Cumbo, V. R., Abrego, D., Kool, J. T., Ainsworth, T. D. & Willis, B. L. (2011). Infection dynamics vary between *Symbiodinium* types and cell surface treatments during establishment of endosymbiosis with coral larvae. *Diversity*, **3:**356-374.

Bayer, T., Aranda, M., Sunagawa, S., Yum, L.K., DeSalvo, M.K., Lindquist, E., Coffroth, M.A., Voolstra, C.R., Medina, M. (2012). Symbiodinium transcriptomes: Genome insights into the dinoflagellate symbionts of reef-building corals. *PLoS ONE*, **7**(4): e35269.

Bertucci, A., Tambutté, E., Tambutté, S., Allemand, D., Zoccola, D. (2010). Symbiosis-dependent gene expression in coral-dinoflagellate association: cloning and characterization of a P-type H+-ATPase gene. *Proc. Biol. Sci.*, **277**(1678): 87-95.

Birkeland, C. (1997). Life and Death of Coral reefs. Chapman and Hall, New York: 536.

Bosch, T.C.G., Adamska, M., Augustin, R., Domazet-Loso, T., Foret, S., Fraune, S., Noriko, F., Grasis, J., Hamada, M., Hatta, M., Hobmayer, B., Kawai, K., Klimovich, A., Manuel, M., Shinzato, C., Technau, U., Yum, S., Miller, D.J. (2014). How do environmental factors influence life cycle and development? An experimental framework for early-diverging metazoans. *Bioessays*, **36**(12): 1185-1194.

Brodersen, K.E., Lichtenberg, M., Ralph, P.J., Kuhl, M., Wang-Praseurt, D. (2014). Radiative energy budget reveals high photosynthetic efficiency in symbiont-bearing corals. *Journal of the Royal Society Interface*, **11**: 20130997.

Brown, T., & Rodriguez-Lanetty, M. (2015). Defending against pathogens – immunological priming and its molecular basis in a sea anemone, cnidarian. *Sci. Re.*, **5**: 17425

Bucher, M., Wolfowicz, I., Voss, P. A., Hambleton, E. A., Guse, A. (2016). Development and symbiosis establishment in the cnidarian endosymbiosis model *Aiptasia* sp. *Sci. Rep.*, **6**: 19867.

Burriesci, M.S., Raab, T.K., Pringle, J.R. (2012). Evidence that glucose is the major transferred metabolite in dinoflagellate-cnidarian symbiosis. *Journal of Experimental Biology*, **215**: 3467-3477.

Cairns, S.D. (1999). Species richness of recent Scleractinia. *Atoll Research Bulletin*, **459**(46).

Cesar, H., Burke, L., and Pet-soede, L. (2003). The Economics of Worldwide Coral Reef Degradation. *Cesar Environ. Econ. Consult. Arnhem, WWF-Netherlands*, **14**: 23.

Chen, M. C., Cheng, Y. M. P., Sung, J., Kuo, C. E., Fang, L. S. (2003) Molecular identification of Rab7 (ApRab7) in *Aiptasia* pulchella and its exclusion from phagosomes harboring zooxanthellae. *Biochem. Biophys. Res. Commun.* **308**(3): 586–595.

Chen, M. C., Cheng, Y. M., Hong, M. C., Fang, L. S. (2004). Molecular cloning of Rab5 (ApRab5) in *Aiptasia* pulchella and its retention in phagosomes harboring live zooxanthellae. *Biochem. Biophys. Res. Commun.*, **324**(3): 1024–1033.

Chen, M.C., Hong, M.C., Huang, Y.S., Liu, M.C., Cheng, Y.M., Fang, L.S. (2005). ApRab11, a cnidarian homologue of the recycling regulatory protein Rab11, is involved in the establishment and maintenance of the *Aiptasia-Symbiodinium* endosymbiosis. *Biochem. Biophys. Res. Commun*., **338**(3):1607-1616.

Coffroth, M. A., Poland, D. M., Petrou, E. L., Brazeau, D. A. & Holmberg, J. C. (2010). Environmental symbiont acquisition may not be the solution to warming seas for reef-building corals. *PLoS ONE*, **5**: e13258.

Coffroth, M.A. & Santos, S.R. (2005). Genetic diversity of symbiotic dinoflagellates in the genus *Symbiodinium*. *Protist*, **156**: 19-34.

Coffroth, M.A., Lewis, C.F., Santos, S.R., Weaver, J.L. (2006). Environmental populations of symbiotic dinoflagellates in the genus *Symbiodinium* can initiate symbiosis with reef cnidarians. *Current Biology*, **16**(23): R985-R987.

Colley, N. J., & R. K. Trench. (1983). Selectivity in phagocytosis and persistence of symbiotic algae by the scyphistoma stage of the jellyfish *Cassiopeia xamachana*. *Proc. R. Soc. Lond*. B, **219**: 61–82.

Conservation International (2008). Economic Values of Coral Reefs, Mangroves, and Seagrasses: A Global Compilation. Center for Applied Biodiversity Science, Conservation International, Arlington, VA.

Cook, C.B., Muller-Parker, G., Orlandini, C.D. (1994). Ammonium enhancement of dark carbon fixation and nitrogen limitation in zooxanthellae symbiotic with the reef corals *Madracis mirabilis* and *Montastrea annularis*. *Mar. Biol.*, **118**(1):157–165.

Cook, C.E., Chenevert, J., Larsson, T.A., Arendt, D., Houliston, E., Lénárt, P. (2016). Old knowledge and new technologies allow rapid development of model organisms. *Mol. Biol. Cell.*, **27**(6):882-887.

Cumbo, V.R., Baird, A.H. & van Oppen, M.J.H. (2013). The promiscuous larva: flexibility in the establishment of symbiosis in corals. *Coral Reefs*, **32**: 111-120.

Dani, V., Ganot, P., Priouzeau, F., Furla, P., Sabourault, C. (2014). Are Niemann-Pick type C proteins key players in cnidarian-dinoflagellate endosymbiosis?. *Molecular Ecology*, **23**(18): 4527-4540.

Davy, S. K., Allemand, D. & Weis, V. M. (2012). Cell biology of cnidarian-dinoflagellate symbiosis. *Microbiol. Mol. Biol. Rev.*, **76**(2): 229- 261.

De'ath, G., Fabricius, K. E., Sweatman, H. & Puotinen, M. (2012). The 27-year decline of coral cover on the Great Barrier Reef and its causes. *Proceedings of the National Academy of Sciences*, **109**: 17995-17999.

deBoer, M.L., Krupp, D.A., Weis, V.M. (2007). Proteomic and transcriptional analysis of coral larvae newly engaged in symbiosis with dinoflagellates. *Comp. Biochem. Physiol. Part D*., **2**(1): 63-73.

Dodson, M. W., Zhang, T., Jiang, C., Chen, S., Guo, M. (2012). Roles of the Drosophila LRRK2 homolog in Rab7-dependent lysosomal positioning. *Hum. Mol. Genet.*, **21**(6): 1350–1363.

Douglas, A.E., Smith, D.C. (1984). The green *Hydra* symbiosis. VIII. Mechanisms in symbiont regulation. *Proc. R. Soc. Lond. B*., **221**:291–319.

Dubaissi, E., Papalopulu, N. (2011). Embryonic frog epidermis: a model for the study of cell-cell interactions in the development of mucociliary disease. *Disease Models and Mechanisms* **4**: 179-192.

Dubaissi, E., Rousseau, K., Lea, R., Soto, X., Nardeosingh, S., Schweickert, A., Amaya, E., Thornton, D.J., Papalopulu, N. (2014). A secretory cell type develops alongside multiciliated cells, ionocytes and goblet cells, and provides a protective, anti-infective function in the frog embryonic mucociliary epidermis. *Development* **141**: 1514-1525.

Dunn, S.R., Weis, V.M. (2009). Apoptosis as a post-phagocytic winnowing mechanism in a coral-dinoflagellate mutualism. *Environ. Microbiol*., **11**(1):268-276.

Ebert, D. L., Jordan, K. B. & Dimond, R. L. (1990). Lysosomal enzyme secretory mutants of *Dictyostelium discoideum*. *J. Cell Sci.,* **96**: 491–500.

Elizabeth Hambleton (2013). Symbiosis specificity and innate immunity in *Aiptasia*, a model system for cnidarian-dinoflagellate symbiosis. PhD Dissertation, Department of Biology, Stanford University.

Fadlallah, Y.H. (1983) Sexual reproduction, development and larval biology in scleractinian corals: *A review. Coral Reefs*. **2**: 129-150.

Fairn, G. D. & Grinstein, S. (2012). How nascent phagosomes mature to become phagolysosomes. *Trends Immunol.*, **33**(8):397–405.

Falkowski, P.G., Dubinsky, Z., Muscatine, L. & Porter, J.W. (1984). Light and the bioenergetics of a symbiotic coral. *BioScience*, **34**: 705-709.

Fay, S. A. & Weber, M. X. (2012). The occurrence of mixed infections of *Symbiodinium* (Dinoflagellata) within individual hosts. *Journal of Phycology*. **48**: 1306-1316.

Fitt, W., Trench R. (1983b). Endocytosis of the symbiotic dinoflagellate *Symbiodinium microadriaticum* Freudenthal by endodermal cells of the scyphistomae of *Cassiopeia xamachana* and resistance of the algae to host digestion. *J. Cell Sci.* **65**:195-212.

Fitt, W.K., Trench, R.K. (1983a). The relation of diel patterns of cell division to diel patterns of motility in the symbiotic dinoflagellate *Symbiodinium microadriaticum* (Freudenthal) in culture. *New Phytol*. **94**:421–432.

Flannagan, R. S., Cosío, G., Grinstein, S. (2009). Antimicrobial mechanisms of phagocyes and bacterial evasion strategies. *Nature Reviews Microbiology*, **7**: 355-366.

Flannagan, R. S., Jaumouill, V., Grinstein, S. (2012). The Cell Biology of Phagocytosis. *Annu. Rev. Pathol. Mech. Dis*, **7**: 61-98.

Goldstein, B. & King, N. (2016). The Future of Cell Biology: Emerging Model Organisms. *Spec. Issue Futur. Cell Biol.*, **26**(11): 818-824.

Grawunder, D., Hambleton, E. A., Bucher, M., Wolfowicz, I., Bechtoldt, N., Guse, A. (2015). Induction of gametogenesis in the cnidarian endosymbiosis model *Aiptasia* sp. *Sci. Rep.*, **5**: 15677.

Hagedorn, M., Carter, V., Zuchowicz, N., Phillips, M., Penfield, C., Shamenek, B., Vallen, E. a., Kleinhans, F. W., Peterson, K., White, M., Yancey, P. H. (2015). Trehalose Is a Chemical Attractant in the Establishment of Coral Symbiosis. *PLoS One*, **10**(1): e0117087.

Hambleton, E. A., Guse, A., Pringle, J. R. (2014). Similar specificities of symbiont uptake by adults and larvae in an anemone model system for coral biology. *J. Exp. Biol.*, **217**(9): 1613–1619.

Harii, S., Yasuda, N., Rodriguez-Lanetty, M., Irie, T. & Hidaka, M. (2009). Onset of symbiosis and distribution patterns of symbiotic dinoflagellates in the larvae of scleractinian corals. *Marine Biology*, **156:** 1203-1212.

Harrison, P.L. (2011) Sexual reproduction of scleractinian corals. In: Dubinsky, Z., Stambler, N. (eds) Coral reefs: an ecosystem in transition. *Springer Science*, Berlin, 59−85.

Harrison, P.L., Wallace, C.C. (1990). Reproduction, dispersal and recruitment of scleractinian corals. *In Coral Reefs*, ed. Z Dubinsky, 133–207. Amsterdam: Elsevier.

Hayashibara, T., Ohike, S., Kakinuma, Y. (1997). Embryonic and larval development and planula metamorphosis of four gamete-spawning *Acropora* (Anthozoa, Scleractinia). *Proc. 8th Int. Coral Reef Sym*. **2:** 1231–1236.

Hill, M.S. (2014). Production possibility frontiers in phototroph:heterotroph symbiosis: trade-offs in allocating fixed carbon pools and the challenges these alternatives present for understanding the acquisition of intracellular habitat. *Frontiers in Microbiology*, **5**: 357.

Hill, M.S., Hill, A. (2012). The magnesium inhibition and arrested phagosome hypotheses: new perspectives on the evolution and ecology of *Symbiodinium* symbiosis. *Biol. Rev*., **87**: 804-821.

Hoegh-Guldberg, O. (1999). Climate change, coral bleaching and the future of the world's coral reefs. *Mar. Fresh. Res.*, **50**:839–866.

Hoegh-Guldberg, O., Mumby, P. J., Hooten, A. J., Steneck, R. S., Greenfield, P., Gomez, E., Harvell, C. D., Sale, P. F., Edwards, A. J., Caldeira, K., Knowlton, N., Eakin, C. M., Iglesias-Prieto, R., Muthiga, N., Bradbury, R. H., Dubi, A. & Hatziolos, M. E. (2007). Coral reefs under rapid climate change and ocean acidification. *Science*, **318**: 1737-1742.

Hohman, T.C., McNeil, P.L., Muscatine, L. (1982). Phagosome-lysosome fusion inhibited by algal symbionts of *Hydra viridis*. *J. Cell Biol*., **94**(1):56–63.

Holbrook, S.J., Schmitt, R.J., Messmer, V., Brooks, A.J., Srinivasan, M., Munday, P.L., Jones, G.P. (2015). Reef Fishes in Biodiversity Hotspots Are at Greatest Risk from Loss of Coral Species. *Plos One*, **10**(5): e0124054.

Hughes, T. P., Baird, A. H., Bellwood, D. R., Card, M., Connolly, S. R., Folke, C., Grosberg, R., Hoegh-Guldberg, O., Jackson, J. B. C., Kleypas, J., Lough, J. M., Marshall, P., Nyström, M., Palumbi, S. R., Pandolfi, J. M., Rosen, B. & Roughgardem, J. (2003). Climate change, human impacts, and the resilience of coral reefs. *Science*, **301**: 929-933.

Huvard, L., Holland, N. (1986). Pinocytosis of ferritin from the gut lumen in larvae of a seastar (*Patiria miniata*) and a sea urchin (*Lytechinus pictus*). *Dev. Growth Differ.*, **28**(1): 43–57.

Ishikura, M., Hagiwara, K., Takishita, K., Haga, M., Iwai, K., Maruyama, T. (2004). Isolation of new *Symbiodinium* strains from Tridacnid giant clam (*Tridacna crocea*) and sea slug (*Pteraeolidia ianthina*) using culture medium containing giant clam tissue homogenate. *Mar. Biotechnol.*, **6**: 378-385.

Jackson, A.E., Yellowlees, D. (1990). Phosphate uptake by zooxanthellae isolated from corals. *Proc. R. Soc. Lond. B*, **242**(1305):201–204.

Jaeckle, W., Smith, K.A. (2013). Feeding modes of larvae of Nematostella vectensis (Cnidarian:Anthozoa). *Student's Professional Presentations and Publications*, Paper 2.

Jeong, H.J., Lee. S.Y., Kang, N.S., Yoo, Y.D., Lim, A.S., Lee, M.J., Kim, H.S., Yih, W., Yamashita, H., LaJeunesse, T.C. (2014). Genetics and morphology characterize the dinoflagellate *Symbiodinium voratum*, n. sp., (Dinophyceae) as the sole representative of *Symbiodinium* Clade E. *J. Eukaryot. Microbiol.*, **61**(1):75-94.

Jones, A. M., Berkelman, R., van Oppen, M. J. H., Mieog, J. C., Sinclair, W. (2008). A community change in the algal endosymbionts of a scleractinian coral following a natural bleaching event: field evidence of acclimatization. *Proceedings of the Royal Society B*, **275**: 1359-1365.

Kamezaki, M., Higa, M., Hirose, M., Suda, S., Reimer, J.D. (2013). Different zooxanthellae types in populations of the zoanthid *Zoanthus sansibaricus* along depth gradients in Okinawa, Japan. *Marine Biodiversity*, **43**(1): 61-70.

Karakashian, M.W., Karakashian, S.J. (1973). Intracellular digestion and symbiosis in *Paramecium bursaria*. *Exp. Cell Res.*, **81**(1):111–119.

Karakashian, S.J., Rudzinska, M.A. (1981). Inhibition of lysosomal fusion with symbiont-containing vacuoles in *Paramecium bursaria*. *Exp. Cell Res*., **131**(2):387–393.

Kasper, L., Seider, K., Gerwien, F., Allert, S., Brunke, S., Schwarzmüller, T., Ames, L., Zubiria-Barrera, C., Mansour, M.K., Becken, U., Barz, D., Vyas, J.M, Reiling, N., Haas, A., Haynes, K., Kuchler, K., Hube, B. (2014). Identification of Candida glabrata Genes Involved in pH Modulation and Modification of the Phagosomal Environment in Macrophages. *Plos One* **9**(5): e96015.

Kayal, E., Roure, B., Philippe, H., Collins, A.G., Lavrov, D.V. (2013). Cnidarian phylogenetic relationships as revealed by mitogenomics. *BMC Evolutionary Biology*, **13**(5).

Kazandjian A, Shepherd, V.A., Rodriguez-Lanetty, M., Nordemeier, W., Larkum, A.W. & Quinnell, R.G. (2008). Isolation of symbiosomes and the symbiosome membrane complex from the zoanthid *Zoanthus robustus*. *Phycologia*, **47**(3):294–306.

Kinzie, R. A. III & Chee, G. S. (1979). The effect of different zooxanthellae on the growth of experimentally reinfected hosts. *Biological Bulletin*, **156**(3): 315-327.

Korolchuk, V., Saiki, S., Lichtenberg, M., Siddiqi, F., Roberts, E., Imarisio, S., Jahreiss, L., Sarkar, S., Futter, M., Mensies, F., O'Kane, C., Deretic, V., Rubinsztein, D. (2011). Lysosomal positioning coordinates cellular nutrient responses. *Nat. Cell Biol*., **13**: 453-460.

Kuniya, N., Jimbo, M., Tanimoto, F., Yamashita, H., Koike, K., Harii, S., Nakano, Y., Iwao, K., Yasumoto, K., & Watabe, S. (2015). Possible involvement of Tachylectin-2-like lectin from *Acropora tenuis* in the process of *Symbiodinium* acquisition. *Fish. Sci.*, 473–483.

LaJeunesse, T. C. (2001). Investigating the biodiversity, ecology, and phylogeny of endosymbiotic dinoflagellates in the genus *Symbiodinium* using the ITS region: in search of a "species" level marker. *Journal of Phycology*, **37**: 866-880.

LaJeunesse, T. C., Thornhill, D. J., Cox, E. F., Stanton, F. G., Fitt, W. K., & Schmidt, G. W. (2004). High diversity and host specificity observed among symbiotic dinoflagellates in reef coral communities from Hawaii. *Coral Reefs*, **23**(4): 596–603.

Lehnert, E. M., Burriesci, M. S., Pringle, J. R. (2012). Developing the anemone *Aiptasia* as a tractable model for cnidarian-dinoflagellate symbiosis: the transcriptome of aposymbiotic *A.* pallida. *BMC Genomics*, **13**: 271.

Lehnert, E. M., Mouchka, M. E., Burriesci, M. S., Gallo, N. D., Schwarz, J. A. & Pringle. J. R. (2014). Extensive differences in gene expression between symbiotic and aposymbiotic cnidarians. *G3 (Bethesda).*, **4**(2): 277–95.

Lewis, C. L. & Coffroth, M. A. (2004). The acquisition of exogenous algal symbionts by an octocoral after bleaching. *Science* **304:** 1490-1492.

Lin, S., Cheng, S., Song, B., Zhong, X., Lin, X., Li, W., Li, L., Zhang, Y., Zhang, H., Ji, Z., Cai, M., Zhuang, Y., Shi, X., Lin, L., Wang, L., Wang, Z., Liu, X., Yu, S., Zeng, P., Hao, H., Zou, Q., Chen, C., Li, Y., Wang, Y., Xu, C., Meng, S., Xu, S., Wang, J., Yhang, H., Campbell, D.A., Sturm, N.R., Dagenais-Bellefeuille, S., Moise, D. (2015). The *Symbiodinium kawagutii* genome illuminates dinoflagellate gene expression and coral symbiosis. *Science*, **350**: 691-694.

Little, A. F., van Oppen, M. J. H. & Willis, B. L. (2004). Flexibility in algal endosymbiosis shapes growth in reef corals. *Science*, **304**: 1492-1494.

Liu, P., Rudick, M., Anderson, R.G.W. (2002). Multiple functions of Caveolin-1. *The Journal of Biological Chemistry*, **277**: 41295-41298.

Manning, M.M., Gates, R.D. (2008). Diversity in populations of free-living *Symbiodinium* from Caribbean and Pacific reef. *Limnol. Oceanogr.*, **53**(5): 1853-1861.

Marlow, H.Q., Martindale, M.Q. (2007). Embryonic development in two species of scleractinian coral embryos: *Symbiodinium* localization and mode of gastrulation. *Evol. And Development*, **9**(4): 355-367.

Matthews, J. L., Sproles, A. E., Oakley, C. A., Grossman, A. R., Weis, V. M., Davy, S. K. (2016). Menthol-induced bleaching rapidly and effectively provides experimental aposymbiotic sea anemones (*Aiptasia* sp.) for symbiosis investigations. *J. Exp. Biol.*, **219**(3): 306–310.

McAuley, P.J. (1985a). Regulation of numbers of symbiotic *Chlorella* in digestive cells of green *Hydra*. *Endocytobiosis Cell Res*., **2**:179–190.

McAuley, P.J. (1985b). The cell cycle of symbiotic *Chlorella*. I. The relationship between host feeding and algal cell growth and division. *J. Cell Sci*., **77**:225–239.

McCook, L. J., Ayling, T., Cappo, M., Choat, J. H., Evans, R. D., De Freitas, D. M., Heupel, M., Hughes, T. P., Jones, G. P., Mapstone, B., Marsh, H., Mills, M., Molloy, F. J., Pitcher, C. R., Pressey, R. L., Russ, G. R., Sutton, S., Sweatman, H., Tobin, R., Wachenfeld, D. R. & Williamson, D. H. (2010). Adaptive management of the Great Barrier Reef: a globally significant demonstration of the benefits of networks of marine reserves. *Proc. Natl. Acad. Sci. U. S. A.*, **107**(43): 18278–85.

McNeil, P.L. (1981). Mechanisms of nutritive endocytosis. I. Phagocytic versatility and cellular recognition in *Chlorohydra* digestive cells, a scanning electron microscope study. *J. Cell Sci.*, **49**:311–339.

Morberg, F., Falke, C. (1999). Ecological goods and services of coral reefs ecosystems. *Ecol. Econom.*, **29**: 215-233.

Muscatine, L. (1990). The role of symbiotic algae in carbon and energy flux in coral reefs, In *Coral Reefs*. *Elsevier* (ed. Zubinsky, Z.): 75–87.

Muscatine, L., Hand, C. (1958). Direct evidence for the transfer of materials from symbiotic algae to the tissues of a coelenterate. *Proc. Natl. Acad. Sci. U. S. A*., **44**(12):1259–1263.

Nitschke, M.R., Davy, S.K., Ward, S. (2016). Horizontal transmission of *Symbiodinium* cells between adult and juvenile corals is aided by benthic sediment. *Coral Reefs*, **35**(1): 335-344.

Nonet, M. L. Staunton, J.E., Kilgard, M.P., Fergestad, T., Hartwieg, E., Horvitz, H.R., Jorgensen, E.M., Meyer, B.J. (1997). *Caenorhabditis elegans* Rab-3 mutant synapses exhibit impaired function and are partially depleted of vesicles. *J. Neurosci.* **17**(21): 8061–8073.

Nyholm, S.V., McFall-Ngai, M.J. (2004). The winnowing: establishing the squid-*Vibrio* symbiosis. *Nat. Rev. Microbiol*., **2**:632–642.

O'Brien, T.L. (1982). Inhibition of vacuolar membrane fusion by intracellular symbiotic algae in *Hydra viridis* (Florida strain). *J. Exp. Zool*., **223**(3): 211–218.

Oakley, C.A., Ameismeier, M.F., Peng, L., Weis, V.M., Grossman, A.R., Davy, S.K. (2016). Symbiosis induces widespread changes in the proteome of the model cnidarian *Aiptasia*. *Cellular Microbiology*, **18**(7):1009-1023.

Pandolfi, J.M., Bradbury, R.H., Sala, E., Hughes, T.P., Bjorndal, K.A., Cooke, R. G., McArdle, D., McClenachan, L., Newman, M.J., Paredes, G., Warner, R.R., Jackson, J.B. (2003). Global Trajectories of the long-term decline of coral reef ecosystems. *Science*, **301**(5635):955-8.

Paulay, G. (1997). Diversity and distribution of reef organisms. In: Birkeland, C. (Ed.), Life and Death of Coral Reefs. Chapman and Hall, New York: 298–345.

Pochon, X. & Gates, R. D. (2010). A new *Symbiodinium* clade (Dinophyceae) from soritid foraminifera in Hawai'i. *Molecular Phylogenetics and Evolution*, **56**: 492- 497.

Pochon, X. & Pawlowski, J. (2006). Evolution of the soritids-*Symbiodinium* symbiosis. *Symbiosis*, **42**: 77-88.

Pochon, X., LaJeunesse, T.C. & Pawlowski, J. (2004). Biogeography partitioning and host specialization among foraminiferan dinoflagellate symbiont (Symbiodinium; Dinophyta). *Marine Biology*, **146**(1): 17-27.

Pochon, X., Montoya-Burgos, J. I., Stadelmann, B. & Pawlowski, J. (2006). Molecular phylogeny, evolutionary rates, and divergence timing of the symbiotic dinoflagellate genus *Symbiodinium*. *Molecular Phylogenetics and Evolution*, **38**: 20-30.

Pool, R.R. (1979). The role of algal antigenic determinants in the recognition of potential algal symbionts by cells of *Chlorohydra*. *J. Cell Sci*., **35**: 367–379.

Porto, I., Granados, C., Restrepo, J.C., Sánchez, J.A. (2008). Macroalgal-associated dinoflagellates belonging to the genus *Symbiodinium* in Caribbean reefs. *Plos One*, **3**(5):e2160.

Pu, J., Schindler, C., Jia, R., Jarnik, M., Backlund, P., Bonifacino, J. S. (2015). BORC, a Multisubunit Complex that Regulates Lysosome Positioning. *Dev. Cell*, **33**(2): 176–188.

Putnam, H. M., Stat, M., Pochon, X. & Gates, R. D. (2012). Endosymbiotic flexibility associates with environmental sensitivity in scleractinian corals. *Proceedings of the Royal Society B*, **279**: 4352-4361.

Quagliata, S., Malentacchi, C., Delfino, C., Brunasso, A.M., Delfino, G. (2006). Adaptive evolution of secretory cell lines in vertebrate skin. *Caryologia*, **59**(2): 187-206.

Quigley, K., Stubbs, L., Kinter, C. (2011). Specification of ion transport cells in the *Xenopus* larval skin. *Development*, **138**: 705-714.

Rands, M.L., Loughman, B.C., Douglas, A.E. (1993). The symbiotic interface in an alga-invertebrate symbiosis. *Proc. R. Soc. Lond. B*, **253**:161–165.

Reis, R., Sorgine, M., Coelho-Sampaio, T. (1998). A novel methodology for the investigation of intracellular proteolytic processing in intact cells. *Eur. J. Cell Biol.*, **74**: 192-197.

Richmond, R.H. (1988). Competency and dispersal potential of planula larvae of a spawning versus a brooding coral. *Proc. 6th. Int. Coral Reef Symp.*, **2**:827–831.

Roa, J. N., Munévar, C. L., Tresguerres, M. (2014). Feeding induces translocation of vacuolar proton ATPase and pendrin to the membrane of leopard shark (*Triakis semifasciata*) mitochondrion-rich gill cells. *Comp. Biochem. Physiol. Part A Mol. Integr. Physiol.*, **174**: 29–37.

Rodriguez-Lanetty, M., Phillips, W.S., Weis, V.M. (2006a). Transcriptome analysis of a cnidarian-dinoflagellate mutualism reveals complex modulation of host gene expression. *BMC Genomics*, **7**:23.

Rodriguez-Lanetty, M., Wood-Charlson, E.M., Hollingsworth, L.L., Krupp, D.A., Weis, V.M. (2006b). Temporal and spatial infection dynamics indicate recognition events in the erly hours of a dinoflagellate/coral symbiosis. *Marine Biology*, **149**: 713-719.

Rosenberg, E., Koren, O., Reshef, L., Efrony, R., Zilber-Rosenberg., I. (2007). The role of microorganisms in coral health, disease and evolution. *Nature Reviews Microbiology*, **5**: 355-362.

Rowan, R. & Powers, D. A. (1991). Molecular genetic identification of symbiotic dinoflagellates (zooxanthellae). *Marine Ecology Progress Series*, **71**:65-73.

Rumpho, M. E., Pelletreau, K. N., Moustafa, A. & Bhattacharya, D. (2011). The making of a photosynthetic animal. *J. Exp. Biol.*, **214**: 303–311.

Salao, K., Jiang, L., Li, H., Tsai, V. W.-W., Husaini, Y., Curmi, P.M.G., Brown, L.J., Brown, D.A., Breit, S.N. (2016). CLIC1 regulates dendritic cell antigen processing and presentation by modulating phagosome acidification and proteolysis. *Biol. Open* **5**: 620-630.

Santos, S. R., Taylor, D. J., Kinzie, R. A., Hidaka, M., Sakai, K. & Coffroth, M. A. (2002). Molecular phylogeny of symbiotic dinoflagellates inferred from partial chloroplast large subunit (23S)-rDNA sequences. *Molecular Phylogenetics and Evolution*, **23**: 97-111.

Schindelin, J., Arganda-Carreras, I., Frise, E., Kaynig, V., Longair, M., Pietzsch, T., Preibisch, S., Rueden, C., Saalfeld, S., Schmid, B., Tinevez, J.-Y., White, D.J., Volker, H., Eliceiri, K., Tomancak, P., Cardona, A. (2012). Fiji: an open-source platform for biological-image analysis. *Nat. Methods*, **9**(7): 676-682.

Schnitzler, C.E., Weis, V.M. (2010). Coral larvae exhibit few measurable transcriptional changes during the onset of coral-dinoflagellate endosymbiosis. *Marine Genomics*, **3**: 107-116.

Schwarz, J. A. (2008). Understanding the intracellular niche in cnidarian-*Symbiodinium* symbiosis: parasites lead the way. *Life and Environment*, **58**(2): 141-151.

Schwarz, J. A., Krupp, D. A. & Weis, V. M. (1999). Late larval development and onset of symbiosis in the scleractinian coral *Fungia scutaria. Biological Bulletin*, **196**: 70-79.

Shinzato, C., Shoguchi, E., Kawashima, T., Hamada, M., Hisata, K., Tanaka, M., Fujie, M., Fujiwara, M., Koyanagi, R., Ikuta, T., Fujiyama, A., Miller, D.J., Satoh, N. (2011). Using the *Acropora digitifera* genome to understand coral responses to environmental change. *Nature*, **476**(7360):320-323.

Shoguchi, E., Shinzato, C., Kawashima, T., Gyoja, F., Mungpakdee, S., Koyanagi, R., Takeuchi, T., Hisata, K., Tanaka, M., Fujiwara, M., Hamada, M., Seidi, A., Fujie, M., Usami, T., Goto, H., Yamasaki, S., Arakaki, N., Suzuki, Y., Sugano, S., Toyoda, A., Kuroki, Y., Fujiyama, A., Medina, M., Coffroth, M. A., Bhattacharya, D., Satoh, N. (2013). Draft assembly of the *Symbiodinium minutum* nuclear genome reveals dinoflagellate gene structure. *Curr. Biol.*, **23**(15): 1399–1408.

Silverstein, R. N., Correa, A. M. S. & Baker, A. C. (2012). Specificity is rarely absolute in coral-algal symbiosis: implications for coral response to climate change. *Proceedings of the Royal Society B*, **279**: 2609-2618.

Smith D.C. & Douglas A.E. (1987). *The Biology of Symbiosis*. Edward Arnold, London, England.

Smith, Amanda Kehr '13 and Jaeckle, William. (2013). Feeding modes of larvae of *Nematostella vectensis* (Cnidaria: Anthozoa). Students' Professional Presentations and Publications. Paper 2.

Spalding, M.D., Ravilious, C., Green, E.P. (2001) World Atlas of Coral Reefs. *University of California Press*, Berkeley.

Stat, M., Carter, D., Hoegh-Guldberg, O. (2006) The evolutionary history of *Symbiodinium* and scleractinian hosts—symbiosis, diversity, and the effect of climate change. *Perspect. Plant Ecol. Evol. Syst*. **8**: 23–43.

Stuart, L. M., and R. a B. Ezekowitz, “Phagocytosis: Elegant complexity,” *Immunity*, vol. 22, no. 5, pp. 539–550, 2005.

Sunagawa, S., Wilson, E. C., Thaler, M., Smith, M. L., Caruso, C., Pringle, J. R., Weis, V. M., Medina, M. & Schwarz, J. A. (2009). Generation and analysis of transcriptomic resources for a model system on the rise: the sea anemone *Aiptasia pallida* and its dinoflagellate endosymbiont. *BMC Genomics*, **10**: 258.

Suzuki, G., Yamashita, H., Kai, S., Hayashibara, T., Suzuki, K., Yukihiro, I., Okada, W., Ando, W., Komori, T. (2013). Early uptake of specific symbionts enhances the post-settlement survival of *Acropora* corals. *Marine Ecol. Prog. Ser.*, **494**: 149-158.

Sweatman, H., Delean, S., Syms, C. (2011). Assessing loss of coral cover on Australia’s Great Barrier Reef over two decades, with implications for longer-term trends. *Coral Reefs*, **30**(2):521-531.

Tang, B.L. (2015). Thoughts on a very acidic symbiosome. *Front. Microbiol*., **6**(816): 4-7.

Technau, U. & Steele, R.E. (2011). Evolutionary crossroads in developmental biology: Cnidarian. *Development*, **138**: 1447-1458.

Thornhill, D. J., Xiang, Y., Pettay, D. T., Zhong, M., Santos, S. R. (2013). Population genetic data of a model symbiotic cnidarian system reveal remarkable symbiotic specificity and vectored introductions across ocean basins. *Mol. Ecol.*, **22**(17): 4499–4515.

Trench, R.K. (1971a). Physiology and biochemistry of zooxanthellae symbiotic with marine coelenterates. I. Assimilation of photosynthetic products of zooxanthellae by two marine coelenterates. *Proc. R. Soc. Lond. B*, **177**(1047):225–235.

Trench, R.K. (1971b). Physiology and biochemistry of zooxanthellae symbiotic with marine coelenterates. III. Effect of homogenates of host tissues on excretion of photosynthetic products in vitro by zooxanthellae from two marine coelenterates. *Proc. R. Soc. Lond. B*, **177**(1047)::251–264.

Trench, R.K. (1974). Nutritional potentials in *Zoanthus sociatus* (Coelenterata, Anthozoa). *Helgolander Wiss. Meeresunters*., **26**(2):174–216.

Vance, J.E., Peake, K.B. (2011). Function of the Niemann-Pick type C proteins and their bypass by cyclodextrin. *Current Opinion in Lipidology*, **22**(3): 204-209.

van Oppen, M. (2001). In vitro establishment of symbiosis in *Acropora* millepora planulae. *Coral Reefs*, **20**(3): 200.

van Oppen, M. J. H., Palstra, F. P., Piquet, A. M.-T. & Miller, D. J. (2001). Patterns of coral-dinoflagelalte associations in *Acropora*: significance of local availability and physiology of *Symbiodinium* strains and host-symbiont selectivity. *Proceedings of the Royal Society B*, **268**(1478): 1759-1767.

Venn, A.A., Tambutté, E., Holcomb, M., Allemand, D., Tambutté, S. (2011). Live tissue imaging shows reef corals elevate pH under their calcifying tissue relative to seawater. *PloS One*, **6**:e13288.

Venn, A.A., Tambutté, E., Lotto, S., Zoccola, D., Allemands, D., Tambutté, S. (2009). Imaging intracellular pH in a reef coral and symbiotic anemone. PNAS, **106**(39): 16574-16579.

von Holt, C., & von Holt, M. (1968). Transfer of photosynthetic products from zooxanthellae to coelenterate hosts. *Comp. Biochem. Physiol*., **24**(1): 73–81.

Voolstra, C.K., Schwarz, J. A., Schnetzer, J., Shinichi, S., DeSalvo, M.K., Szmant, A.M., Coffroth, M.A., Medina, M. (2009). The host transcriptome remains unaltered during the establishment of coral-algal symbiosis. *Mol. Ecol.*, **18**: 1823-1833.

Wakefield, T. S., Kempf, S. C. (2001). Development of host- and symbiont-specific monoclonal antibodies and confirmation of the origin of the symbiosome membrane in a cnidarian-dinoflagellate symbiosis. *Biol. Bull.*, **200**(2): 127–143.

Wakefield, T.S., Farmer M.A., Kempf, S.C. (2000). Revised description of the fine structure of in situ "zooxanthellae" genus *Symbiodinium*. *Biol. Bull.* **199**(1):76–84.

Weis, V. M., Davy, S. K., Hoegh-Guldberg, O., Rodriguez-Lanetty, M. & Pringle, J. R. (2008). Cell biology in model systems as the key to understanding corals. *Trends in Ecology and Evolution*, **23**(7): 369-376.

Weis, V.M. (2008). Cellular mechanisms of Cnidarian bleaching: stress causes the collapse of symbiosis. *J. Exp. Biol*. **211**:3059–3066.

Weis, V.M., Reynolds, W.S., deBoer, M.D., Krupp, D.A. (2001). Host-symbiont specificity during onset of symbiosis between the dinoflagellate *Symbiodinium* spp. and the planula larvae of the scleractinian coral *Fungia scutaria*. *Coral Reefs*, **20**:301–308.

Wernegreen, J. J. (2012). Endosymbiosis. *Curr. Biol.*, **22**: R555-R561.

Wicks, L.C., Sampayo, E., Gardner, J.P.A., Davy, S.K. (2010). Local endemicity and high diversity characterise high-latitude coral–*Symbiodinium* partnerships. *Coral Reefs*, **29**:989–1003.

Wilkinson, C. R. (1996). Global change and coral reefs: impacts on reefs, economies and human cultures. *Global Change Biology*, **2**: 547-558.

Wolfowicz, I., Baumgarten, S., Voss, P.A., Hambleton, E.A, Hatta, M., Voolstra, C., Guse, A. (2016). *Aiptasia* sp. larvae as a model to reveal mechanisms of symbiont selection in cnidarians. *Sci. Rep*. **6**: 32366.

Xiang, T., Hambleton, E. A., DeNofrio, J. C., Pringle, J. R. & Grossman, A. R. (2013). Isolation of clonal axenic strains of the symbiotic dinoflagellate *Symbiodinium* and their growth and host specificity. *J. Phycol*., **49**(3): 447-458.

Xiang, T., Nelson, W., Rodriguez, J., Tolleter, D., Grossman, A. R. (2015). *Symbiodinium* transcriptome and global responses of cells to immediate changes in light intensity when grown under autotrophic or mixotrophic conditions. *Plant J.*, **82**(1): 67–80.

Yacobovitch, T., Benayahu, Y., Weis, V.M. (2004). Motility of zooxanthellae isolated from the Red Sea soft coral *Heteroxenia fuscescens* (Cnidaria). *J. Exp. Mar. Biol. Ecol*., **298**:35–48.

Yamashita, H., G. Suzuki, T. Hayashibara, and K. Koike. (2013). *Acropora* recruits harbor 'rare' *Symbiodinium* in the environmental pool. *Coral Reefs*, **32**(2): 355–366.

Yamashita, H., Koike, K. (2013). Genetic identity of free-living *Symbiodinium* obtained over a broad latitudinal range in the Japanese coast. *Phycological Research*, **61**:68-80.

Yamashita, H., Suzuki, G. Kai, S., Hayashibara, T., Koike, K. (2014) Establishment of Coral–Algal Symbiosis Requires Attraction and Selection. *PLoS ONE*, **9**(5): e97003.

Yellowlees, D., Rees, T. A. V. & Leggat, W. (2008). Metabolic interactions between algal symbionts and invertebrate hosts. *Plant, Cell, and Environment*, **31**: 679-694.